UiT The Arctic University of Norway

Department of Safety and Technology

Preventing Atmospheric Icing in Aviation

Passive Repulsion of Super Cooled Water Droplets through Hydrophobic Nanocomposites

Gøran Frantzen Hobitz

TEK-3901 Master's thesis in Technology and Safety 13.07.2020

Adapted from thepointsguy.com (Zach, 2020)

Preface

The following master's thesis is prepared by me, Gøran Frantzen Hobitz, at the Department of Technology and Safety – Arctic University of Norway. This master thesis is the completion of my master's degree and is an independent work by the author. The motivation behind writing a dissertation about the Aviation industry is because of the broad and complex subject around safety challenges. This thesis contains approximately 24500 words, 80 figures, and 9 tables.

With a master's thesis's limitations, it will be advisable with more extensive quality assurance of the product; further work to commercialize the product should follow a recognized qualification procedure, for example, the procedure as suggested by DNVGL (2019).

Acknowledgements

The following thesis has been written as a final part of the master's program in "Safety and Technology in The High North" at the University of Tromsø. The project has been conducted from January 2020 to June 2020.

First and foremost, research of this matter is never a solitary task. Therefore, I want to acknowledge my mentors Ove Tobias Gudmestad, André Rogander Karlsen, and Jørgen Holst for exceptional guidance through the thesis and providing knowledge regarding the main objective and the risk management in general. Secondly, I have benefited significantly from the supervision of Federico Banno, who have been assisting me through the whole process of creating a hydrophobic coating.

13.07.2020

Gøran Frantzen Hobitz

Abstract

The aviation industry already consists of a complex system of strict regulations related to operation and maintenance, where severe weather conditions further challenge flight operations. Recent research has shown that most aircraft accidents are caused by icing externally, where severe icing conditions lead to the critical degradation of the aerodynamic effectiveness – increasing the stall speed. If only a thin film of ice accumulates on the airframe, it will rapidly increase the risk for a fatal accident to occur.

The following thesis addresses critical icing conditions that might substantially affect the aerodynamic performance and propose an accessible method of a hydrophobic coating to mitigate the risk of ice accretion on planes.

The results show that the most exposed phase within in-flight icing occurs at cruising altitude, with glaze ice accretions. A risk assessment of components suggests that the wing part has the most significant effect on aerodynamic sustainability. A further CFD analysis of the wing section of an Airbus A320neo, at cruising altitude, was simulated and compared with and without glaze ice conditions. The ice formation led to a mass of 2.3 kg after 100 seconds, while measurements determined that the drag capacity was increased significantly. The lifting capacity was virtually unaffected.

Furthermore, a feasibility study has been conducted with the underlying goal of identifying the most promising of anti-icing coatings for aircraft. To date, there are no coatings capable of independently functioning as a passive anti-icing system. However, findings reveal two promising methods that were further carried out for testing.

The preparation of a highly hydrophobic and ice phobic coating based on Zinc Stearate (ZnSt) and a curable Polydimethylsiloxane (PDMS) was carried out. Indicatively, the coating showed high water repellent and ice repellent properties by measuring the ice adhesion, which reduced the interaction between the aluminum surface and freezing water droplets by over 50%.

Table of Contents

List of Tables

List of Figures

Glossary of Terms and Abbreviations

Abrasion resistance: The ability of an adhesive to withstand wear due to contact with another surface.

Adiabatic Process: Expansion where no heat is added nor subtracted from the air, which cools during the expansion because of the work done by the air.

Airfoil: Cross-sectional shape of the wing.

Anti-icing: Application of a substance that can prevent and continuously delay ice formation for a specific period.

Composite: Combination of two materials with different properties that becomes stronger when merged.

Copolymer: Different types of monomers connected in the same chain.

Cross-linking: A bond that links one polymer chain to another.

Curing/curable: The process in which the polymer is made tougher/harder.

Curing agent: Substance used to harden a surface.

De-icing: The process of actively removing snow or ice accretion form a surface.

Deposition: Occurs when the pressure of a substance is so low that the atoms detach from the solid phase during heating and go directly to gaseous form. The opposite of deposition is sublimation.

Dispersion: A mixture where particles of one substance are spread throughout another substance, creating a solution/suspension.

Hybridization: Process in which atomic orbitals[1] are mixed to form new, identical orbitals.

Icephobic[ity] - Icephobic[ity] is the ability of a solid surface to repel ice because of the low adhesion strength due to a certain topographical structure of the surface (Sojoudi, Wang, Boscher, McKinley, & Gleason, 2016).

JAR-OPS: The general aviation requirements for commercial air transport. Any commercial airliner in the European Directive needs to comply with these provisions.

[1] Definition of the areas an electron can appear around an atom.

Liquid water content: A measure of water mass in a cloud.

Median Volumetric Diameter: A measure of droplet size.

Monomer: Monomers are simple molecules that, when bonded, can join long-chain molecules, so-called polymers.

Partial vacuum: A section of low atmospheric pressure.

Polymer: Polymers or macromolecules means many monomers (see monomers).

Shear modulus: The ratio of shear stress and shear strain. A value that indicates how resistant a material is to shear deformation.

Sublimation: When a solid material turns directly to a gas without going through an intermediate phase as liquid. E.g., when a surface of ice turns into fog without melting (Robards, Haddad & Jackson, 2004).

Substrate: A molecule upon which an enzyme act.

Substance: Any materials that have a definite chemical composition. E.g. water.

Thermal inversion: Usually, the air temperature decreases with altitude. In a thermal inversion the temperature increases with height because the surface of the earth cools more rapidly. The phenomenon is referred to as thermal inversion.

AOPA: Aircraft Owners and Pilots Association.

DC: 1-dodecanethiol - $C_{12}H_{26}S$

DMF: dimethylformamide - C_3H_7NO

EASA: European Aviation Safety Agency is the EUs bureau for aircraft safety.

FAA: Federal Aviation Administration.

FAR-25: Federal Aviation Regulations, Part 25.

HMDSO: Hexamethyldisiloxane - $\boldsymbol{C_6H_{18}OSi_2}$

ICAO: International Civil Aviation Organization.

IPS: Ice Protection Systems.

LWC: Liquid Water Content.

MVD: Median Volumetric Diameter.

Pt: Platinum.

PDMS: polydimethylsiloxane - $(C_2H_6OSi)n$

PMTFPS: Polymethyltrifluoropropylsiloxane - $(C_4H_7F_3OSi)n$

PFPE: Perfluoropolyether.

PTES: 1H,1H,2H,2H-perfluorooctyltriethoxysilane – $C_{14}H_{19}F_{13}O_3Si$

PTFE: Polytetrafluoroethylene – $(C_2F_4)n$

PVDF: Polyvinylidene - $(C_2H_2F_2)n$

REACH: The European Chemicals Regulation.

SLD: Supercooled Large Water Droplets.

SLIPS: Slippery Liquid-Infused Porous Surfaces.

SWD: Supercooled Water Droplets.

WCA: Water Contact Angle.

WT%: Weight percentage (mass fraction of the solvent times a hundred).

ZnSt: Zinc Stearate - $C_{36}H_{70}O_4Zn$

ZnO: Zinc Oxide - OZn

Other flight-related expressions that may be appropriate to know before reading can be seen in Figure 1.

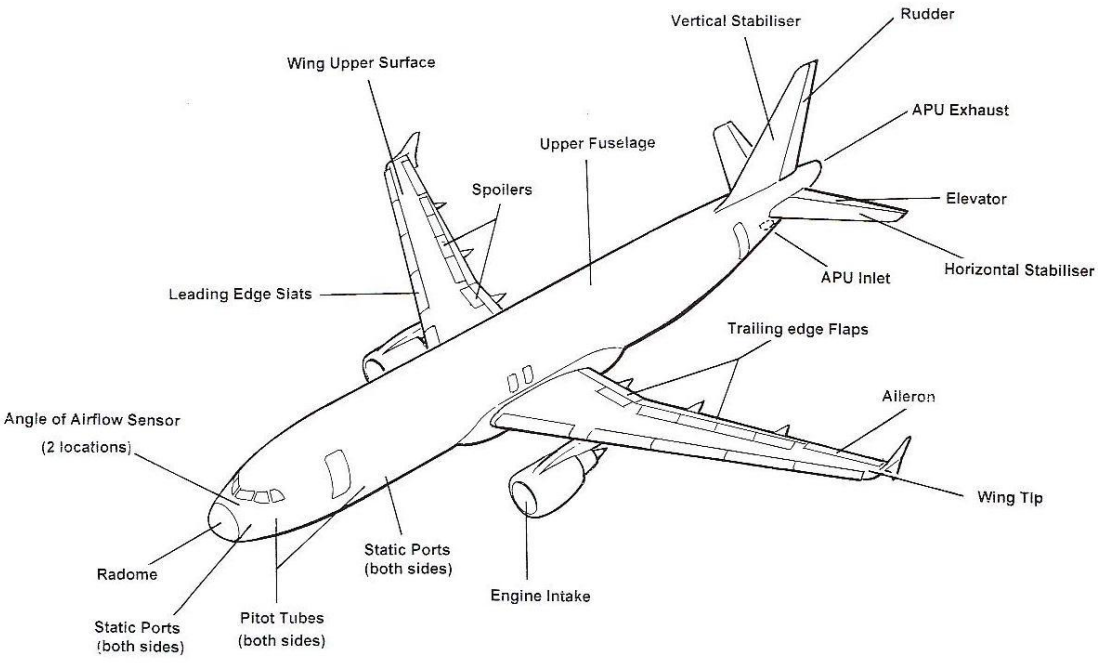

Figure 1: Parts of an Airbus A320 (Commons, 2007).

Introduction

Global warming is a significant threat to today's society and industry. In the northern areas, new hot air pockets are formed, creating more polar lows and colder winters. The aviation industry already consists of a complex system of strict regulations related to operation and maintenance, where the rapidly changing weather conditions further challenge minor airports in the Arctic. The aviation industry faces tough challenges when it comes to the future of air travel and expected climate change.

According to Perrow (1999), aviation is one of the most complex industries in terms of safety, where human error often can be claimed as a factor for unwanted events. Such events sometimes originate from natural phenomena, where accidents caused by weather are reported as a cause in about 50% of cases. It is stated by Mahapatra et al. (1999) that weather conditions affect aviation in several subtle ways and are a constant factor in the industry when overlooking periodic accidents.

Airplanes are designed to operate in frigid climates because the temperature at march height is well below 0°C. So why do ice formations still appear on the surface of the plane, and what makes the aviation industry spend billions of dollars on de-icing fluids, while accidents still are caused by icing?

The process of icing on aircraft can be defined as the accumulation or accretion of supercooled liquid or water onto an airplane during flight. Recent research has shown that most of the aircraft accidents are caused by icing externally (Lankford, 2000). According to the National Transportation Safety Board, airframe icing has led to more than 583 accidents and more than 800 fatalities from 1982 to 2000, only in the US (NTSB, 2004).

When ice accumulates on the airframe, the aerodynamics can change and reduce its efficiency, potentially impair critical parts – which may lead to a disaster. Because de-icing operations heavily rely on mechanical removal (Klein-Paste & Potova, 2014), ice also disrupts flight schedules and causes repercussions in delayed aircraft (Sparaco, 2011).

Airplanes are especially susceptible to the pernicious consequences of ice formation. Small amounts of ice on the structural surface can significantly reconstruct flight characteristics, which can be critical to the aircraft's airworthiness (Rutherford & Dudman, 2001).

Since the establishment of the aviation industry, there have been many attempts to impair ice formations on airplanes. Different methods have been tested, with thermal systems, chemical compounds, and mechanical creations, without ample impacts (ICAO, 2000).

In today's industry, measures are being taken to reduce safety challenges in an ever-changing climate, hence newer and more modern technology that may become more resilient to adverse events. To combat some of the shortcomings caused by accumulation of ice, the development of passive anti-icing systems in the form of special icephobic coatings has been actively conducted in recent years.

In the following thesis, one will study and assess critical icing conditions that affect the aerodynamics of an airplane and propose an accessible method of a hydrophobic coating to mitigate the risk of ice accretion on planes.

1.1 Background

1.1.1 Laws and regulations

Aircraft maintenance is regulated by the European directive and is enshrined in the Aviation Act, and shall ensure that the aircraft is airworthy and that both operating systems and emergency equipment are functional, including through the following measures (Lovdata, 2018):

- *"(1) Performing pre-departure inspection"*
- *"(3) Completion of all maintenance in accordance with the carrier's approved maintenance program"*
- *"(4) Analysis of the efficiency of the carrier's approved maintenance program"*

1.1.2 Weather conditions

The International Civil Aviation Organization (ICAO) demands requirements prior to flights. The following definitions from ICAO annex 6, section A13, Part I, 4.3 are utilized in this chapter (COSCAP, 1984):

"A flight to be operated in known or expected icing conditions shall not be commenced unless the aeroplane is certificated and equipped to cope with such conditions.

A flight to be planned or expected to operate in suspected or known ground icing conditions shall not take off unless the aeroplane has been inspected for icing and, if necessary, has been given appropriate de- icing/anti-icing treatment. Accumulation of ice or other naturally occurring contaminants shall be removed so that the aeroplane is kept in an airworthy condition prior to take-off."

1.1.3 Clean aircraft

The Association of European Airlines (2008), section 3.10 states the following hazards after applying de-icing chemicals:

All essential aircraft surfaces should be clean of all frost, snow and ice accumulations under the following requirements:

Wings, tail and control surfaces

"Wings, tail and control surfaces shall be free of ice, snow, slush, and frost except that a coating of frost may be present on wing lower surfaces in areas cold-soaked by fuel between forward and aft spars in accordance with the aircraft manufacturer's published manuals.

Pitot heads and static ports

Pitot heads and static ports shall be clear of ice, frost, snow and fluid residues.

Engines

Engine inlets, exhaust nozzles, cooling intakes, control system probes and ports shall be clear of ice and snow. Engine fan blades or propellers (as appropriate) shall be clear of ice, frost and snow, and shall be free to rotate.

Air conditioning inlets and exits

Air conditioning inlets and exits shall be clear of ice, frost and snow. Outflow valves shall be clear and unobstructed.

Landing gear and landing gear doors

Landing gear and landing gear doors shall be unobstructed and clear of ice, frost and snow.

Fuel tank vents

Fuel tank vents shall be clear of ice, frost and snow.

Fuselage

Fuselage shall be clear of ice and snow. Frost may be present in accordance with the aircraft manufacturer's manuals."

1.1.4 Airworthiness

Airworthiness deals with various factors that relate to the legal and physical condition of an aircraft. De. Florio (2016) defines airworthiness as airborne systems' ability to

operate in air and on the ground, without constituting a significant danger to passengers, aircraft, crew, and third parties.

1.1.5 Continuous Airworthiness

Continuous airworthiness describes the process in which the aircraft maintains its airworthiness beyond its expected lifespan. Explicitly: Technically suitable for flying. One uses the definition according to ICAO, which describes the phenomenon as follows:

"*All of the processes ensure that, at any time in its life, an airplane complies with the technical conditions fixed to the issue of the Certificate of Airworthiness and is in a condition for safe operation."* ICAO (2014).

By EASA, one can derive the aforementioned definition under Regulation No 216/2008, which describes continuous airworthiness as all processes ensuring that the aircraft at all times during its service life complies with current airworthiness requirements, while at the same time in a reliable condition (EC, Commission Regulation, 2016).

1.2 Research objective

The purpose of this thesis is preferably to examine ice formations that can affect an aircraft aerodynamic ability, and likewise propose solutions that may help mitigate the overall risk of icing, juxtaposed to an Arctic climate. In the introduction, there were made references to such correlations between weather conditions and airworthiness, especially in a cold climate. Therefore, one would like to investigate the following research questions further:

RQ1: How do different ice formations affect the aircraft's aerodynamic performance?
RQ2: How can one create a passive anti-icing system for aircraft, and improve risk mitigation through hydrophobic nanocomposites?

The effects of ice accretion are both wide-ranging and unpredictable (ICAO, 2000), while icephobic surfaces remain an unresolved issue (Zhuo et al., 2020). Therefore, the complexity of the second research question is seen as quite comprehensive. To be able to do thorough research, it has been created a landscape assessment to provide a basis for the research question.

The purpose of the "landscape assessment" is:
- *to investigate the known methods for creating icephobic coatings/surfaces;*
- *to identify among the latter the most promising for commercial implementation;*
- *to give a technical assessment and recommendations for further development.*

1.3 Limitations

Limitations, according to the dissertation, are primary resources and scope, especially given the ongoing pandemic. With limited access to laboratory testing and chemical substances, this study will only show a prediction. The study is reserved for civil aviation and limited within a European directive, but one will nevertheless look at theory with a more substantial aspect.

The task mainly deals with risk factors that correlate according to preventive regulations set by the European Aviation Safety Agency (EASA), and operational standards set by the International Civil Aviation Organization (ICAO). The following research does not concern the European aviation alone, but a study which can be seen in the context of aviation's challenges in a cold climate.

The aviation industry is seen as one industry and will not be separated in the task. The industry has many different challenges related to atmospheric icing. These conditions, as part of in-flight icing, will be in focus. Thus, ice that accumulates at a given altitude above ground level.

The research will only address monoplanes[2], neglecting drones and military aircraft. The de-icing principle will be considered as an operational parameter to erase icing from aircraft, as opposed to "anti-icing," which is a passive system to prevent ice accumulation. The thesis emphasizes the challenges that can be directly or indirectly linked to a cold climate.

[2] Monoplane is an aircraft with one set of wing surfaces (Rathakrishnan, 2013).

1.4 Structure of the thesis

The thesis will go through four main chapters, and these chapters are as follow:

- The literature review and theory will present the most relevant metrological phenomena during atmospheric icing and the related theory in creating an ice repellent coating.

- Discussion, analysis, and methodology will address methods where different assessments will be performed on topics such as structural icing, flight phases, components, landscape assessment, and so forth.

- One will also discuss and present results from the analysis within each method used. The risk assessment leads to CFD-analysis. Moreover, the landscape assessment will go through known methods for creating an icephobic coating.

- Based on this landscape assessment, one does a final analysis by preparing a highly hydrophobic coating.

- The final chapter will present a conclusion that sums up the results and discussion by answering research questions 1 and 2. This part will also go through future work with thoughts on what could be done regarding this subject.

2 Literature review and theory

In the following chapter, one explains the selected theory to provide a basic understanding of key themes and concepts. The section will provide a basis for the discussion and analysis of the research.

2.1 Overview

Table 1 provides an overview of fundamental meteorological phenomena that occur during atmospheric icing and the related theory in creating an ice repellent coating.

Table 1: Overview.

<table>
<tr><td rowspan="4">Atmospheric Icing</td><td rowspan="2">Homogeneous Freezing</td><td rowspan="4">Super Cooled Water Droplets</td><td>Structural icing</td><td>Glaze Ice
Rime Ice
Mixed Ice
Frost</td></tr>
<tr><td>Aerodynamics</td><td>Lift
Drag
Angle of attack
Wing stall</td></tr>
<tr><td rowspan="2">Heterogeneous Freezing</td><td>Ice phobic coatings</td><td>Silicone coating
Fluoropolymer coating</td></tr>
<tr><td>Nanocomposites</td><td>Hydrophobicity
Water contact angle
Ice adhesion</td></tr>
<tr><td colspan="5">Airfoil/Airframe</td></tr>
</table>

The listed expressions will be discussed in the following chapters.

2.1 Ice

There are several general definitions of ice. One adheres to The Federal Aviation Administration´s definition of ice:

"Ice is the solid form of frozen water and is formed when the water temperature falls below freezing (0 ° C)" (FAA, 2016).

Icing refers to any formation of ice on an aircraft. In aviation, different ice formations are defined according to icing that is critical to the aircraft's operation, flight stability, and hazards of take-off, cruise and landing.

2.1.1 Atmospheric Icing

At temperatures below sub-zero, clouds either contain supercooled liquid or ice. Ice particles can form at temperatures as "warm" as -10°C, opposed du supercooled water droplets that may remain in a liquid state even at a temperature of -40 °C. Supercooled water droplets are most commonly found in temperatures between -15°C and 0°C and freeze immediately upon impact with a structure such as an aircraft. The process of which supercooled water droplets hit an object in mid-air is referred to as *in-cloud icing*. Ice particles that form due to wet snow, freezing rain, or by deposition of water vapor (frost) is generally known as *precipitation icing* (Cattin, 2012; Lester. F, 1995). According to Fikke, Heimo, & Säntti (2007), each of these processes is generally referred to as *atmospheric icing*.

Physical properties such as humidity, temperature, shear strength, compression, and duration of the ice accretion are essential factors to define the accreted ice (Vindportalen, (n.d)). The dimension and the wind direction of the object exposed are critical preconditions to define the significance of any type of ice accretion. Based on that ice particles may form by either freezing[3] or by deposition[4], they can, in each case, be produced by either: Homogenous freezing,

[3] A substance changes directly from a liquid to a solid.

[4] The substance changes directly from a gas to a solid without going through the liquid phase

heterogeneous freezing, or heterogeneous deposition. (Since the latter do not occur under atmospheric conditions and there is no evidence that this is an important atmospheric process, one will only focus on the first two (Centre For Atmospheric Icing (n.d)).

2.1.2 In-cloud icing

Clouds are formed by moist air rising upwards, expanding and cooling down adiabatically. Upon sufficient cooling, the water vapor will be condensed on aerosols to form droplets. The cloud droplets are water droplets with an approximate diameter of 10µm. The droplets can grow and thus fall with higher speed, and eventually, it falls out of the cloud as either rain or snow reaching the ground.

The freezing point at 0 ◦C is the temperature at which water and ice are in thermodynamic equilibrium[5]. However, for a given amount of water to freeze, a crystallization process must be initiated. This means that random fluctuations of some of the water molecules spontaneously form an ice spire (Waagbø, 2013).

2.1.3 Clouds

Stratiform clouds

Stratiform clouds have about 3000-4000 feet in thickness, generally forming rime and mixed ice conditions. Although stratiform clouds form trace to moderate icing conditions at the top of the cloud, the danger lies in the horizontal distribution (O'Brien et al., 1990). Low-level stratiform clouds warmer than -20°C are known to be more prone to icing conditions (Federal Aviation Administration & National Weather Service, 2016).

Cumuliform clouds

Cumuliform clouds are smaller but extend longer vertically than stratiform clouds. Icing in these clouds is usually glazed or mixed. Principally, there are variable ice conditions in such cloud conditions, because it depends entirely on where the cloud is at the development stage. Icing can occur from lighter to severe icing intensities, but is most dangerous as cumulus

[5] When all parts in a physical or chemical system have the same temperature, the state of the system is in thermal equilibrium (store norske leksikon, 2017).

congestus, the stage before it develops into cumulonimbus (O'Brien et al., 1990). Cumulative clouds are most intense at the upper part of the cloud, where there is an abundance of SLD, and where they can exist at temperatures down to -40C (Federal Aviation Administration & National Weather Service, 2016).

2.2 Supercooled water droplets (SWD)

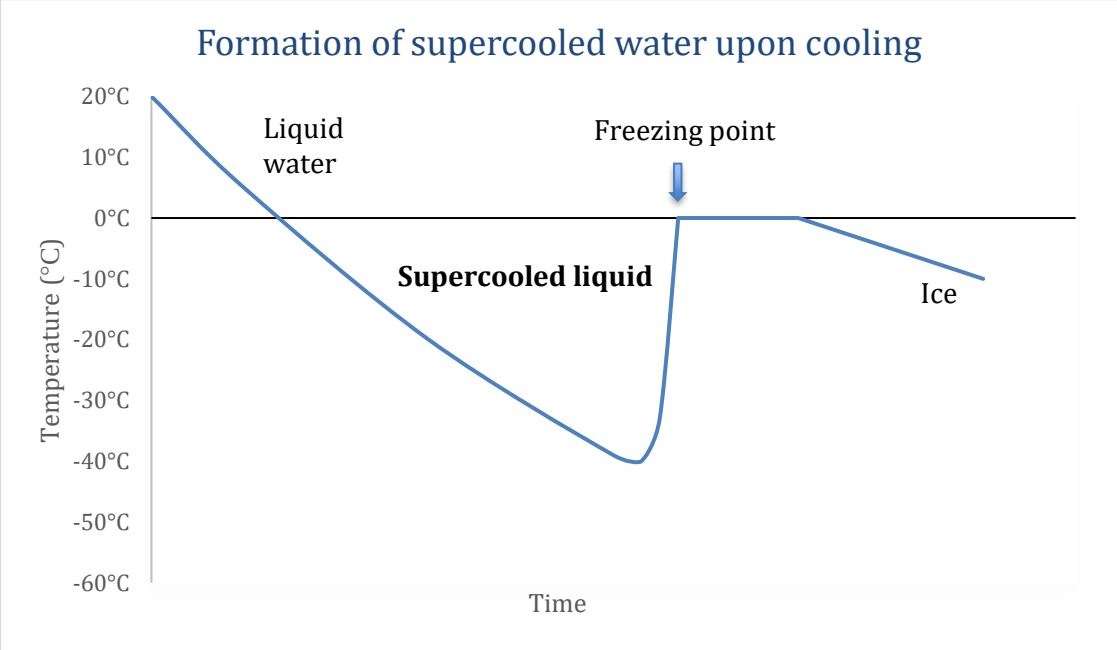

Figure 2: Supercooled water remains liquid below melting point.

Aircraft icing occurs due to supercooled water droplets (SWD) in the atmosphere. SWD is water in a liquid state, even though the temperature is below 0°C, figure 2. (Bureau of Meteorology, 2013). The phenomenon happens due to the absence of freezing nuclide, which usually consists of aerosol particles such as salt, dust, pollen, or smoke particles. A surface or substance is needed to initiate the freezing process for a droplet of water to freeze. Without it – freezing is delayed or even prevented. SWD can exist in the atmosphere at temperatures as low as -40°C. However, what one needs to consider is how these water droplets act when they encounter an aircraft, which is also below 0 °C.

In order to understand how SWD freeze when they hit objects in mid-air, it is essential to illustrate the distinction between cloud droplets and a regular raindrop. Cloud droplets are so small (10 µm) that even though the temperature is well below 0°C, it can take a long time for

the molecules to be correctly oriented to reach freezing. The thermodynamic properties of droplets from a cloud are vastly different from other types of water accumulations (Waagbø, 2013). The aspect-ratio has been illustrated in figure 3.

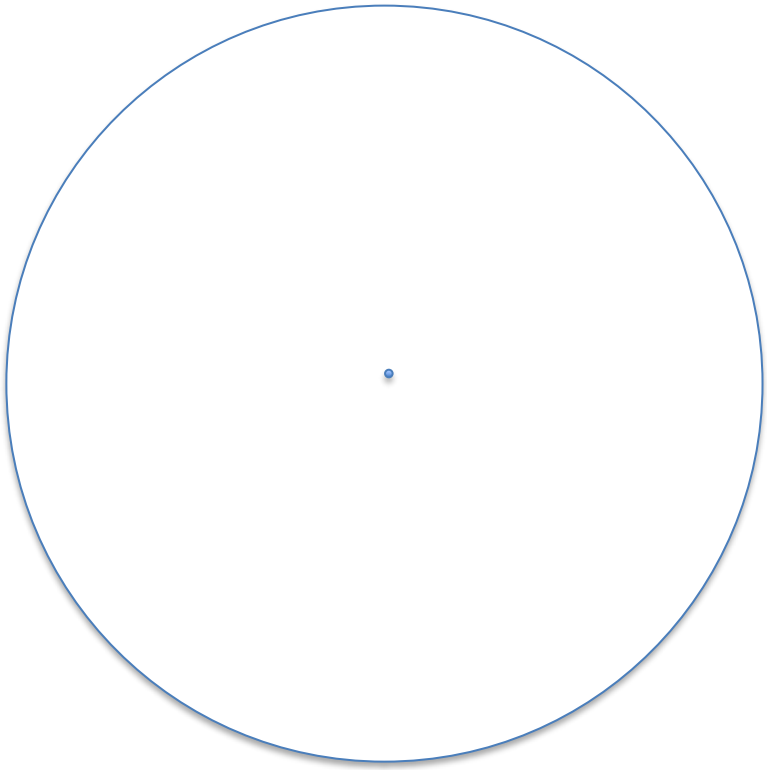

Figure 3: Illustration of the typical aspect ratio of a raindrop (radius 1mm) to a cloud-droplet (radius 10µm) (Waagbø, 2013).

SWD come in a wide variety of sizes. Their size does not only control the type of icing but the severity of it. Smaller droplets freeze at lower temperatures than larger ones, which is simply because larger droplets are more likely to contain freezing nuclei than smaller droplets, and therefore freezes more quickly (Jung, Tiwari, & Poulikakos, 2012).

2.2.1 Supercooled large droplets (SLD)

The accurate definition of Supercooled Large Droplets (SLD) is a droplet with a diameter greater than 50µm. Compared to other precipitation in an atmospheric environment, an aircraft certified for a flight can only handle droplets with a median volumetric diameter (MVD) up to 40 µm. Because of the latter, the inertia of SLD is more preeminent and less influenced by the airflow surrounding the aircraft, causing it to stick more easily to the surface of the plane (FAA, 2014).

In recent years, the attention towards SLD has grown, creating regulations according to the airworthiness, such as the FAR-25 Appendix. The reason behind the corresponding regulations is because of the significant hazard towards flight safety, affecting aerodynamics performance (Cao, Wenyuan & Wu, 2018).

2.2.2 Homogenous freezing

According to the Centre for Atmospheric Science (n.d), Homogenous freezing is the process in which a supercooled water droplet freezes without assistance from an ice nucleus[6], figure 1. Homogenous freezing usually takes place at -38°C (Häusler, Witek, Felgitsch, Hitzenberger & Grothe, 2017).

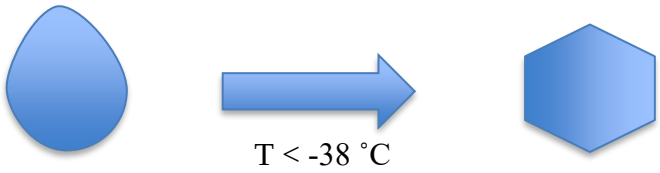

Figure 4: Water droplet freezes without a Nuclei

2.2.3 Heterogeneous freezing

Heterogeneous freezing initiates when a supercooled water droplet freezes with the assistance of an ice nucleus. It usually takes place at temperatures warmer than −38°C (Pruppacher & Klett, 1997). The process operates via several different modes, figure 5-7:

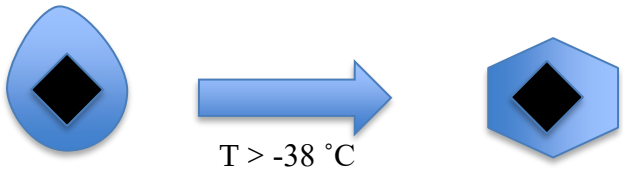

Figure 5: Immersion nucleation: Aerosol particle within a drop acts as a nucleus and the droplet freezes.

[6] Ice nucleus is a particle that appears as the nucleus without the physical processes involved.

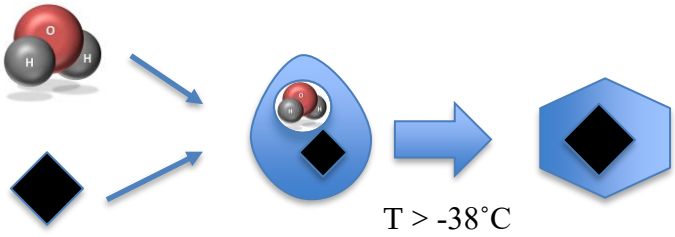

Figure 6: Condensation nucleation: Water vapor condensates on an aerosol particle to act as an immersion nucleus before the droplet freezes.

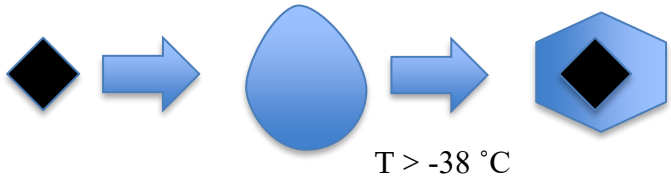

Figure 7: Contact nucleation: A solid aerosol particle collide with an existing droplet and initiates freezing.

2.3 Aerodynamics

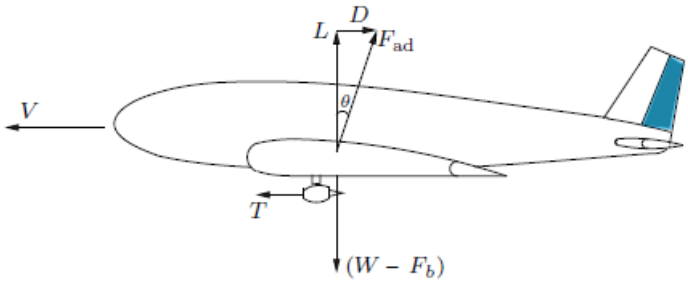

Figure 8: Forces acting on a plane (Rathakrishnan, 2013)

Aerodynamics is the theory of how air moves around an object and is determined by the aerodynamic forces acting on an aircraft (NASA, 2011). In fluid dynamics, Archimedes' law defines that the buoyancy of the aircraft will be determined by a force equal to the weight of air displaced by it, which means that the buoyancy force (F_b) acts upwards, while the weight (W) of the plane acts downwards, as seen in figure 8. The resultant force is, therefore ($W - F_b$). According to Newton's first law, the net force acting on an airplane must maintain a constant velocity ($= 0$) unless there is an external force (F_{ad}) changing it (Rathakrishnan, 2013).

The sum of vectorial forces on an airplane is, therefore:

$$T + (W - F_b) + F_{ad} = 0, \quad [2.1]$$

2.3.1 Lift

Lift and drag are functions of the resulting force (F_{ad}). Lift is only a vertical force acting perpendicular to the direction of flight (V) or opposite to the weight (W) of the aircraft. (Rathakrishnan, 2013).

Lift is mainly produced through the wing structures of a plane and is created when fluids act upon the curved airfoil. According to Bernoulli's principle: *"as the velocity increases, the pressure decreases."* Fast-moving fluids above the wings surface travel further with a higher velocity than underneath, creating lower pressure at the top of the wing, figure 9. The lower pressure exerts a suction, which creates the pressure difference and thus generating lift (Johnson, 1998).

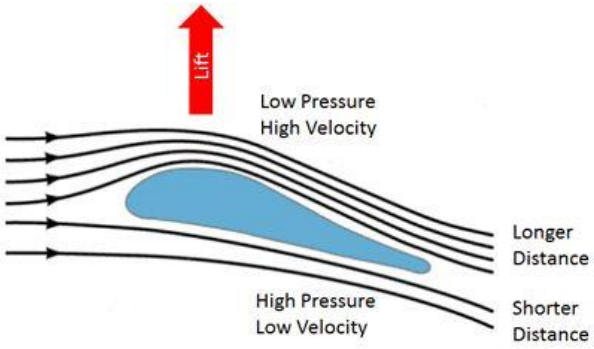

Figure 9: Bernoulli's lift theory (Electropaedia, n.d)

Even though one can make arguments to use or combine Newton's theory to explain lift, one adheres to the Bernoulli principle because of the fluid dynamics and airflow related to a possible CFD analysis later in the research (NASA, 2015; Eastlake, 2002).

Lift coefficient (C_L)

$$C_L = \frac{2L}{\rho \times v^2 \times A} \quad [2.2]$$

The lift coefficient is a value used to explain lift contingencies (inclinations, shape, and flow conditions). The lift coefficient is the ratio of lift produced by the dynamic pressure times the area. (NASA, 2015)

The maximum value of the lift coefficient (CL_{max}) depends on various factors, such as (Sforza, 2014):

- *"Wing aspect ratio."*
- *"Taper ratio."*
- *"Sweep back angle."*
- *"Trailing edge flap design and deflection angle."*
- *"Leading edge flap design and deflection angle."*

2.3.2 Drag

Drag is the horizontal force acting opposite to the direction of flight (V) or thrust (T). It relates to every component of the aircraft and represents the object's resistance through a fluid. Drag is often expressed in terms of the drag coefficient (C_D) (NASA, 2015).

$$C_d = \frac{D}{p \times \frac{V^2}{2}} \qquad [2.3]$$

2.3.3 Angle of Attack (AoA)

The Angle of Attack (AoA) is simply explained as the difference between the flight path angle and the pitch angle, as seen in figure 10.

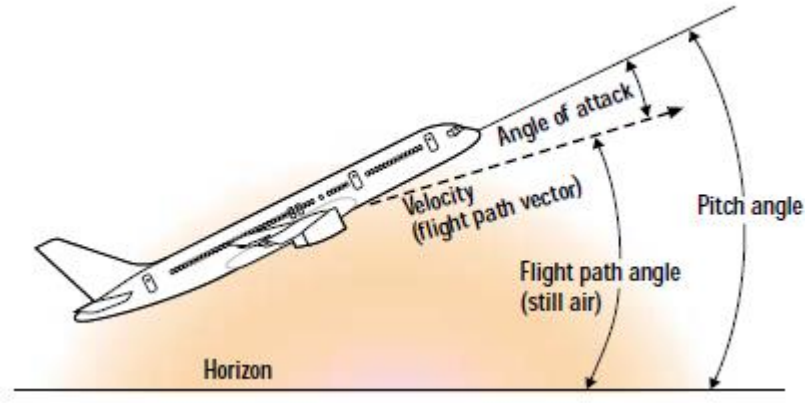

Figure 10: The principal of AoA (Boeing, 2000).

The reference line is usually different when talking about the airfoil, (figure 11).
An increased AoA increases both lift and drag. As AoA increases to the point around 15°, the airflow on the upper surface of the wing becomes detached, and the lift is lost, figure. This is known as a stall. For every circumstance, an increase in AoA increases the lift coefficient (C_L), until stall (Boeing, 2000).

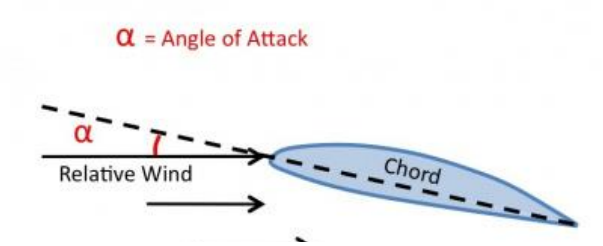

Figure 11: Airfoil displaying the Angle of Attack in contrast to relative wind and wing chord (Ideas Engineering, 2016).

2.3.4 Wing stall

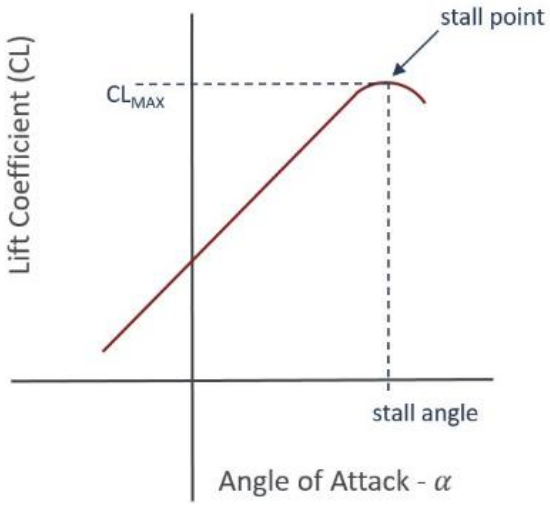

Figure 12: The relationship between the angle of attack and the lift coefficient (Aerotoolbox, 2017).

When an aircraft rotates upwards, it creates higher angles to the flow and separates air molecules needed to create the lift. The separation of the molecules, called the boundary layer, will cause a wing stall (figure 12). The lift generated depends on the type of airfoil, shape, and how the aircraft moves through the air. Therefore, with thin airfoils, the AoA (α) is proportional to the lift coefficient (C_L) compared to thicker airfoils, which is a more complicated matter (NASA, 2018).

With a layer of ice, FAA (2015) states that the maximum lift coefficient $C_{L_{max}}$ is significantly decreased, as well as the AoA becomes lower at which a stall occurs (Figure 13).

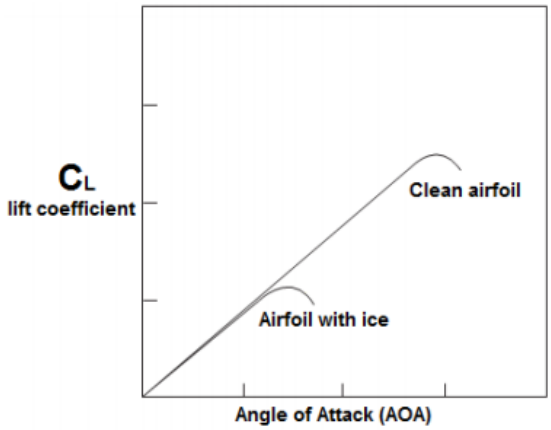

Figure 13: The relationship between the angle of attack and the lift coefficient with ice accretion (FAA, 2015).

Besides the reduced lift, the drag coefficient (C_D) increases proportional to the ice accumulation, as shown in figure 14. An airfoil drag increase of 100%-200% is not uncommon.

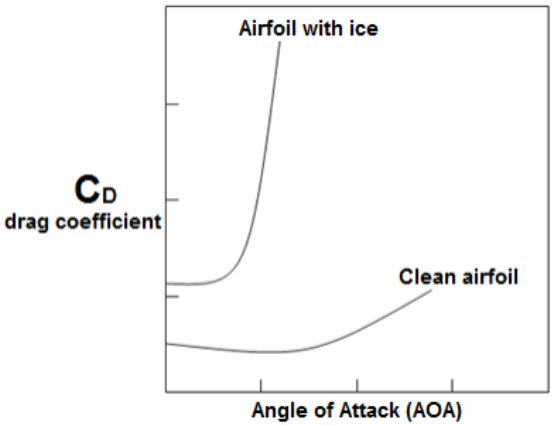

Figure 14: The relationship between the angle of attack and the drag coefficient with ice accretion (FAA, 2015).

2.4 Nanocomposites

Nanocomposites are a multiphase solid material, and has the following characteristics (Chen et al., 2008):

- Material consisting of several components.
- Contains different phase domains.
- At least one phase is continuous.
- At least one phase has a dimension in the nanoscale.

2.4.1 Hydrophobicity

The Greek word *Hydrophobicity* is known in the field of chemistry as the ability of a substance or surface to repel water. *Hydro* is Greek for water, while *phobicity* means a lack of affinity (Law, 2014).

2.4.2 Water contact angle

Hydrophobicity is defined by the static water contact angle (θ), as determined by Young's equation (Young, 1805).

$$\gamma_{LV}\cos\theta = \gamma_{SV} - \gamma_{SL}, \qquad [2.4]$$

Where Y_{LV} = liquid surface tension, Y_{SV} = solid surface tension, Y_{SL} = solid/liquid surface tension, and θ = Water contact angle.

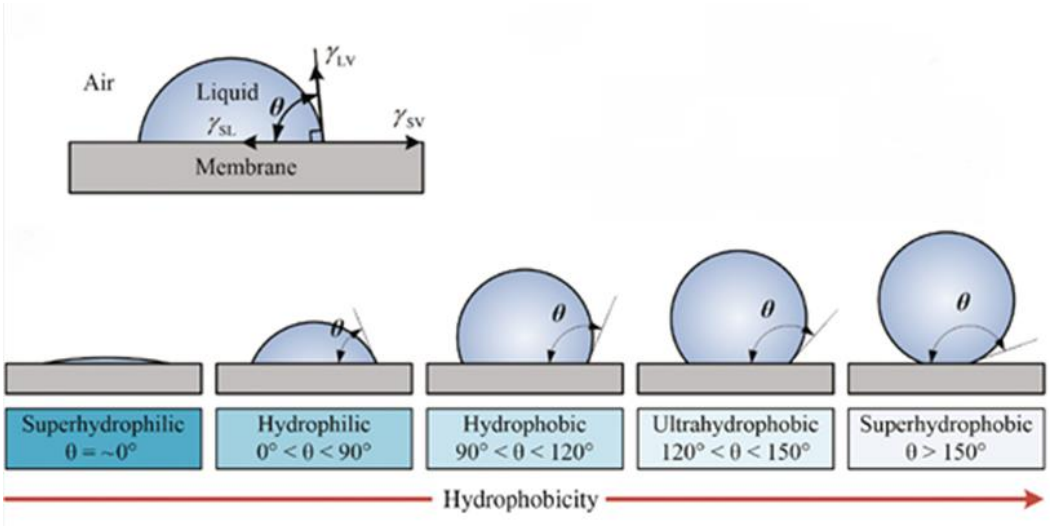

Figure 15: Characteristics of hydrophobic surfaces (Himma, Prasetya, Anisah, & Wenten, 2019). The angle (θ) is the water contact angle.

A surface is said to be hydrophobic when θ > 90°, and superhydrophobic when θ > 150°, as seen in figure 15.

Contact angle hysteresis (CAH) and sliding angle (SA)

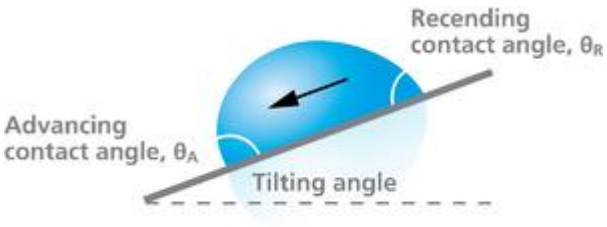

Figure 16: Contact angle hysteresis (Biolin Scientific, 2018).

A contact angle hysteresis (CAH) is often observed when a water droplet starts to slide. CAH is the difference between the advancing and the receding angles of a droplet before it starts to move, figure 16. (Biolin Scientific, 2018). The Sliding angle (SA) determines the coefficient of static friction and is obtained by tilting the surface to a certain degree until the droplet starts to slide.

2.4.3 Ice adhesion

Ice adhesion is the physical and chemical process between the solid and ice surfaces. Petrenko & Ryzhkin (1997) proposed that the electrostatic attraction between the ice and metal surfaces influences the ice adhesion strength. According to Ghalmi, Menini & Farzaneh (2009), hydrogen bonding is responsible for the solid ice cohesion from the liquid. The liquid layer on the solid-ice surface, influence the ice adhesion. (Beeram, 2017)

The method to estimate the characteristics of ice adhesion is called the Work of Adhesion; it can be defined as the maximum amount of free energy required to remove the ice from the solid surface.

$$Ice\ Adhesion\ Strength = \frac{Maximum\ Force}{Contact\ Area} \qquad [2.5]$$

Figure 17 illustrates a droplet of water on the solid layer for the three-phase system, where the liquid is the droplet of water, the solid is the surface. The water droplet shape can be determined by the solid-liquid, solid-gas, and liquid-gas interaction energies, denoted by γSL, γSG, and γLG, respectively.

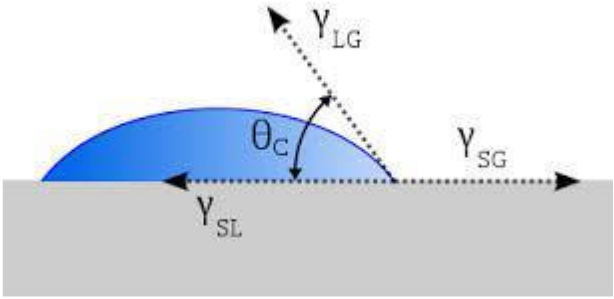

Figure 17: Water surface placed on the solid surface with contact angle (Nanoproject, 2013).

As the contact area θ_c, has an indirect relation with the solid-liquid interaction. If the contact area is high, there will be low interaction, and if the contact area is low, there will be high interaction. If the surface energies of ice and water become the same, the work of water adhesion is approximately equal to ice adhesion (Makkonen, 2012). So, one can say the ice removal is dependent upon the contact angle. If the contact angle is low, there will be high ice adhesion strength; if the contact angle is high, there will be low ice adhesion.

2.5 Icephobic coatings

According to Huang et al. (2019), icephobic or ice-phobic coatings are characterized by their chemical composition, surface properties, and application approaches.

To be called icephobic, a coating must have at least one of the following functions:

- Water repellent, such that they detach from the coated surface before freezing.
- Carries a delay before freezing,
- Ice-to-surface adhesion strength reduction. For passive systems, this parameter should be less than 20 kPa.

The dimensions and features of the final product also matter. Essential details such as aircraft components are economically achievable to process using standard methods such as dip, spray,

brush, or electrostatic deposition[7]. For such cases, coatings made using polymers are usually most suitable. However, it is rational to coat expensive small-sized components using more technologically complicated processes that involve the use of enclosed chambers (Huang et al., 2019).

2.5.1 Silicone-based coating

Silicones include a group of macromolecular compounds, where the siloxane unit having various organic elements acts as a monomer. It has been determined that due to their low surface energy and low elastic modulus, silicones have icephobic properties (Golovin et al., 2016).

2.5.2 Fluoropolymer coating

Fluoropolymers are polymers bonded by multiple fluorocarbons and have properties that other polymers do not have. It is, therefore, very compatible on the surface of a substrate. Some of the most known non-stickable coatings are:

- Polytetrafluoroethylene (PTFE)
- Tetrafluoroethylene- hexafluoropropylene copolymer (FEP)
- Ethylene tetrafluoroethylene copolymer (ETFE)
- Polyvinylidene fluoride (PVDF)

PVDF is the only fluoropolymer that is made of thermoplastic and has previously been used for paint since it was difficult to dissolve in organic solvents. In recent decades, new fluoropolymers have been developed with successful curable[8] features, most commonly used as weather-resistant coatings (Stoye & Freitag, 1998).

[7] The deposition of material in liquid form followed by evaporation of the solvent, creating a solid coating.

[8] A curable substance is a substance that starts out in a liquid phase and is hardened into a solid, in this case, by use of a curing agent (Pham & Marks, 2005).

2.6 Icing conditions and subsequent effects

2.6.1 Structural Icing

There are three main types of ice formations that affect an aircraft during the flight (Thompson, Bruintjes, Brown & Hage, 1997). The type of structure and how each affects an aircraft are further discussed below.

2.6.2 Rime Ice

Ahrens (2007) and O'Brien et al. (1990) define rime ice as a whitish and rough ice deposit with an opaque texture, figure 18. It is generated by small supercooled droplets (MVD <50 µm) encountered in either stratiform or cumuliform clouds where the temperature varies from -10°C and -20°C. Rime ice freezes instantly upon impact with a sub-zero surface of the aircraft. Because of the small size of the SWD, the droplets trap air inside them, generating an instant transition to ice crystals. The freezing process happens so rapidly that the droplets will strike the wings' leading edges, creating porous and brittle ice crystals. Rime ice is usually favorable in cold temperatures with low Liquid Water Content (LWC).

Figure 18: Rime ice (Federal Aviation Administration & National Weather Service, 1975).

Rime ice mainly accumulates on the leading edges of both wings, stabilizers and air inlets. This type of ice mainly affects the aircraft by altering the plane's aerodynamics and may choke the orifices of the carburetor in the process.

2.6.3 Glaze ice

Glaze ice (clear ice) is glossy, transparent and caused by Supercooled large droplets (SLD). As Lynch & Khodadoust (2001) reported, the most favorable conditions for glaze ice are between 0°C and -3°C with higher LWCs. It usually occurs in areas of freezing rain, and forms on the aircraft's wings and antennas, but have a more substantial aerodynamic effect on the wings (FAA, 2016). Because the MVD of SLD exceeds 50um, the droplet does not freeze instantly upon contact with the wings surface. Only a portion of the droplets will freeze on the leading edge, but the droplet's excess will flow towards the trailing edge, creating a robust, transparent, and unnoticeable ice film, figure 19 (Ahrens, 2007).

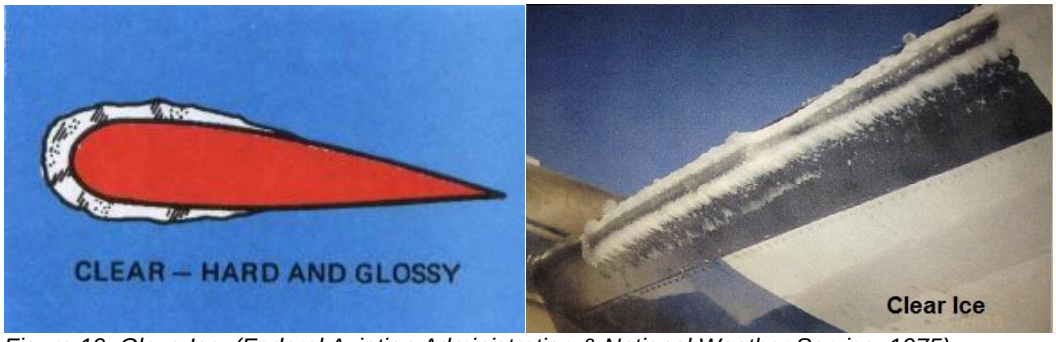

Figure 19: Glaze Ice. (Federal Aviation Administration & National Weather Service, 1975).

Glazed ice massively disrupts the airflow around the airfoil and is known as the most hazardous structural ice, where even modern de-icers may be insufficient in removing the structures (Ahrens, 2007; O'Brien et al., 1990). Since glaze ice has high ice adhesion strength, de-icing fluids prior to take-off needs to be repeated to remove glaze ice (Association of European Airlines, 2008).

2.6.4 Mixed Ice

Figure 20: Mixed Ice. (Federal Aviation Administration & National Weather Service, 1975).

On most occasions, one would not just experience one type of icing, but both types called mixed ice (figure 20). Mixed ice incorporates both rime and glaze ice characteristics and is the most common form of icing since droplets of different MVD usually occur in the cloud. It is most likely to occur in temperatures between -10°C and -15°C and is characterized by being irregular, rough, and whitish.

With a mixture of frost, glaze, and rime, mixed ice can accumulate quickly, making it more difficult to remove compared to rime ice. This ice type usually affects take-off by increasing stall speed and reducing lift (Federal Aviation Administration & National Weather Service, 2016).

2.6.5 Frost

Figure 21: Frost vs. Ice (Federal Aviation Administration, 2008)

Frost (figure 21), or hoar frost, is a type of icing that can be formed under clear weather conditions, both in-flight and in-ground conditions. When the surface temperature falls below 0°C, particles on the surface of the airplane can act as aerosol particles (FAA, 2008). Water vapor can turn directly to ice, and hoarfrost can be seen as the ice crystals are created (Bureau of

Meteorology, 2013). Frost differs from the ice because of their independent growth and granular texture, though heavy frost may have frictional similarities to other icing types.

At ground conditions, the aircraft surface may be below 0°C. The water vapor in the air that encounters the surface will freeze on impact through a sublimation, thus forming hoar frost.

In-flight frost can be formed when the aircraft climbs through a thermal inversion, from an air layer below 0°C to an air layer above 0°C (figure 22). The plane will then be below the freezing point, allowing hot air to freeze on the aircraft's surface through sublimation (Oxford Aviation Academy, 2010).

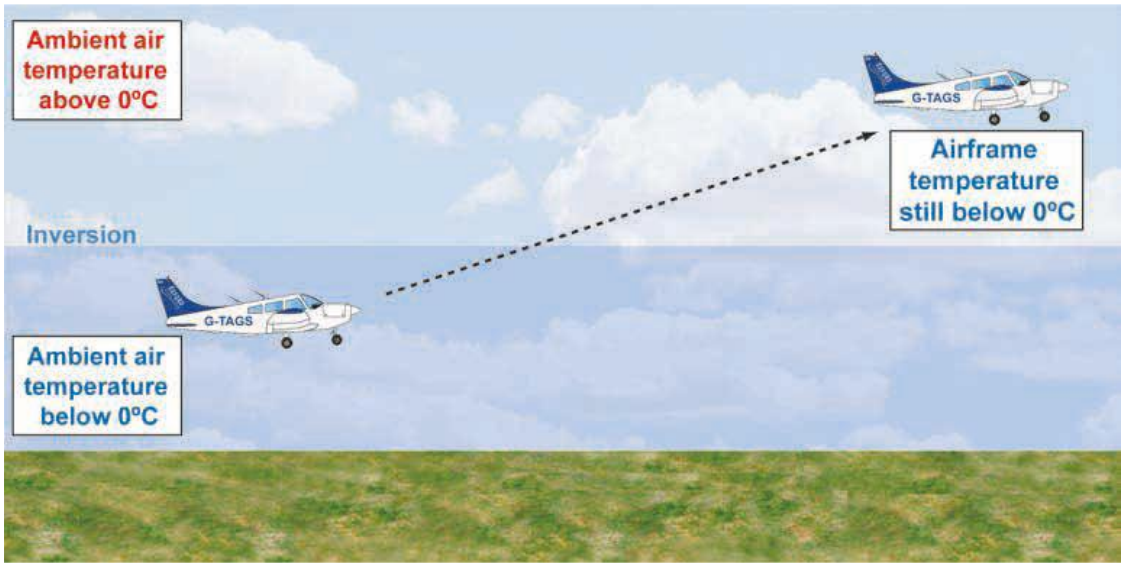

Figure 22: Frost may accumulate when climbing from air temperatures below 0°C, into warmer air (Oxford Aviation Academy, 2010).

As seen in figure 23, in-flight frost may also occur during a descent during typical inversion, where the surface of the aircraft is above 0°C, while the layer of air underneath is below 0°C (Oxford Aviation Academy, 2010).

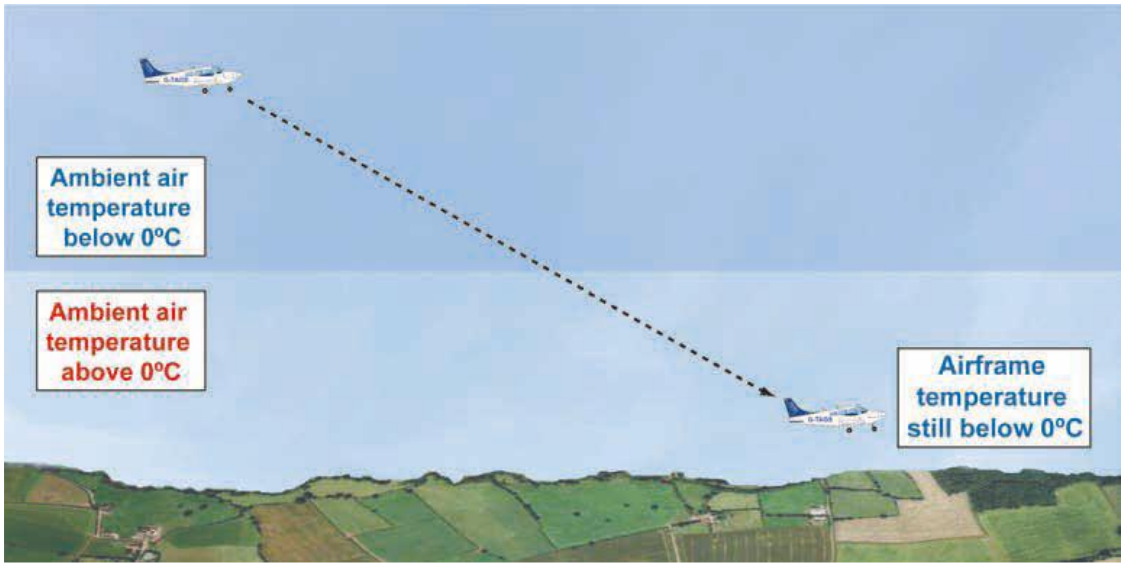

Figure 23: Frost may accumulate when descending rapidly from air temperatures below 0°C, into warmer air (Oxford Aviation Academy, 2010).

Frost caused by inversion is challening to detect because it will most often be situated on the underside of the aircraft's wings, where the fuel tanks are located. The reason is that the fuel takes longer to heat than the rest of the surface (ICAO, 2000). See figure 24.

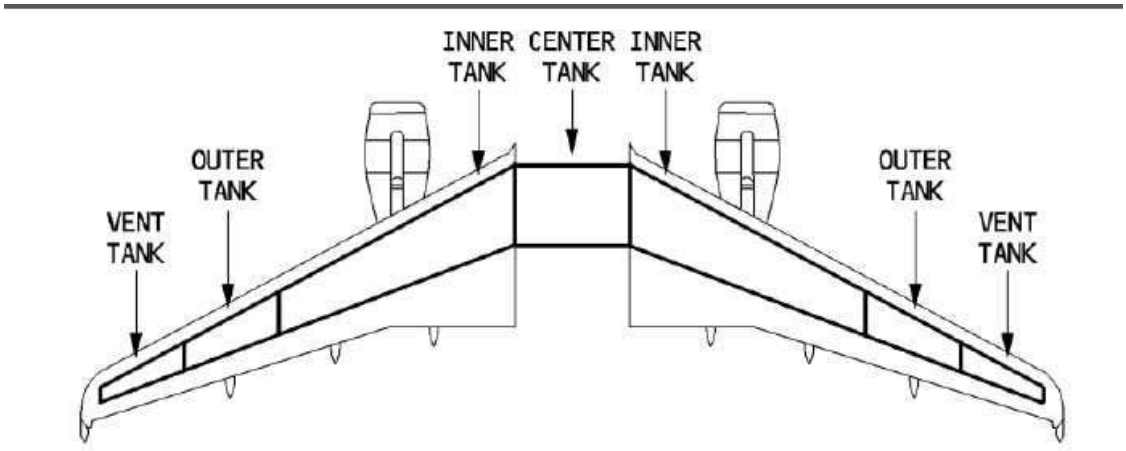

Figure 24: Fuel tanks Schematic (Frega, 2018).

2.7 Precipitation

Precipitation is a wide-ranging definition of any atmospheric water vapor that condenses and falls to the earth's surface. Examples are rain, snow, hail, ice pellets, etc. (American Meteorological Society, 2012). Figure 25 illustrates the risk of precipitation and SWD in various altitudes.

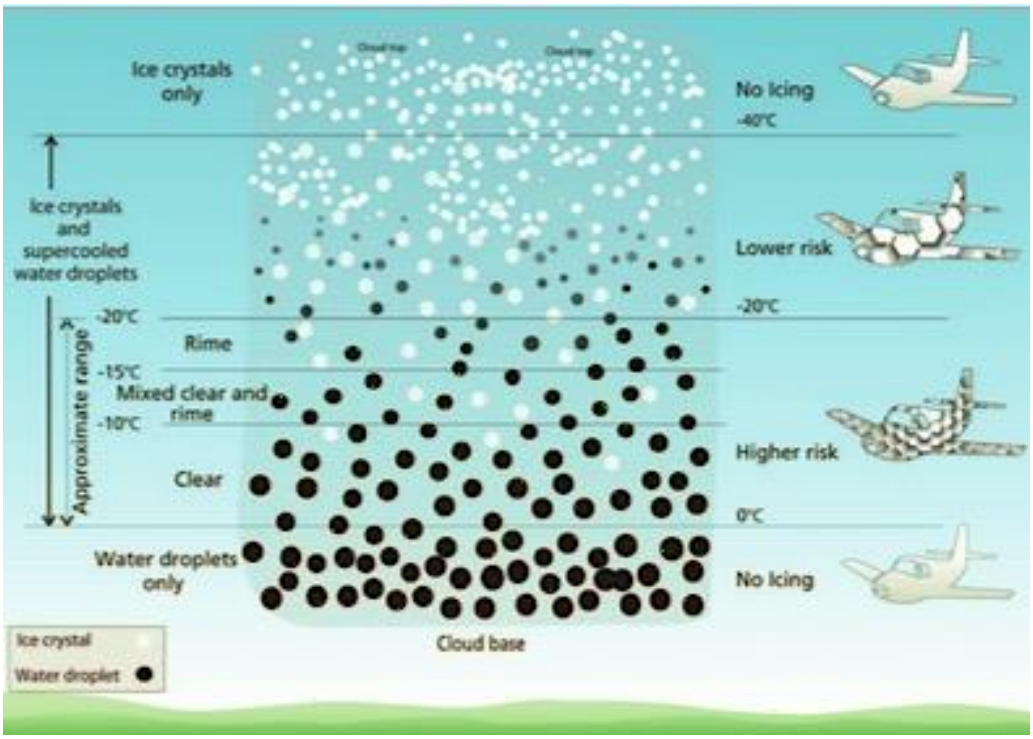

Figure 25: Aircraft icing. (Bureau of Meteorology, 2013).

2.7.1 Freezing rain

Freezing rain is the most hazardous to aircraft operations and is characterized by droplets that exceed 50µm. It occurs when frozen precipitation falls from a warm air mass (>0°C) into a cold layer of air - where they become supercooled. For this to happen, there must be a layer of air above 0°C, overlying a layer of air below 0°C, as seen in figure 26 (Bernstein 2000; Rauber, Olthoff, Rama-murthy, & Kunkel, 2000; Skybrary, 2019c).

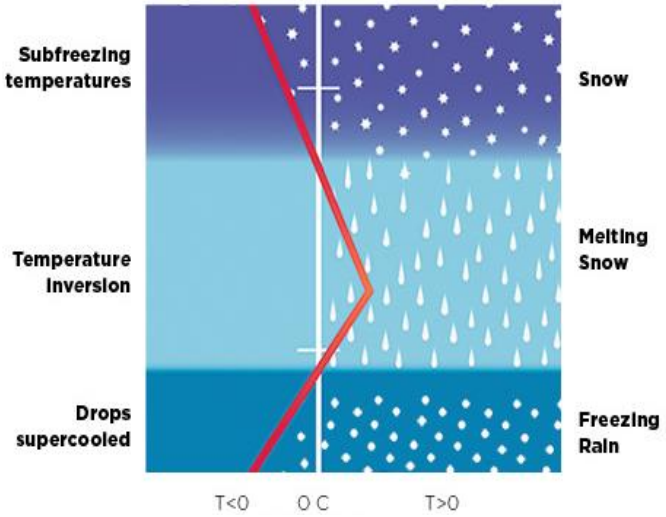

Figure 26: How snow melts and becomes supercooled through temperature inversions (AOPA, 2010).

When rain falls into the zone with below 0°C, it may become supercooled. If an aircraft were to fly within this area, then the airframe temperature will be below 0°C, and Supercooled Water Droplets (SWD) will hit the airframe. The rate of accumulation is so severe that within a short time, the aircraft may not be able to sustain flight. This type of icing can occasionally be found associated with a warm front: The diagram in figure 27 shows where warm air overlies air below 0°C.

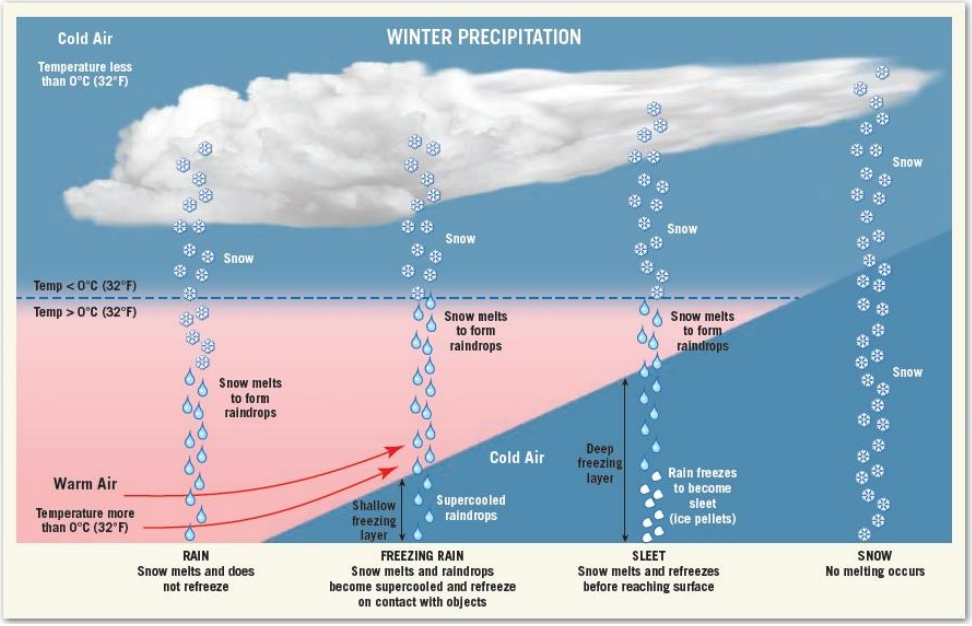

Figure 27: The diagram shows the cloud and rain formation within the warm layer. (Richoffmanclass, n.d.)

Airplanes, heading towards a front, can have a significant impact on ice accretion, especially if the air ahead of the front is cold. (Bureau of Meteorology, 2013; Federal Aviation Administration & National Weather Service, 1975; Federal Aviation Administration, 2008).

2.7.2 Freezing drizzle

Freezing drizzle can happen due to either collision-coalescence (CC) or the classical melting process (CMP) (Bocchieri 1980; Huffman and Norman 1988; Ohtake 1963).

Previous studies have shown that the CC process is the primary process for the propagation of freezing drizzle in more than 80 percent of the time (Bernstein 2000; Kajikawa, Kikuchi, Asuma, Inoue, & Sato, 2000; Rauber et al., 2000; Skybrary, 2019c).

The CC process usually occurs in clouds where the temperature is between 0 and – 10°C, where supercooled droplets are commonly produced due to low concentrations of ice nuclei (Cortinas Jr, Bernstein, Robbins, & Strapp, 2004).

Freezing drizzle occurs when some droplets in a cloud develop to roughly 30 µm, and they begin falling fast enough to collide with smaller droplets, creating a coalition. These droplets are now even more significant in size and have a better chance of capturing smaller droplets. Under the right conditions, the process may generate drizzle-sized drops with a diameter of between 50 and 500 µm, typically at the top of a supercooled cloud. When entering a freezing drizzle, one should not expect a warmer layer of air to exist above the conditions (Skybrary, 2019c).

2.8 Ice-exposed flight conditions

2.8.1 Icing in mountainous area

Orographic lifting

When stable air currents rise above a mountain, the wind cools adiabatically by the leeward side of the hill, thus having a higher density than the air around it. Air mass then falls towards the bottom of the mountain before it produces fluctuations at the equilibrium level, (figure 28). The phenomenon is called orographic lift (Whiteman, 2000).

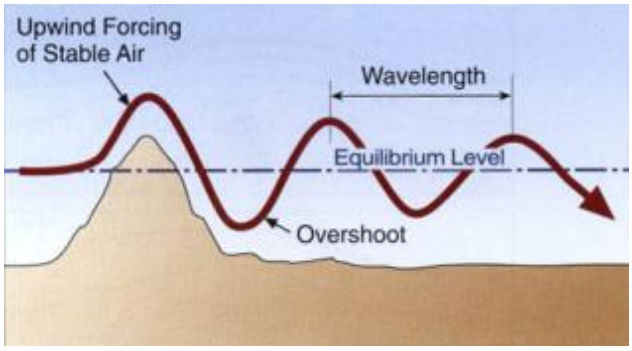

Figure 28: Orographic waves. (Whiteman, 2000).

Orographic lifts are known to create hazardous flying conditions, especially by the ridges on the windward side, where the zone can extend to over 5000 ft, (figure 29). (AOPA Air Safety Foundation, 2008; Federal Aviation Administration & National Weather Service, 2016; O'Brien et al., 1990). If there is enough moisture in the atmosphere and perpendicular clouds are visible (lenticular clouds), there is a significant chance of freezing drizzle (Whiteman, 2000).

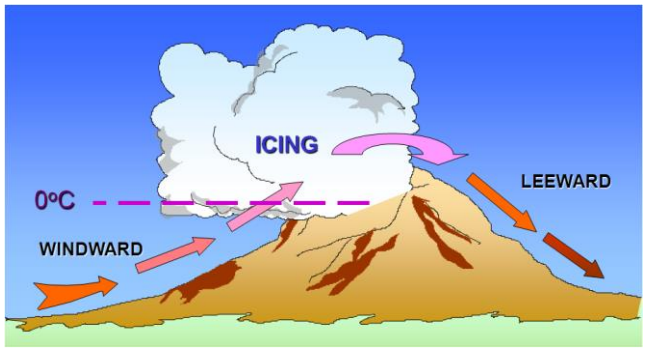

Figure 29: Icing with mountains (FAA, 2016).

Since freezing drizzle is known to produce small supercooled droplets, the layer of clear ice accumulating on a plane will be transparent, and significantly harder to notice for pilots. Moreover, it can mask the aerodynamic effects. Should the aircraft be exposed to freezing drizzle from the windward side, the maximum lift coefficient ($C_{L_{max}}$) will be reduced to the point that the aircraft is unable to ascend over the mountain. Neither will the plane be capable of descending to safer conditions because of the terrain elevation (AOPA Air Safety Foundation, 2008; Federal Aviation Administration & National Weather Service, 2016).

2.8.2 Icing in frontal area

The definition of a front is a distinction between two air masses, which are different in temperature, stability, and humidity. When these two air masses coincide, the hot air rises above the cold air (Yr, 2009). frontal areas are known for freezing rain and freezing drizzle, (figure 30).

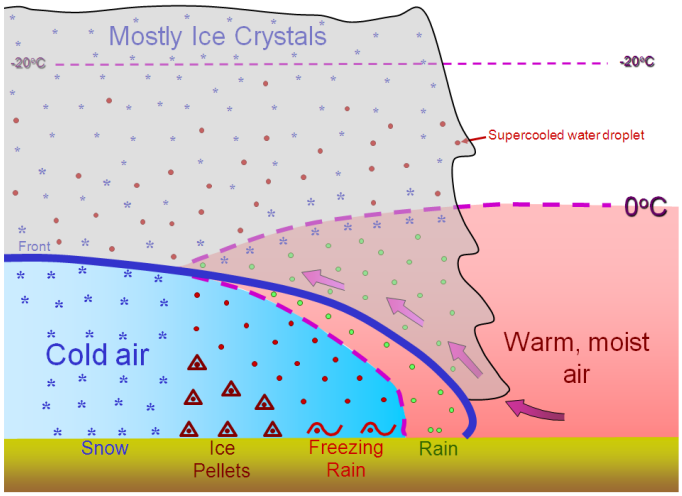

Figure 30: Icing with fronts (Federal Aviation Administration & National Weather Service, 2016).

One will mainly distinguish between three types of fronts: Warm fronts, cold fronts, and occluded fronts, (stationary fronts).

Warm front

A warm front occurs when warm air gradually exceeds cold air, (figure 31). Production of freezing rain and freezing drizzle are typical in a warm front, where rime, clear or mixed icing is frequent. (O'Brien et al., 1990).

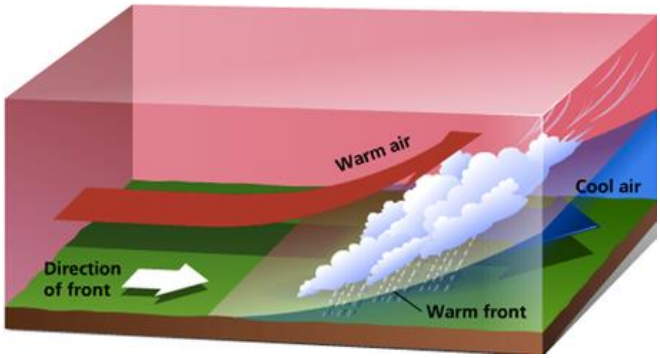

Figure 31: Warm front (Ahrens, 2007).

When hot air passes over a sub-freezing air mass through cold winters, the conditions create a higher risk of freezing rain and freezing drizzle (NASA, 2016; Federal Aviation Administration & National Weather Service, 2016).

On monoplanes, frontal icing can become extremely hazardous, according to NASA (2016). It is relatively critical because it is unpredictable, but also because under such conditions, freezing precipitation may extend horizontally over 10.000 ft., making lateral deviations almost impossible. However, the probability of such events is usually exceptional, and they commonly extend to no more than about 3000 ft., making a vertical deviation less hazardous. (Federal Aviation Administration & National Weather Service, 2016; NASA, 2016; O'Brien et al., 1990)

Cold front

Cold fronts are produced when a cold layer of air mass supersedes the warm layer of air, (figure 32). Because of the high density, cold fronts stay close to the ground, forcing the warmer air to ascend above the cold mass. Due to the rapid climb, the temperature decreases - creating cumuliform clouds (FAA, 2016).

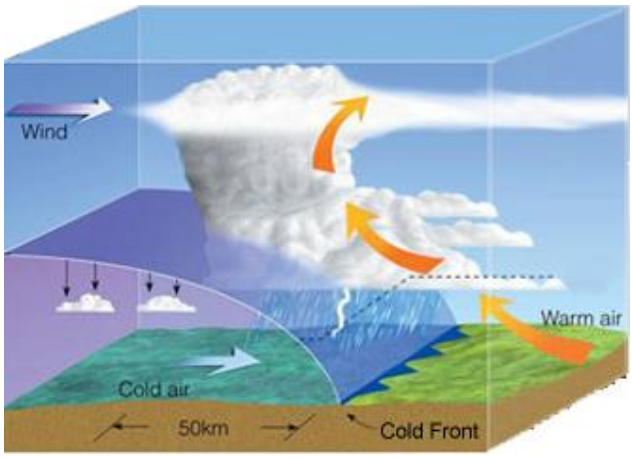

Figure 32: Cold front (Ahrens, 2007)

The rapid lifting associated with a cold front may cause severe icing conditions, usually with a high Liquid Water Content (LWC). Although a vertical deviation of 3000 ft. may avoid in-flight icing, it can become hazardous since the end passage of cumuliform clouds is known for the intense production of SLD. Moreover, cumuliform clouds in cold fronts will be about 10.000 ft. thick (NASA, 2016; O'Brien et al., 1990).

The main difference between a cold and a warm front is the violent activity along the cold front, as opposed to a warm front with more limited movement before the front line. According to O'Brien et al., 1990, a cold front is portrayed by extreme weather that develops quickly (up to 100 km/h), often without warning, opposed to a warm front that moves relatively slowly (25-40 km/h) with the possibility of advance notice (FAA, 2016).

Occluded front

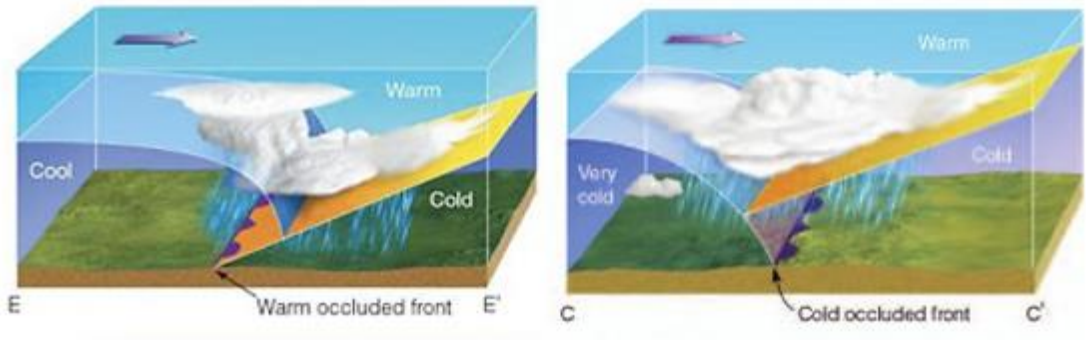

Figure 33: Warm occluded front compared with a cold occluded front (Ahrens, 2007).

Occluded fronts are known for their substantial rate of precipitation with both stratiform and cumuliform clouds, consisting of glaze, rime, and mixed ice.
Ahrens (2007) describe a cold occlusion as when very frigid air accelerates too quickly to catch the less cool air mass, forcing the warm air mass to rise above the cold front, (figure 33). Cold occluding fronts have stable air mass and a mixture of weather associated with both cold- and warm front weather conditions.

A warm occlusion front follows the same process as a cold front, except that the front air is colder than the air mass at the front, which causes the cold mass to drift over the warm.

The most dangerous flight conditions transpire most often by a warm occlusion since the cold air forced over the heat is often unstable. The phenomenon contributes to stratiform clouds with an icing zone up to 20.000 ft. with heavy freezing rain and freezing drizzle (NASA, 2016; FAA, 2016).

2.9 Icing intensities

The type of ice accumulation and the intensity are reported through PIREPs, which is the pilot weather report. Intensity is categorized according to the rate of accumulation, the effectiveness of de- and anti-icing chemicals, and how pilots must act toward the different scenarios of ice, table 2 (Lester, 1995).

Table 2: Icing intensities (Lester, 1995).

Intensity	*Airframe Accumulation*	*Pilot Action*
Trace	*Ice becomes perceptible. Rate of accumulation of ice is slightly greater than the rate of loss due to sublimation.*	*Unless encountered for one hour or more, de-icing/anti-icing equipment and/or heading or altitude change not required.*
Light	*The rate of accumulation may create a problem if flight in this environment for one hour.*	*De-icing/anti-icing required occasionally to remove/prevent accumulation or heading or altitude change required.*
Moderate	*The rate of accumulation is such that even short encounters become potentially hazardous.*	*De-icing/anti-icing required or heading or altitude change required.*
Severe	*The rate of accumulation is such that de-icing/anti-icing equipment fails to reduce or control the hazard.*	*Immediately heading or altitude change required.*

In **trace** conditions, ice becomes barely visible, and there is ordinarily no need for action unless exposed for one hour or more.

Light icing is usually not an obstacle, though conditions in glaze conditions are might considered more severe than rime ice.

In **moderate** icing, a deviation may be crucial because of the rate of ice accumulation. The rate may cause a hazardous situation.

In **severe** icing conditions, the accumulation rate is such that de-icing may fail to reduce the potential hazard. Therefore, an altitude change is vital to evade additional accumulation and flight impairments (Lester, 1995).

The severity of ice accretions depends on the type of aircraft and which kind of de-icing is used. The higher the cloud's LWC, the more quickly ice accumulates on the surfaces. The quantity of water can also influence the ice shape. Nevertheless, the MVD of the droplet is an essential factor in determining the intensity of ice accumulations (FAA, 2014).

3 Discussion, Analysis and methodology

3.1 Risk assessment

The previous chapter addressed factors that affect the aircraft's aerodynamics. Facts reveal that different ice formations of structural ice have a variable impact on the aircraft's lift and drag capacity. Icing incidents occur under the right conditions and is dependent on the environment. As structural icing is a leading factor for such occurrences to happen (figure 34), this chapter will discuss the challenges of such ice formations and further assess the risk against different flight phases.

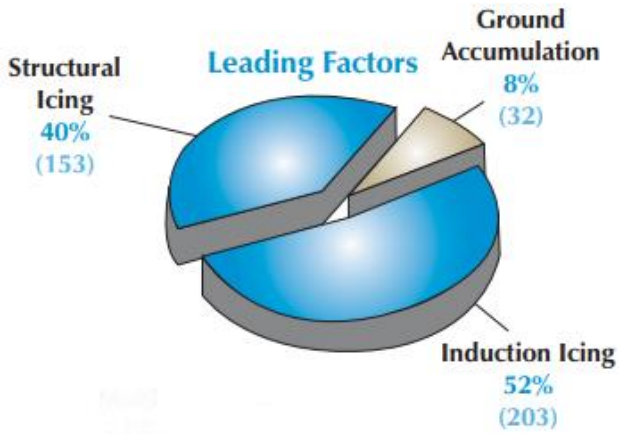

Figure 34: Report from 1990-2000 reveals that structural icing is one of the leading factors for accidents to occur (AOPA Air Safety Foundation, 2008).

"*AT43, en-route, Folgefonna Norway, 2005 (On September 14, 2005, an ATR 42-320 operated by Coast Air AS experienced a continuous build-up of ice in the climb, despite the activation of de-icing systems aircraft entered an uncontrolled roll and lost 1500ft in altitude*" (Skybrary, 2019a).

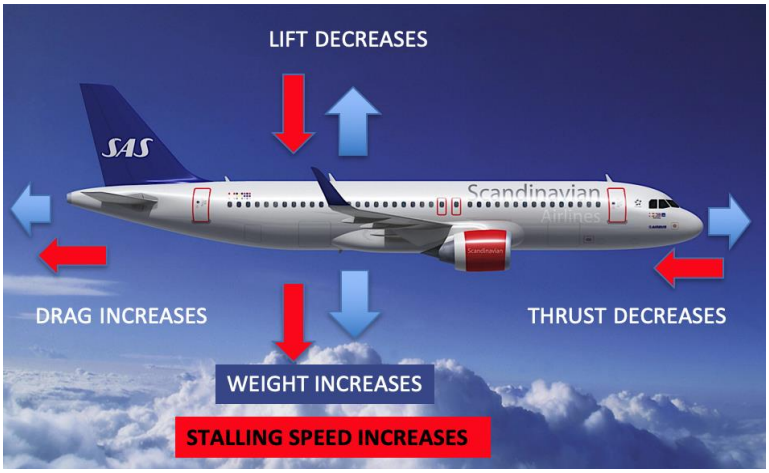

Figure 35: Aerodynamic effects of icing. (Foto: Airbus.com)

The wing of an airplane has been designed to exact the aerodynamic standards. The wing design is made to produce lift and decrease drag. Structural icing that accumulates on the airframe will be detrimental to both factors, as seen in figure 35. As ice accumulates on the airframe, the weight grows, and the plane reduces lift. Gradually the ice forms on the wings, changing its aerodynamics, resulting in increased drag and reduced airspeed (Federal Aviation Administration & National Weather Service, 1975).

3.1.1 Rime ice

According to a study by Cao, Zhang, & Sheridan (2008), rime ice grows critically faster with a Median Volume Diameter (MVD) in the higher spectrum, as seen in figure 36. The latter is merely explained by the fact that larger droplets are less affected by the airflow, which leads to more extensive ice accumulation.

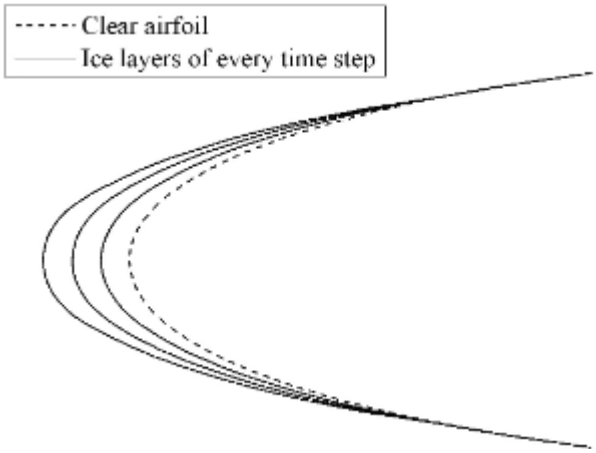

Figure 36: Rime ice with a MVD of 50 µm. Shows accumulation of rime ice on airfoil in 0° AoA after 60, 120, 180 seconds (Cao, Zhang, & Sheridan, 2008).

The unlimited various ice structures, especially those of rime ice, are dependent on numerous variables (speed, temperature, LWC, AoA, MVD, type of cloud, technical reasons, and so forth). Because of the latter, it is impossible to make an accurate and comprehensive study of ice shapes related to a given flying condition (Airbus Industry, 2000).

However, there have been reported several icing accidents concerning cruising conditions (1982-2000, US). Statistically, 40 % of all accidents caused by airframe icing have correlated with the in-phase flight (0-3° AoA). Moreover, 50% was fatal (Petty & Floyd, 2004).

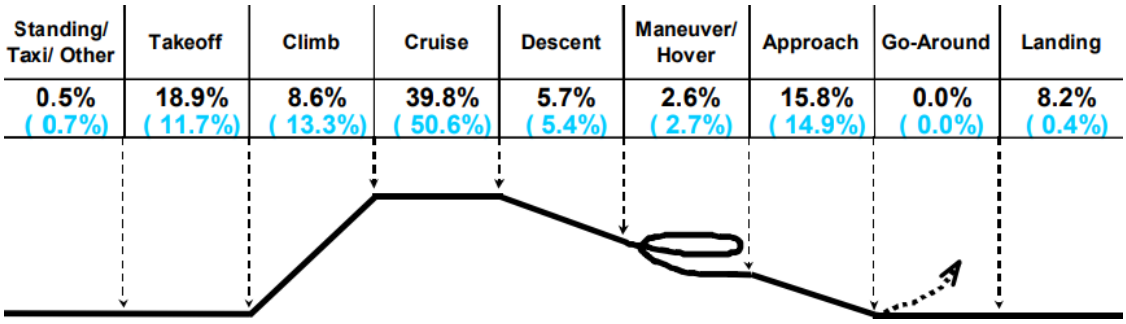

Figure 37: Percentage of accidents represented in blue color and fatal accidents represented in black writing (Petty & Floyd, 2004).

Figure 37 displays that under cruising conditions, the risk of icing accidents is much higher than in other flight phases. According to Aopa Air Safety Foundation (2008), only about 0.33 mm ice thickness on airfoils is enough to reduce the lift by 30% with an increased drag by 40%. However, NASA (1984) researched the effects of rime ice compared to glaze ice on two different flights. They found that even though one of the flights encountered rime ice 77%

longer than the glazed plane, the drag was only 1/3 compared to the flight with glazed ice. Despite research done in severe rime ice conditions (Lynch & Khodadoust, 2001), ice accretion was twice as much compared to glaze conditions. Nevertheless, drag reduction was only 15% compared to 47% and 62% drag decrease in glazed conditions. The aerodynamic penalties are less critical for rime ice due to the low accretion rate but may become hazardous after prolonged exposure since rime ice may be viewed as a function of time (Zhang, Wu, & Min, 2017).

3.1.2 Glaze ice

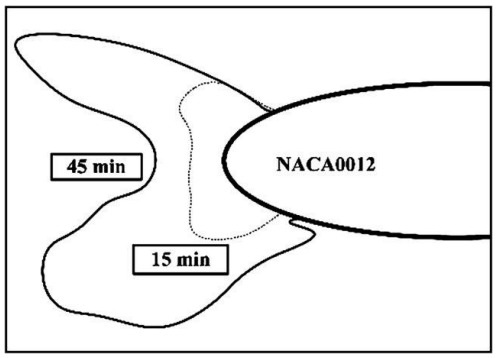

Figure 38: Typical shape of an airfoil with glaze ice. After more prolonged exposure, it forms as a horn (Cao, Wenyuan & Wu, 2018).

Glaze ice is a more severe type of icing not only because it is difficult to spot, but because it tends to form as a horn near the leading edge of the wings (figure 38). This poses a more substantial obstruction for the air to flow evenly above the airfoil Federal Aviation Administration & National Weather Service (2016).

According to Cao et al. (2008), glazed ice accretions have a much higher degradation rate on the airfoils aerodynamic performance compared to rime ice. Moreover, SLD and runback ice's consequences (towards the trailing edge) just aft of the Ice Protection System (IPS) surfaces may result in about 80% reduction in C_{Lmax} (Lynch & Khodadoust, 2001). According to Cao, Wenyuan & Wu (2018), the proportional drag coefficient (C_D) can increase by 300% under glaze ice conditions.

Nasa (2008) collected incident and accident data from NTSB and FAA in the span from 1988-2003, considering the US. Icing-related incidents sorted by flight phase indicated that most of the occurrences happened in cruising altitude, table 3.

Table 3: Most of the icing accidents in the US was caused in an in-flight phase (NASA, 2008).

Flight Phase	Number of Incidents
Climb-out	98
Cruise	325
Descent	193
Ground	106
Landing	133

Although the current evaluation of structural ice is based on prediction, the current evaluation indicates that icing significantly impacts the phase of cruising. Since rime ice is a minor risk factor compared to glaze ice, one could conclude by assuming that glaze ice has a more significant impact because of the adverse aerodynamic effects.

3.1.3 Mixed Ice

Mixed ice tends to form like glaze ice, except the distinct hollowing in the middle, as seen in figure 39.

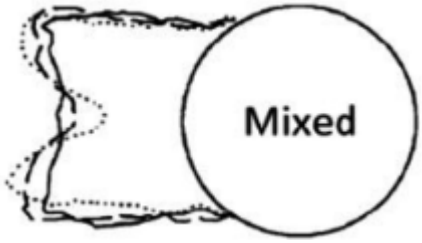

Figure 39: Mixed ice shape on the leading edge of the airfoil (Han, 2011).

As explained in subchapter 4.1.3, mixed ice is a combination of rime ice and glaze ice formed from SWD of various droplet sizes. It mainly affects the take-off and initial climb phase. However, since it occurs below the flight level, it may become hazardous also under descent (Baumert, Bansmer, Trontin, & Villedieu, 2018). Lynch & Khodadoust (2001) compared glaze ice to mixed ice in a wind tunnel and found that the drag penalty for glaze ice conditions was twice as much as mixed ice (75% versus 31% and 38%), even though the amount of mixed ice

was 50% greater than glaze ice. For a single wing, the drag penalty for glaze ice was six times as much as mixed ice.

3.1.4 Frost

The aerodynamic functions of the aircraft may not be severely affected by frost. However, the contours and size of the frost could pose a potential hazard for ice to distort and slow down the airflow over an exposed wing area, especially when the aircraft is climbing in altitude (Oxford Aviation Academy, 2010). The following claim is sustained by an accident report from 2002:

"On January 4, 2002, a Canadair Challenger—a small jet—was taking off from Birmingham, England [...]. Immediately after liftoff, the aircraft started to bank rapidly to the left, and two seconds after liftoff the bank angle had reached 50 degrees. [...] "The left winglet contacted the runway shoulder, the outboard part of the left wing detached and the aircraft struck the ground inverted, structurally separating the forward fuselage, which caught fire. The crash killed the jet's two pilots and all three passengers aboard" (AOPA, 2016).

As described in the report from the Aircraft Investigation Branch (2004), the jet almost rolled upside down right before the initial crash. It confirms that the left-wing was accumulating frost more rapidly compared to the right-wing, which reduced its lifting capacity and increased the stall speed tremendously.

A substantial and dense layer of frost may affect the lift characteristics of the wing by reducing $C_{L_{max}}$. Furthermore, it will lead to an increase in the risk of stall speed by 5-10 % (AOPA, 2019; Hoth, 2012; Skybrary, 2019b). Also, considering that frost is a discrete ice type and difficult to notice for pilots (Federal Aviation Administration & National Weather Service, 1975). If one considers a more fundamental approach in assessing the risk factor, it would be relevant to think of an approximate reduction in the probability variable according to detecting the danger in time, as described by Hoth (2012).

To summarize the effects, frost is both challenging to notice and possesses greater danger in larger quantities, especially during climbing. In-flight, frost represents an equal threat if not noticed in time. According to Oxford Aviation Academy (2010), frost accumulation during

descent does not constitute a significant hazard compared to other types of icing. The Civil Aviation Authority (2000) states that controlled descents will help eliminate the accumulation of frost.

3.1.5 Thermal de-icing

According to the Aircraft Investigation Branch (2004), the wings had not been checked of frost, making the left-wing accumulate a substantial amount of frost. The frost's contour and irregularity reduced the angle of attack, while the stall warning system had stopped functioning. Even though both the pilots confirmed the use of thermal anti-icing, the plane stalled almost immediately after take-off. As mentioned by Alizadeh et al. (2013) and ICAO (2000), electric thermal heating systems may not have a substantial effect of removing already existing frost and can decrease flight operating efficiency. Due to the aircraft design, there are limited numbers of generators to produce enough wattage to maintain an ideal surface temperature of 38°C – 54°C (Vertuccio, De Santis, Pantani, Lafdi, & Guadagno, 2019). The reduced wattage is also consistent with Baumert, Bansmer, Trontin, & Villedieu (2018), who investigated an airfoil of type NACA 0012, in mixed clouds. They found that the thermal flux[9] only generated 0.31 W/m^2, which is far too low to create a significant melting process of the ice accretion. There are different liquid-based thermal systems; however, they possess a delay before heat is transferred to the outer surface of the airfoil (Pourbagian, Talgorn, Habashi, Kokkolaras, & Le Digabel, 2015). It is, therefore, essential that the thermal system is activated before entering icing conditions. Active ice protection systems (IPS) are nevertheless the most effective method to actively remove ice in the aviation industry, yet the system exhibits weaknesses and is dependent on the pilots both observing the danger in time and actively activating the system before entering icing conditions (NTSB, 2008). All these parameters affect the reliability of the system.

As mentioned at the outset, aviation is one of the most complex industries concerning safety. If this is seen according to Perrow's (1999) system focus, thermal systems can be dependent on three parameters: (1) Timing. (2) Pilots' risk perception and (3) system reliability. Compared

[9] Thermal flux/heat flux is the amount of heat energy passing through a particular surface (Cochrane, Hertleer, & Schwarz-Pfeiffer, 2016).

to Reasons' (1997) Swiss cheese model, the right conditions were in place for the weaknesses of each barrier to run parallel to each other and cause the accident. On the other hand, these redundancy applications can make the system even more complex and counterproductive, and instead increase the risk of accidents (Perrow, 1999). AOPA (2010), FAA (2014), and Lester (1995) also claim that under particularly severe icing conditions, current anti-icing and de-icing systems may not be sufficient to reduce a potential hazard. In aviation, where safety is a decisive factor, developing a more reliable solution would have to be fundamental to eliminating current problems in frost and icing conditions. Thermal solutions still are not as effective as desired, and often supported with de-icing chemicals.

3.1.6 Icing hazard assessment

Flight phase

Based on Ryerson (2011), a combination of risk matrix and cross-tabulation (table 1) was developed to assess and summarize the icing severity in different phases of flight. The different ice types are determined by the degree of impact on the aircraft's aerodynamics, while the flight phase is ranked based on which phase of flight the specific ice types are most likely to occur. For example: Compared to rime ice, glaze ice has a more significant impact on aerodynamic performance in the final approach (e.g., increased stall speed when reducing the speed, precipitated area, holdover time, etc.).

Table 4: ice impact on aerodynamics by flight phase. Black square denotes that frost is not included in these specific phases of flight.

	Flight phase probability rating	Glaze	Mixed	Rime	Frost
Ice type hazard rating		**10**	**8**	**7**	**5**
Cruising altitude	**10**	100	80	70	
Initial approach	**8**	80	64	56	
Initial climb	**7**	70	49	49	35
Take-off	**7**	70	56	49	35
Final approach	**6**	60	48	42	30
Landing	**3**	30	24	21	15
Climb (flaps up)	**3**	30	24	21	15
Taxi/Hold/De-icing	**1**	10	8	7	5

In the assessment of flight phases, it is also taken into consideration that de-icing fluids have a limited holdover time[10], regardless of the type of fluid applied, which increases the probability rate after the de-icing phase.

Components

In order to simulate the severe impact of structural ice, it is essential to understand the characteristics that influence the aerodynamic effects. The most crucial factor for assessing and simulating structural icing is to identify the amount of SWD water content, temperature, and MVD of the droplets. Various characteristics: Size, shape, amount, and roughness of the ice type, are dependent on environmental circumstances, such as flight conditions, aircraft design, the time spent in icing, and the specific component being exposed (NASA, 2008b).

To determine the necessity of de-icing equipment on airplanes, Heinrich et al., (1993) claimed that all aircraft could be examined with the following questions under icing conditions:

1. Will ice accumulate, and to what extent?
2. Will the ice accretion influence the component's function?
3. If the component is affected, will it influence the safe flight?
4. Will the downstream components have a substantial impact on ice accumulation?

Based on the evaluation done by both Vukits (2002) and Heinrich et al., (1993), it will be reasonable to claim that any severe structured ice can impair that specific component to the extent that the aerodynamic effects will no longer function. To simplify the questions into one fundamental question: **"Which individual components of the system can be removed during continuous flight and still sustain the aerodynamic functionalities?".**

One of the central answers to this question was the aerodynamic effect it caused on surfaces, especially the wings (Heinrich et al., 1993). Vukits (2002) categorized several aircraft components by minor, moderate, and significant risk under icing conditions. The assessment made was similar to Heinrich's conclusion. One of the individual major risk factors was "Lifting or control surfaces leading edges - Reduction in aircraft stability and/or control."

[10] Estimated time for how long a specific de-icing fluid protects against icing.

To follow up on the alleged theory, one wants to further analyze the wing's aerodynamic functionality under glaze ice conditions.

3.2 Aerodynamic CFD-analysis

A Computational Fluid Dynamics (CFD) analysis has been carried out using Ansys Fluent. Because of previous findings related to various icing occurrences in the in-phase flight, the CFD analysis examines the wing structure of airliner Airbus A320neo, in cruising conditions at 0° AoA. The simulation compares the aerodynamic performance, with and without structural ice. The following model has been chosen since the A320neo will replace the current Boeing 737-800 from 2020-2023, incorporating many countries, including several Norwegian domestic and international routes.

3.2.1 Introduction

A Computation fluid dynamics simulation is conducted on an Airbus A320 Neo wing to calculate the drag and lift forces produced when the airplane is cruising at an altitude of 35000ft. The temperature is set to -55°C, which is common at this altitude. The surface temperature of 0°C has been used to replicate the most favorable conditions for SWD to accumulate.

The analysis provides necessary data to analyze the aerodynamics of the airbus wing. The variation in the temperature due to the ice formation on the wing was also simulated. It was carried out to examine how the temperature varies due to the airflow over the wing.

3.2.2 Setup

There is a possibility to use both ICING Fluent and FENSAP-ICE to simulate ice on the wing. In this case, ICING FLUENT was used, although both workbenches are equivalent.

The solution obtained from the steady-state simulation was combined with the airflow in "Icing Fluent" before droplets, and glaze ice was simulated on the wing surface.

After simulating the ice, the "displaced grid fluent" option was used to modify the mesh without the winglet or "sharklet." The removal of the sharklet was done since the geometry gave an unknown error with ice accretion. Figure 40 displays the workflow in Ansys.

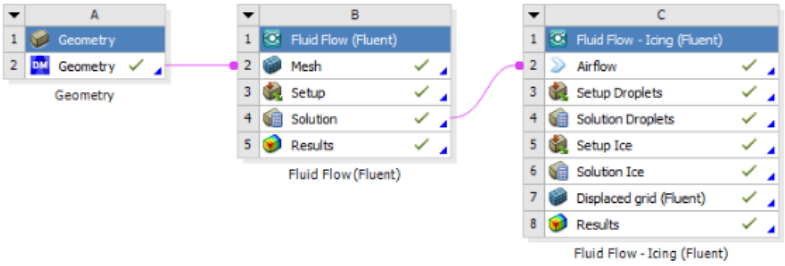

Figure 40: Workflow in Ansys.

3.2.3 Material properties

Table 5: Material properties.

Sr. No.	Property	Value
	Altitude	35000ft
	Mean Molecular Weight	28.9644 kg/kmol
	Kinetic Temperature	218.9242 K
	Molecular Temperature	218.9242 K
	Pressure	23909 Pa
	Density	0.38046 kg/m^3
	Speed of Sound	296.6141 m/s
	Dynamic Viscosity	0.000014341
	Kinematic Viscosity	0.000037694
	Coefficient of Thermal Conductivity	0.019696

3.2.4 Mesh data

Table 6: Nodes and elements.

Domain	Nodes	Elements
Fluid-domain	129.507	718.689
Plane Wing	118.639	660.109
All Domains	248.146	1.378.798

3.2.5 Procedure

The simulation study of the wing was done in three parts:

- Preprocessing
- Solution
- Post-processing

3.2.6 Pre-processing

The pre-processing part includes the 3d model development, domain modeling and meshing. The 3d model of the Airbus A320 Neo was obtained from and online source (Shaylesh, 2020). The wing part was extracted from it and simplified by removing unnecessary features such as surface features before it was transformed into a solid body.

Figure 41: Airbus A320neo (Adapted from Shaylesh, 2020).

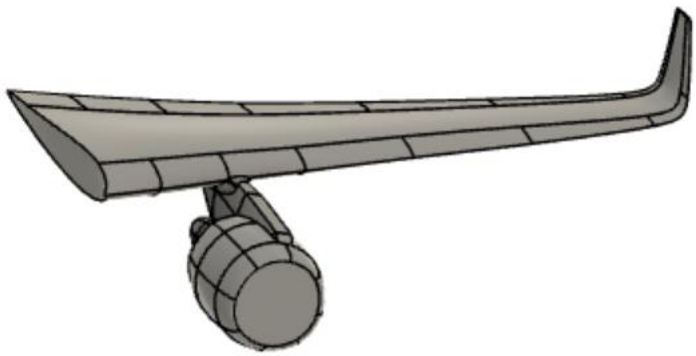

Figure 42: (Extracted wing part).

After the 3d model was complete, an enclosure was created around the plane wing to represent the fluid volume, (figure 42).

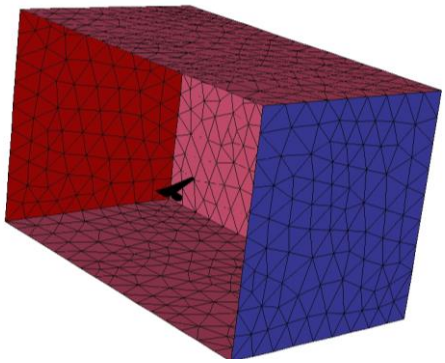

Figure 44: Enclosure.

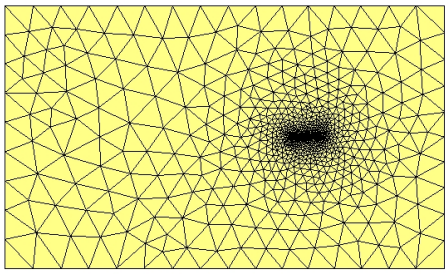

Figure 43: Mesh.

After the creation of fluid volume, a mesh was created, which is the discretization of the whole 3d model into small elements, (figure 43-44).

3.2.7 Solution

In the solution part of the analysis, the boundary conditions are applied:

Inlet Velocity: 257m/s

Wing Area: 122,6 m^2

Wingspan: 35,81 m

Wing surface temperature: 0°C

Air temperature: -55°C

Analysis settings: Pressure based

Gravity: On

Energy Equation: On

Flow model: K-epsilon 2 equation-Realizable-Enhanced wall Treatment

Wing area and wingspan were retrieved from Airbus (n.d).

3.2.8 Post Processing

The following images show the results obtained from CFD analysis. The velocity, pressure, and temperature are based on the Navier-Strokes equation (Zhang, 2019); to determine the airflow around the wing structures.

Figures 45-46 illustrates the pressure and velocity at different cross-section 1:

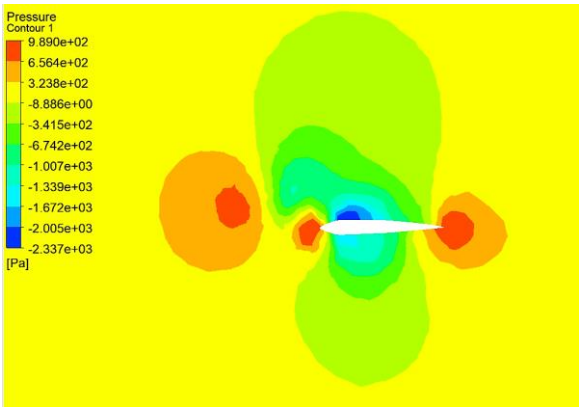

Figure 45: Pressure at cross section 1.

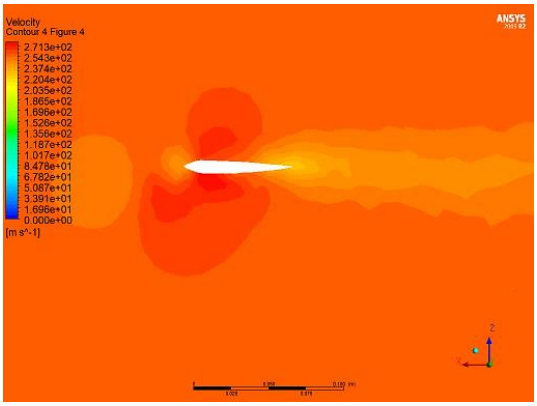

Figure 46: Velocity at cross section 1.

The cross-section of the wing profile is an airfoil shape. Figure 45 and figure 46 displays the velocity around the wings structure. It is evident by the red contours that the air on the upper surface has a higher velocity compared to the leading and trailing edge of the airfoil, a factor for creating lift. (The reason for the increased velocity underneath the wing surface is merely a result of the thrust). It indicates that the pressure at the wing's upper side is lower than the pressure underneath the wing, which, combined with the velocity, produces lift (Johnson, 1998).

Note: Additional pictures are available in appendix B.

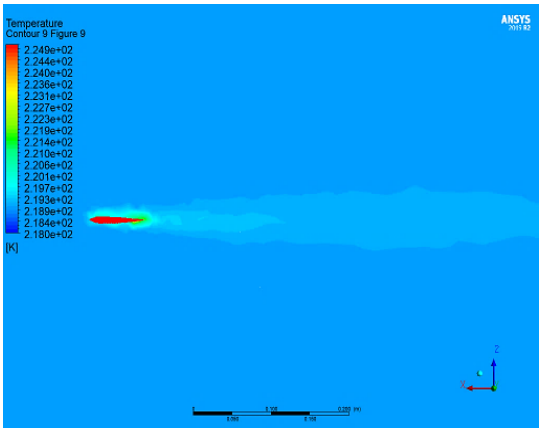

Figure 47: Temperature at cross section 1.

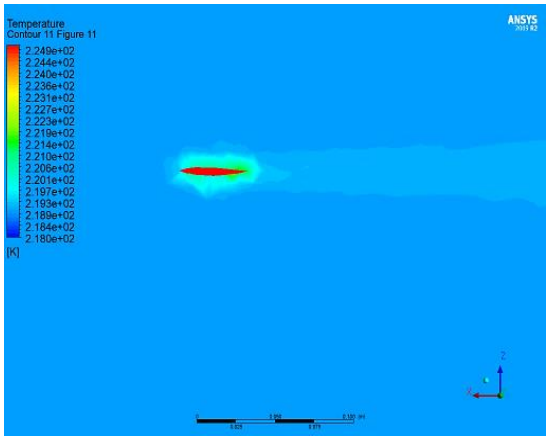

Figure 48:Temperature at cross section 3.

Figure 47-48 shows the local change in temperature of the air as it flows over the wing surface at different cross-sections.

Since cold air is denser than warmer air, one will usually be able to detect an increase in aerodynamic performance, as low temperatures are not a dependent factor in affecting the aerodynamics. The obstruction usually correlates with the structural ice and the change of shape in the wing's airfoil.

Note: The temperature applied on the wing surface is 273K. The air velocity and flow rate are very high, and the far-field average temperature is constant at 218K. Therefore, to capture the small temperature change as compared to the overall temperature of the airflow, the maximum and minimum values were user-specified to obtain these results.

3.2.9 Ice condition contours

Table 7: Ice property.

Output parameters	
Total mass of ice - Kg	2.334

Table 7 shows the mass of ice applied to the wing in kg. The ice simulation was carried out for 100 seconds.

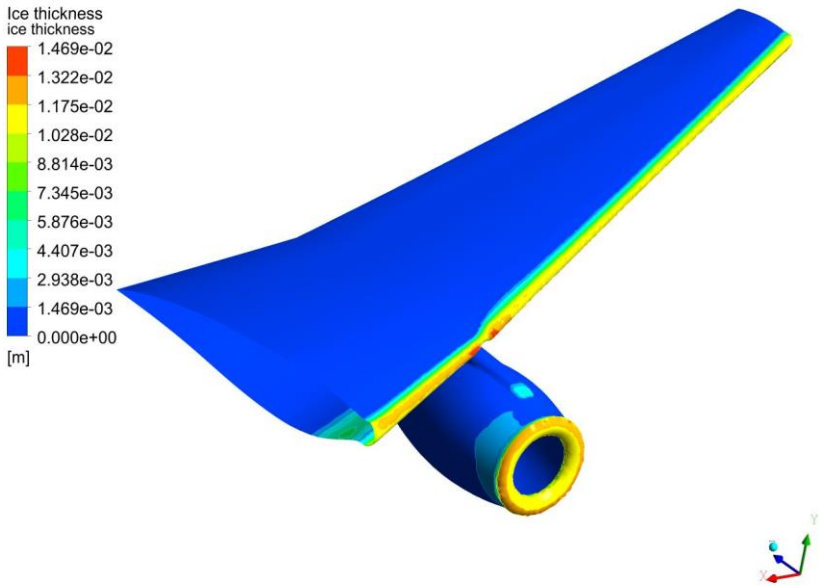

Figure 49: Ice thickness contour (isometric view).

Figure 49 shows the ice thickness contour from an isometric view with glaze ice accretions, after 100 seconds.

Figure 50: Glaze ice on the wing surface (isometric view).

Figure 50 illustrates the ice thickness from an isometric view with glaze ice accretions, after 100 seconds.

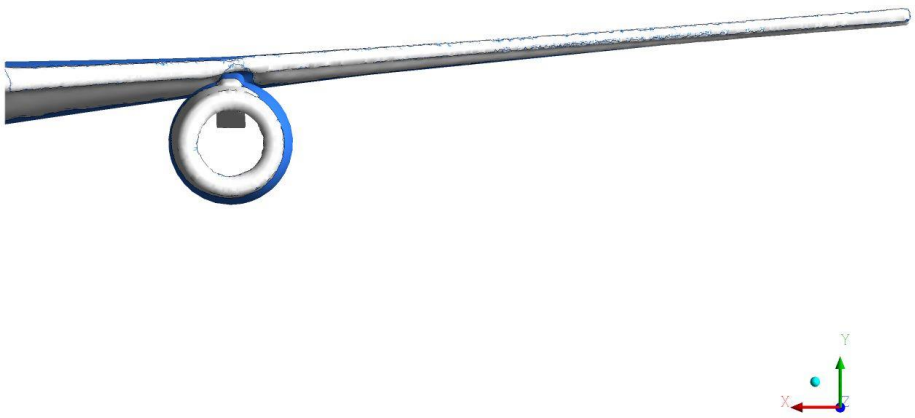

Figure 51: Glaze ice on the wing surface (front view).

Figure 51 illustrates the ice thickness from a front angle with glaze ice accretions, after 100 seconds.

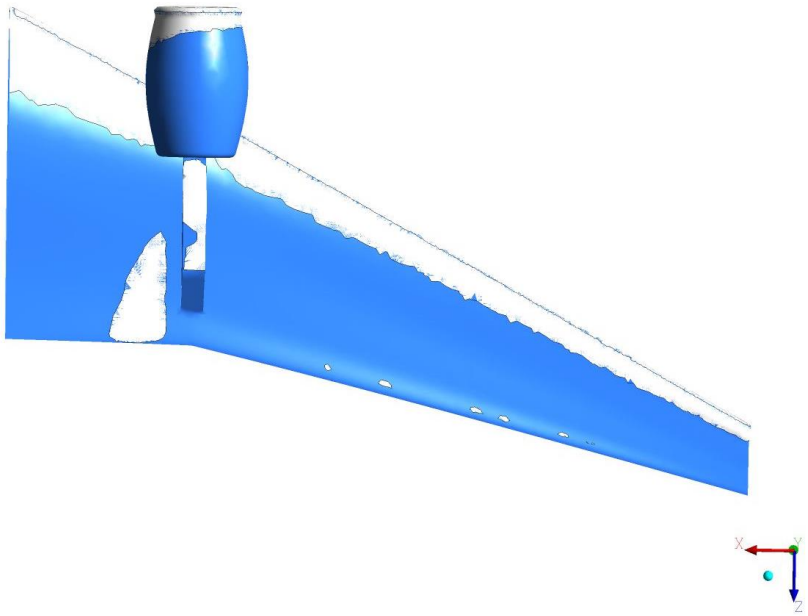

Figure 52: Glaze ice on the wing surface (bottom view).

Figure 52 illustrates the ice thickness from underneath with glaze ice accretions, after 100 seconds.

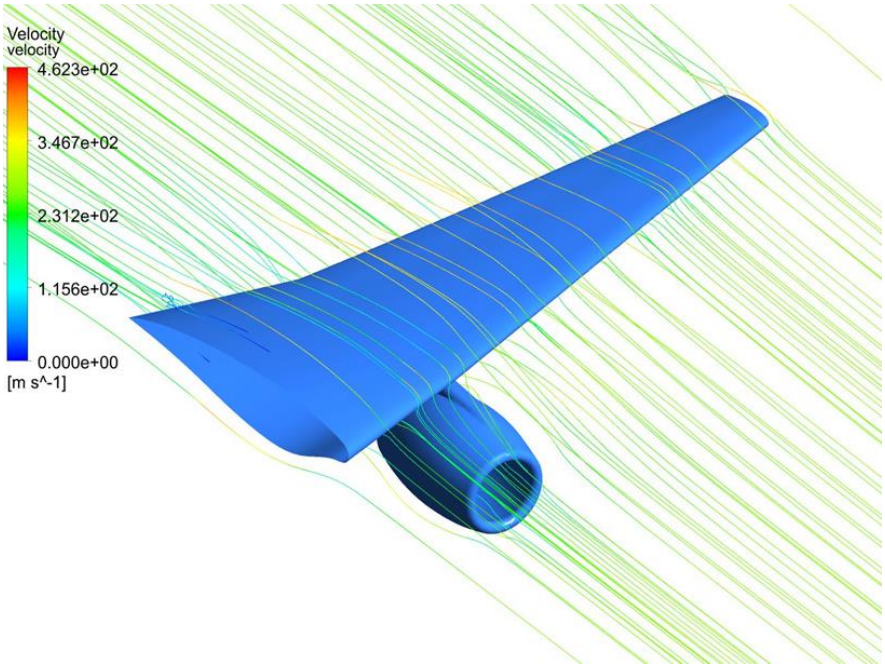

Figure 53: Velocity streamlines without glaze ice (isometric view).

Figure 53 illustrates the streamlines from an isometric view without glaze ice. These streamlines show the path followed by different particles of air over the wing.

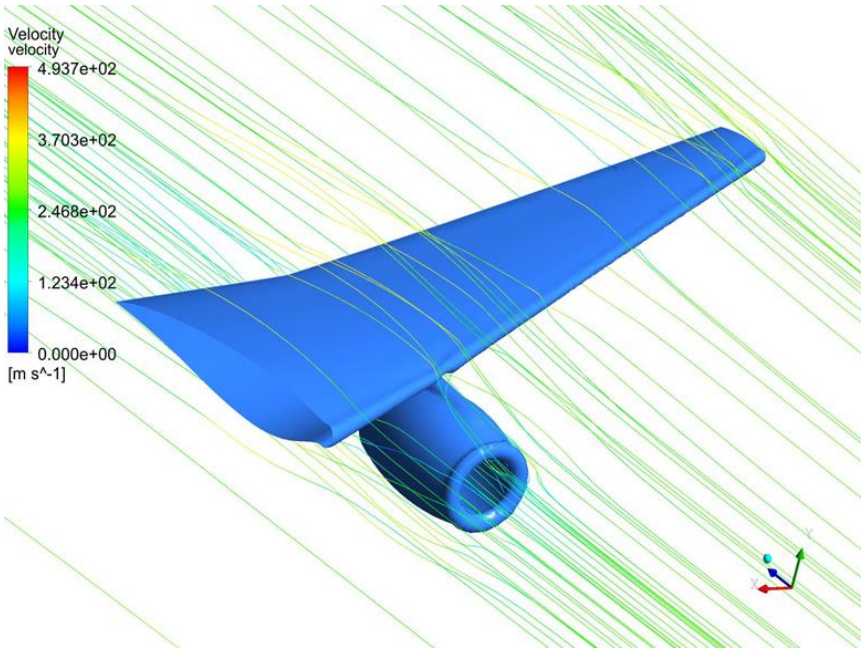

Figure 54: Velocity streamlines with glaze ice (isometric view).

Figure 54 illustrates the streamlines from an isometric view with glaze ice accumulations, after 100 seconds. These streamlines show the path followed by different particles of air over the wing.

Figure 55: Velocity streamlines without glaze ice (front view).

Figure 55 illustrates the streamlines from a front view without glaze ice. These streamlines show the path followed by different particles of air over the wing.

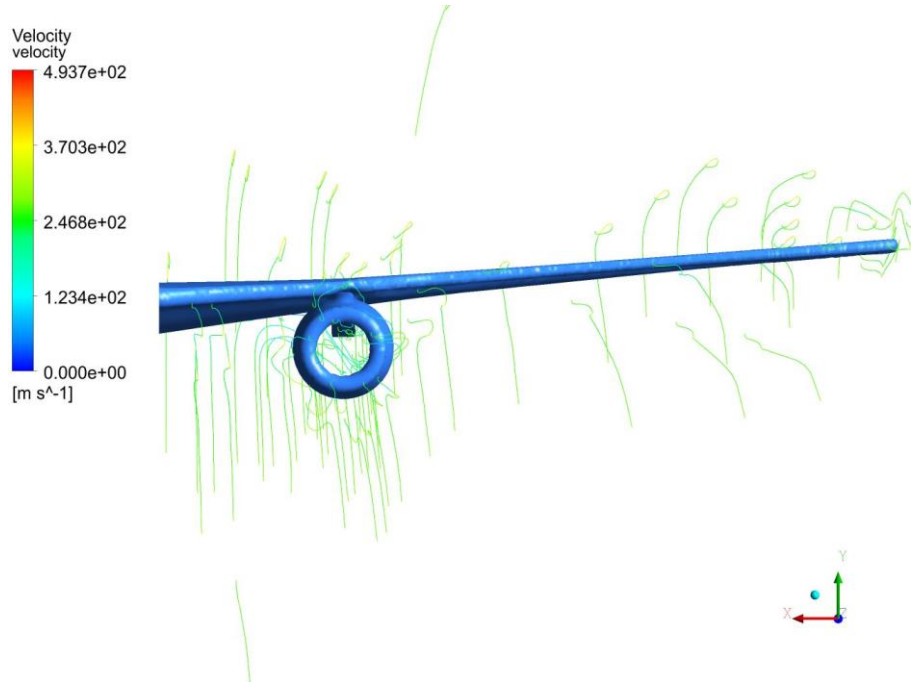

Figure 56: Velocity streamlines with glaze ice (front view).

Figure 56 illustrates the streamlines from a front view with glaze ice accumulations, after 100 seconds. These streamlines show the path followed by different particles of air over the wing.

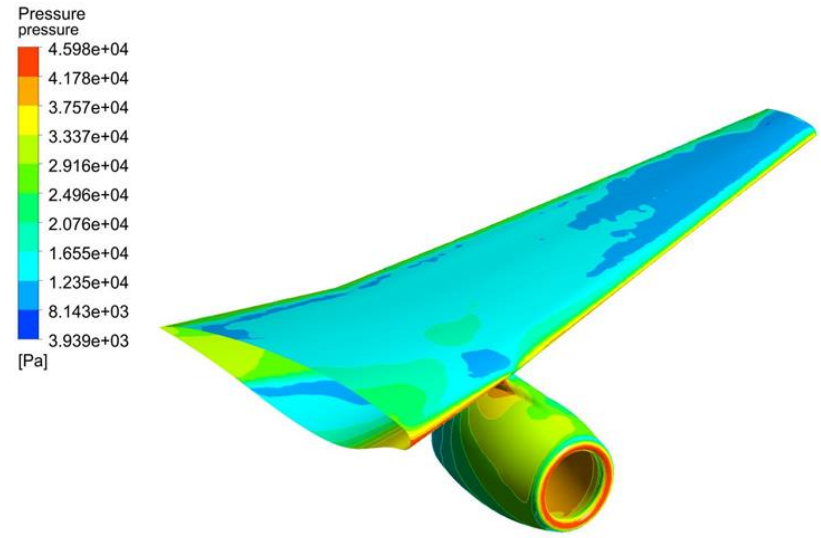

Figure 57: Pressure on the wing surface without glaze ice (isometric view).

Figure 57 shows the pressure contour from an isometric view without glaze ice.

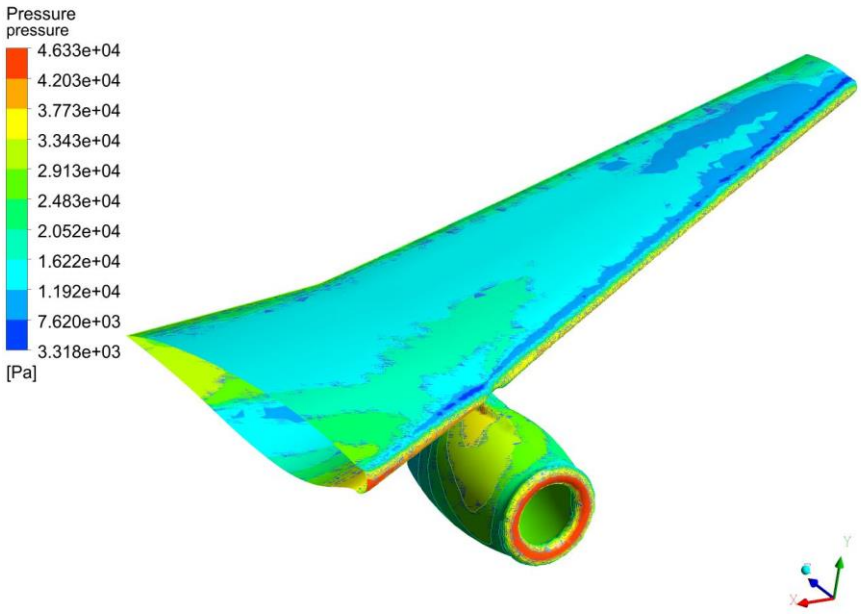

Figure 58: Pressure on the wing surface with glaze ice (isometric view).

Figure 58 shows the pressure contour from an isometric view with glaze ice accumulations, after 100 seconds.

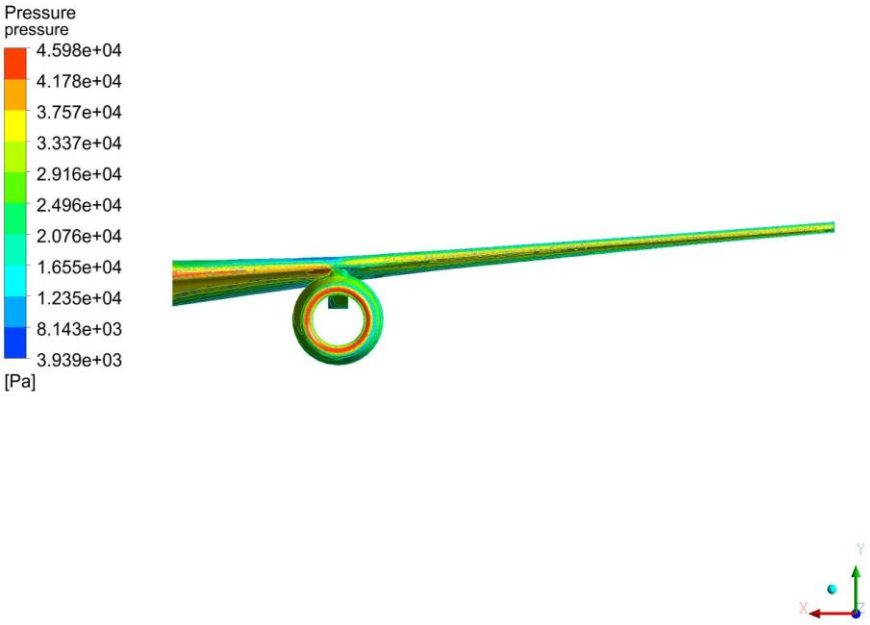

Figure 59: Pressure contour without glaze ice (front view).

Figure 59 shows the pressure contour from a front view without glaze ice accretions.

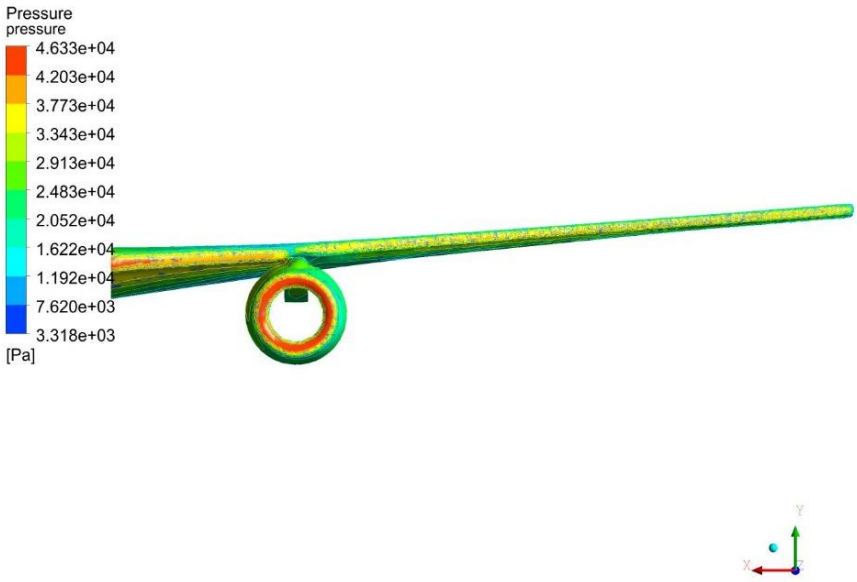

Figure 60: Pressure contour with glaze ice (front view).

Figure 60 shows the pressure contour from a front view with glaze ice accumulations, after 100 seconds.

Note: Additional illustrations are available in appendix B.

3.2.10 Lift and drag

The coefficient of lift was calculated using the lift coefficient formula [3.2]:

Without ice:

$$C_L = \frac{2L}{\rho \times v^2 \times A} = \frac{2 \times 7789{,}42}{0{,}98046 \times 257^2 \times 122{,}6} \approx 0{,}00506 = \underline{0{,}0051}$$

With ice:

$$C_L = \frac{2L}{\rho \times v^2 \times A} = \frac{2 \times 7777{,}85}{0{,}98046 \times 257^2 \times 122{,}6} \approx 0{,}00505 = \underline{0{,}0051}$$

The coefficient of drag was calculated using the drag coefficient formula [3.3].

Without ice:

$$C_d = \frac{D}{p \times \frac{V^2}{2}} = \frac{2138{,}49}{0{,}98046 \times \frac{257^2}{2}} = \underline{0{,}066}$$

With ice:

$$C_d = \frac{D}{p \times \frac{V^2}{2}} = \frac{2490{,}94}{0{,}98046 \times \frac{257^2}{2}} \approx 0{,}0769 = \underline{0{,}077}$$

Table 8: Lift and drag forces were obtained from Ansys.

Conditions	Lift (N)	Drag (N)	
Ice Conditions	7777.85	2490.94	
No Ice Conditions	7789.42	2138.49	

The lift coefficient obtained was 0,0051 without ice accretion and the lift force 2139N. The lift coefficient due to ice accretion was 0,0051, and the lift force 2491N. The results imply that the ice accretions reduced the airfoil lift by 11,57N, which is a total reduction of barely 0,15% lift force.

The drag coefficient obtained was 0,066 without ice accretion and the drag force 2139N. The drag force due to ice accretion was 2491N. The results imply that the ice accretions increased the airfoil drag by 352.45N, which is a total reduction of 17% drag force.

3.2.11 Results

Glaze ice accumulates at a very high rate. After 100 seconds of simulation, the total mass of accreted ice was around 2.3kg. Under glazed ice, airflow's primary obstruction correlates with the structural reformation in the airfoil, as the change in velocity streamlines and pressure is evident. The aerodynamic impairment resulted in an approximately 17% increment in airfoil drag, while the wing lift was almost unaffected with a decrement of 0,15%. The relationship between the velocity and pressure in glazed conditions indicates that a constant AoA of 0° will have a prominent increment in the drag coefficient (C_D). Simultaneously, the lift coefficient (C_L) is close to stagnant in both conditions at 0° AoA.

The results only show a prediction since the simulation is assessed on a single wing. The winglet that was omitted from the simulation may influence lift and drag variables. Other uncertainty factors, such as SWD water content, temperature, MVD of the droplets, size, shape, amount, and roughness of the ice type, are dependent on various environmental circumstances.

3.3 Landscape Assessment

Based on published research, the following chapter will attempt to approximate a hydrophobic coating that may be suitable for further research and testing.

3.3.1 Purpose

The purpose of this "landscape assessment" is:

- To investigate the known methods for creating icephobic coatings/surfaces.
- To identify among the latter the most promising for commercial implementation.
- To give a technical assessment and recommendations for further development.

3.3.2 Icephobic coatings

According to Wong et al. (2011), the following icephobic coatings are most actively studied:

- Coatings having a structure which mimics the surface microstructure of water repellent plants (such as Lotus leaves),
- Coatings with a nanostructure with a lubricating fluid locked to it, like mechanisms shown by certain pitcher plants (the Nepenthes pitcher plant structure).

Measurements of ice adhesion have shown that polymers with elastic properties, such as rubber, tend to have lower ice adhesion than thermoplastics[11]. The lower ice adhesion is due to their viscoelasticity, allowing for slippage and initiation of cracks in the ice. Most of these polymers are attractive substances because of their low ice adhesion, and the scale on which they are produced makes them inexpensive. The two polymer types which have regularly performed better than all others (without modification) are fluorinated organic polymers, and polyorganosiloxanes (silicones).

[11] Plastic that becomes flexible at elevated temperature and solidifies/hardens upon cooling.

3.3.3 Silicone Based coatings

Susoff et al. (2013) studied the viscoelastic silicon rubber; coatings made up of polydimethylsiloxanes. He found that the silicon coating caused the reduction in ice adhesion strength about 100 times as compared to the bare aluminum. Researchers usually consider a high WCA and a low sliding angle (SA) to cause a reduction in the water adhesion strength/ice adhesion strength. Such as, Li et al. (2012) generated a modified composite coating based on polydimethylsiloxane (PDMS) to reduce ice formation on glass insulators. The superhydrophobic properties of the obtained coating had a WCA of about 161°, and significantly higher efficiency in reducing ice accumulation compared with a non-modified silicone coating (Li, Zhao, Hu, Shu & Shi, 2012).

By two steps, Mobarakeh, Jafari & Farzaneh (2013) used a plasma spray process (plasma polymerization) to develop a superhydrophobic surface with icephobic properties:

1. Anodization[12] of the aluminum surface.
2. Plasma polymerization of hexamethyldisiloxane (HMDSO) for application of functional group with low surface energy. The WCA found 158° and SA around 8° in the result of the coating on the anodized aluminum surface. On the application of the superhydrophobic film, they found a reduction in ice adhesion strength 3.5 times lower compared to an untreated aluminum surface.

Yang et al. (2015) designed a method to generate a superhydrophobic ZnO/PDMS composite coating using hydrophobized oxide[13] particles on an aluminum substrate. The resulting coating reduced the accumulation of ice within the temperature range of -5°C to -15°C. Additionally, the composite could withstand the repeated cycle of icing and de-icing and could revive itself.

Hong, Wang, Huang, & Liu (2019) designed a mechanically robust and self-cleaning icephobic coating. They combined the micro-scaled particles of poly-hexeafluorobisphenol A-co-cyclotriphosphazene (PHC) with adhesive PDMS. The result indicated high values of hydrophobicity: WCA about 164° and SA about 3.7° when they treat a surface with such combination of

[12] Surface treatment that improves protection against corrosion.

[13] Oxygen-compund with a higher electropositive element.

particles; they found exceptional mechanical durability against different types of stresses caused by the synergistic [14]effects of surface structures. They also found quite stable bonding between the PDMS and microparticles. The surface showed excellent water repellent and ice repellent properties at the lower temperature about -15°C, higher humidity of 70%, delayed formation of ice, and reduction in ice adhesion after the coating. This mechanism provides benefits from the flexibility of composite and microspheres of PHC and nanoscale structure of the PDMS. Furthermore, the process of preparation is suitable for different substrates and cost-effective so that it can be used for many applications, like aircraft components.

Several commercially available icephobic silicone coatings are already known. For example, AMES corporation offers a range of products. AMES uses proprietary materials such as silicone, fluorosilicone, fluoroelastomer, whether alone or in combination to provide erosion-resistant icephobic coatings for the aviation industry (Amescorp, n.d). Some NuSil brand silicone coatings are also icephobic. Watson et al. (2015) developed and patented an erosion-resistant anti-icing coating using NuSil R-2180 silicone composition. Susoff, Siegmann, Pfaffenroth & Hirayama (2013) estimate NuSil R-1009 silicone as a promising icephobic material. NuSil R-1009 is a silicone system that can be used by simple dip-coating (figure 61) from a solution of 50% by weight concentration in toluene.

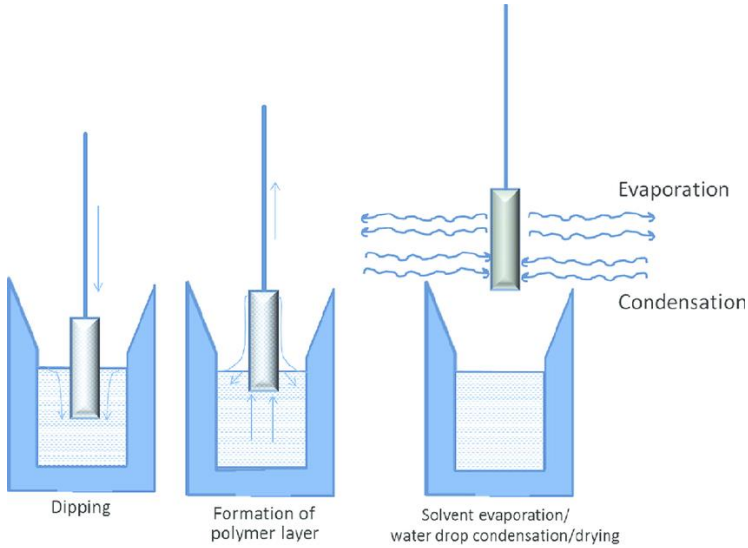

Figure 61: The process of dip-coating (Instras scientific, 2013).

[14] Interaction between substances that make the cooperative effects greater than each individual substance.

3.3.4 Fluoropolymer coatings

A fluoropolymer coating is quite suitable for the anti-icing materials because is it has extremely low surface energy, and due to this property, it may not adhere to water.

Yang et al. (2015) examined the characteristics of materials based on fluoropolymers. They found that Polytetrafluoroethylene (PTFE) with a flat and smooth surface has a low strength of ice adhesion at a specific temperature range. Although fluorinated coatings have a WCA up to 158°; at low temperatures, the surface structure leads to a significant increase in ice adhesion strength. In another study done by Susoff et al. (2013), they treated the aluminum substrate with perfluoropolyether (PFPE) by dip-coating (figure 46). Their results showed that a decrease of 20-folds had been observed in comparison to bare aluminum.

Another method was to prepare a polyvinylidene fluoride (PVDF) coating, where PVDF is dissolved in dimethylformamide (C_3H_7NO) before ammonium bicarbonate (NH_4CO_3) is dispersed in the resulting solution. The dispersion is applied to the substrate and dried at 80°C. At this temperature, the bicarbonate decomposes to gaseous products - forming a coating with a microstructure (Peng et al., 2012). The authors mentioned 156° for WCA while 2° sliding angle. When spraying supercooled drops of water onto the resulting surface at −10 °C, a very slight accumulation of ice was observed for 50 minutes compared to the bare sample.

In order to enhance the mechanical durability of the coating, PVDF porous structure can also be prepared as a composite system using nanoparticles (epoxy-siloxane modified SiO2 (Wang et al., 2011), fumed silicon dioxide (Basu & Paranthaman, 2009), or graphene (Zha et al., 2011). Zou et al. (2011) studied the ice adhesion strength's dependence on surface roughness and surface energy. By depositing a silicon-doped hydrocarbon film and fluorinated-carbon film on smooth and sandblasted aluminum surfaces, the coating could reduce the ice adhesion strength by over 50%. On the rough surface, due to sandblasting, they found a great increase in the WCA (Zou et al., 2011).

To obtain the advantages of three different polymers (fluoropolymers, silicones, and acrylates), Li, Zhao, Li & Yuan (2014) investigated the icephobic properties of several coatings based on Polymethyltrifluoropropylsiloxane (PMTFPS) block copolymers[15]. The research revealed that such copolymers are excellent candidates for use as an icephobic coating since they exhibit a synergistic effect from the combination of fluorine and silicone. Both a delay in the freezing process of 186 seconds at −15°C and a decrease in ice adhesion strength of 300 Kilo Pascals were observed. Cross-linked networks composed of hyperbranched fluoropolymers (HBFP) and polyethylene glycol (PEG) can delay the freezing process due to the complex structure (Zigmond et al., 2016). As in the case of silicones, particles of metals or oxides are used to give the necessary texture for coatings based on fluoropolymers. In one study, they examined treated aluminum plates with a suspension[16] of nanopowders. Even though the coating exhibited a reduction in ice adhesion up to 5.7 times after the first icing cycles, the coating loses required properties after several cycles of icing and de-icing due to the low mechanical durability of the obtained nano-texture of the surface (Farhadi, Farzaneh & Kulinich, 2011; Kulinich & Farzaneh, 2009). Wang, He & Tian (2012) applied a thin fluorocarbon coating on a substrate of copper in order to get the superhydrophobicity. A water droplet on a flat surface of copper achieved a WCA ~84°. However, the icing process of the superhydrophobic copper surface was initiated at around 220 seconds because of the reduction in the contact area of the water droplets. The time to notice an entirely ice accreted surface on the superhydrophobic copper surface was much higher as compared to the bare copper surface and showing the delay in ice formation.

3.3.5 Slippery Liquid-Infused Porous Surfaces (SLIPS)

There are two kinds of anti-wetting surfaces, one is lotus leaf surfaces (superhydrophobic surfaces), and the other is pitcher plant surfaces, Slippery Liquid-Infused Porous Surface (SLIPS). Icephobic surfaces are usually achieved by using the principle of a superhydrophobic surface inspired by the lotus leaf. However, due to the larger surface area under the conditions of high humidity, there is the disadvantage of water condensation, an increase in ice adhesion, and frost

[15] Polymers from one or several different monomers are called copolymers.

[16] A mixture of a finely distributed but insoluble solid in a liquid.

accretion. To avoid the challenges with superhydrophobic surfaces, they used characteristics of the pitcher plant surface to construct the anti-icing method, SLIPS (Bohn & Federle, 2004).

SLIPS is a potential alternative to superhydrophobic surfaces. There is quite a low contact angle hysteresis, which causes no pinning during the sliding down of condensed water droplets from the surface. Nguyen, Park, Jung & Lim, (2019) investigated the anti-icing ability of various types of lubricants that can penetrate aluminum surfaces. They found that the lubricants were not able to reduce the ice adhesion significantly. Nevertheless, they found another combination of infused lubricants and high-water repellency of porous surface that caused an effective reduction in the ice adhesion strength on SLIPS. Zhu et al. (2013) designed a coating based on silicon infused PDMS, caused a significant reduction in the ice adhesion on the surface. Zhang, Gu & Tu, (2017) developed a double-layered SLIPS on the magnesium alloy by the coating of double-hydroxide carbonate CHO_4^{-3} composite and an infused porous layer on the top, that infused porous layer was consist of 1H, 1H, 2H, 2H perfluorooctyltriethoxysilane (PTES) with infused PFPE-lubricant in the layer. The results indicated that the SLIPS reduced the corrosion and shown excellent anti-icing performance. Wong et al. (2011), inspired by a pitcher plant and invented SLIPS that was made up of penetrating the lubricating liquid in the surface, which formed a homogenous and smooth film on the surface. They developed two different kinds of porous surfaces and penetrated the perfluorinated lubricants in the pores and form a smooth and homogeneous surface with the roughness value of approximately 1nm. The resulted SLIPS showed less than 2.5° of contact angle hysteresis and repelled a series of different liquids like blood, crude oil, and water. At the temperature of -4 °C and humidity level of 45%, the SLIPS found with no signs of ice adhesion, and it has taken only milliseconds in order to fix the physical damage and keep the wettability. They also noticed that the infused lubricant inside the pores of the surface wasn't undisturbed at the pressure of 680 atm.

Kim et al. (2012), produced a SLIPS-coated aluminum surface that was quite efficient in reducing the ice accumulation and strength of ice adhesion. Kim at el. coated an organic polymer, namely polypyrrole (PPy), on the aluminum substrate by using the method of electrodeposition. It was transformed into a hydrophobic coating using chemical vapor deposition of trichlorosilane (tridecafluoro-1,1,2,2-tetrahydrooctyl), as shown in figure 55. Finally, SLIPS was fabricated by putting few perfluoroalkyl liquid drops on the coated aluminum substrates. The results indicated that the droplets of condensed water rolled off rapidly before the freezing, and

the accreted ice was detached under the action of gravity with a low angle of tilting. These materials held an ice adhesion strength of approximately 15KPa, and these materials were found quite useful in outdoor anti-icing applications.

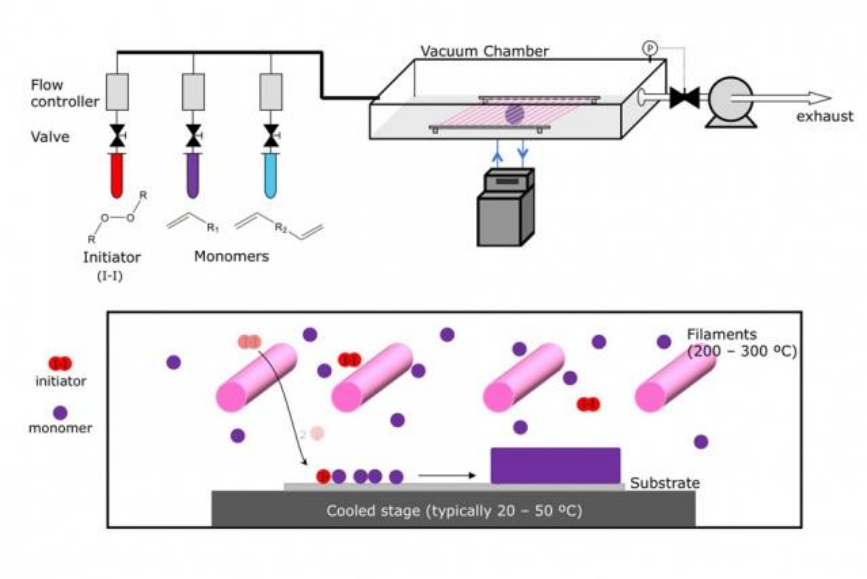

Figure 62: The Chemical vapor process (CVD): The monomers in the blue and purple cylinders are evaporated before entering the vacuum chamber where the surface is being coated. The initiator speeds up the process, making the monomers link up in chains to create polymers (Massachusetts Institute of Technology, 2015).

Wang et al. (2017), used the hot suspension of decahydronaphthalene and hydrophobic silicon dioxide polyethylene on different surfaces, including the aluminum and fabricated a stable superhydrophobic surface. These engineered surfaces indicated exceptional mechanical durability against corrosion, abrasion, and drop impact. However, at the temperature less than 0°C, the water droplets pinned on the engineered superhydrophobic surface, showing meager anti-icing ability. Thus, SLIPS was engineered by the penetration of various lubricant liquids in the pours structure of the superhydrophobic surface. At the temperature of -20°C, it is noticed that the water droplets smoothly slipped off the SLIPS, while at all other temperatures, the water droplets remained pinned on the superhydrophobic surface. They also made research and generated a superhydrophobic coating by spraying the fluorinated silicon dioxide on the surface, which demonstrated an excellent water repellent property.

Liu et al. (2018), performed experimentation in which they saturated fluorinated lubricants in the spin-coated PTFE film, as shown in figure 63. The result of their experiment showed admirable anti-icing property.

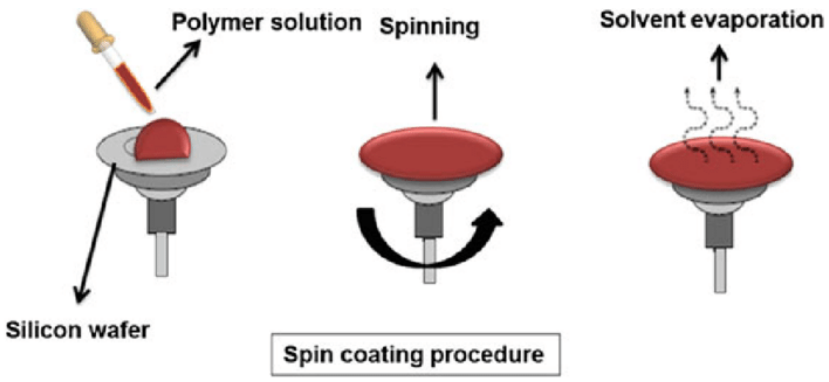

Figure 63: Spin-coating technique (Hosseini et al., 2015).

Cao et al. (2016), compared the wetting ability of pitcher plant based lubricant invaded surfaces and the lotus leaf based superhydrophobic surfaces. The silicon-based superhydrophobic (SUB) coating was made on the glass surface by dipping it in the homogenous suspension of hydrophobic fumed polydimethylsiloxane. This resulted in WCA approximately150° and SA around 4.3°. The silicon oil was absorbed on the SUB surface and resulted, liquid infused slippery (LIS) surface with the WCA around 96° and SA with an approximate of 7.8°. Both of the surfaces, SUB and LIS, have their advantages and disadvantage. On the requirement during different environmental conditions, suitable surface can be used.

In recent time, Zhang et al. (2018) used a low-priced lubrication liquid named as polyols, to invade in the pours structure of magnetic nanoparticles, results showed the capability of thermal de-icing. Wan et al. (2015) saturated a cross-linked polymer network by using the liquid paraffin (LP) and invented a type of anti-icing gel. The network of polymer holds the paraffin in the cross-linked network in order to keep safe during the removal of accrued ice. The swelled LP crossed-inked PDMS originate to show ultra-low strength of ice adhesion (1.7 ± 1.2 kPa) even under the temperature of −70°C. They experimented with 35 cycles of icing/de-icing and kept it exposed in an ambient environment; results showed the ice adhesion strength on the LP-

OG endures under the 10KPa. Overall results are showing that the LP-OG has an outstanding ability to anti-ice coating with good durability and ultra-low ice adhesion.

3.3.6 Icephobic coatings based on cross-link density and interfacial lubricant

Recently, many researchers have moved away from directly adding the hydrophobicity of a surface with its anti-icing properties. In this sense, the newer and more promising methods are described in the following approaches:

1. Preparation of coatings based on polymers with a low cross-link density.
2. Creation of structured systems with a chemically enclosed interfacial lubricant.

Using these approaches leads to partial mobility of the polymer chains inside the elastomeric matrix, which reduces the strength of ice adhesion. Previously, Golovin et al. (2016) studied a series of coatings from various elastomeric systems. For example, the use of PDMS with a low cross-link density made it possible to produce a coating with the ice adhesion of 33 kPa. Further, this parameter was even reduced to 6 kPa with the addition of the lubricants. In this work, much attention was paid to the study of the durability of the obtained system. Indicatively, the coatings did not lose their icephobic properties after a series of icing / de-icing cycles.
Moreover, new and better coatings can tolerate abrasion better in comparison with previously known materials. It was revealed that this approach could be applied to other polymer systems (polyurethane, fluorinated polyurethane, and perfluoropolyether), making it more promising for practical implementation. Gao et al. (2019) studied a similar approach. In their work, they developed new types of PDMS slippage coatings. They displayed an ultra-low ice shear strength, which remarkably enhanced the icephobic durability and abrasion resistance as well. The coatings combined a polyhedral oligomeric silsesquioxane (POSS) cross-linker with a PDMS elastomer matrix. This type of elastomer matrices displayed excellent durability and stability of icephobic with the ice share strength of 11.2 ± 2.7 KPa. They performed 50 cycles of icing/de-icing, and the results showed the value of ice shear strength below the 14 KPa. Besides, the implementation of POSS can prevent the waste of lubrication liquids and cause a significant impact on the abrasion resistance, which can be maintained the low ice shearing strength even after the 175 cycles of abrasion.

Beemer, Wang, & Kota (2016) developed an inexpensive, environmentally friendly, non-corrosive new PDMS gel that offers low adhesion to ice (about 5.2 kPa). It also showed exceptional mechanical durability even after the unlimited cycles of icing/de-icing and up to 1000 cycles abrasion with no significant alteration in the strength of ice adhesion. Zhuo et al. (2019) described another promising approach by using slide-ring materials[17], which are cross-linked molecular networks of polyrotaxane. It has been given much attention recently because of its mechanical characteristics. The architecture of slide-ring materials yields a low Young's modulus in comparison with the traditional cross-linked polymer in the same density. In addition to this, slide-ring material coatings display high abrasion resistance due to flexibility. Slide-ring materials with an effectively designed molecular structure can be served as a good candidate for durable anti-icing/de-icing applications. These sorts of characteristics cause an ultra-low strength of ice adhesion about 13 ± 1.3 kPa and excellent durability. The ice adhesion strength on the surface was sustained at an approximate value of 12 kPa during 20 cycles of icing/de-icing, with an increment to ~22 kPa after approximately 1000 cycles.

3.3.7 Technical considerations

Current aircraft ice mitigation strategies can include anti-icing equipment, which can be activated before encountering icing conditions. It is manufactured to avoid ice from forming, generally by maintaining above freezing point temperature. Such equipment may include electro-thermal heating systems and anti-icing systems that use hot compressed air from the compressor portion of the engine to avoid ice formation on critical components of the engine, such as air intakes and turbine guide vanes[18] (Pellissier, Habashi and Pueyo, 2011). The fluid system contains an organic liquid with a freezing temperature lower than water. It is also widely used on the aircraft surface to prevent icing and frost. Equipment is fabricated in order to remove ice as it starts to accrue on the airframe. For instance, pneumatic boot systems which expand on ice-exposed areas of the aircraft (ICAO, 2000).

The systems of electric thermal heating can decrease the efficiency of flight operation while fluids are only convenient for the shorter duration and can be harmful to the environment. The passive energy doesn't need the energy input to perform the function, so the passive approach

[17] Formed as a necklace of molecules consisting of three different materials. Also known as polyrotaxane.

[18] Number of blades within the turbine inlet that can adjust the flow rate through the turbine.

is more attractive. Regardless of the ongoing research to develop icephobic coating, there is no universal coating solution currently available to repel the formation of ice for various icing conditions, including the completely wetted state under the conditions of high-speed water droplet impingement and condensation from moist environments (Alizadeh et al., 2013). Since water in both liquid and ice forms has similar surface energy and surface tension, most researchers have suggested that coatings that repel liquid water should also be effective against ice. In this sense, superhydrophobic coatings with a microstructure like water-repellent plants seem to be a promising icephobic material.

In the laboratory, it is challenging to reproduce the exact conditions that the surface of an aircraft encounters during flight. Therefore, researchers must test superhydrophobic coatings at temperature, speed, and humidity quite different from the actual operating conditions. Nevertheless, already in 1987, a work was published where the details of ice formation under various conditions were studied in the Icing Research Tunnel at the NASA Lewis Research Center (Scavuzzo & Chu, 1987). The authors revealed a direct dependency between the droplet impact momentum (droplet size and wind velocity) and the ice adhesion strength. In the same work, it was determined that surface roughness could seriously affect the increase in adhesion. Yeong et al. obtained similar results (2017), they tested several superhydrophobic coatings under conditions sufficiently close to the conditions of ice formation during the aircraft flight (airspeed of 50 m/s and 70 m/s while the air temperatures of -5°C and -15°C). Their tests showed that the water-repellent characteristics of the coating do not necessarily provide low ice adhesion in the aviation industry. Whenever a water droplet would impact velocities, the strength of ice adhesion to a superhydrophobic surface also increases. When developing coatings for the aviation industry, it is crucial to test under conditions as close to practice. The results of the above studies indicate that micro-textured superhydrophobic surfaces can not only be ineffective but even complicate the problem in conditions of frost formation. It is known that as earlier as a minimal ice layer forms on the coating, the surface becomes hydrophilic. Therefore, the property of a surface to repel ice depends not only on the properties and characteristics of the surface itself but also on the conditions under which ice formation occurs.

Varanasi & Deng (2010) studied ice nucleation on a superhydrophobic surface in real-time. They fabricated a series of hydrophobic silicon posts and coated them with a thin hydrophobic layer of trichlorosilane. Then they gradually increased the humidity in the test chamber at lower temperatures. The results showed that ice forms in each part of the surface without any partiality, which caused the loss of superhydrophobic properties. Moreover, the textured surface's high contact area causes more strength of ice adhesion as compared with a smooth surface (Varanasi, Deng, Smith, Hsu, & Bhate, 2010). Thus, under different icing conditions, if the surface has not been specially designed to prevent frost formation, superhydrophobicity cannot be a direct indicator of icephobicity. However, this applies only to micro-textured systems.

There are disputes whether superhydrophobic surfaces can act as a repulsive anti-icing system, especially in high humidity conditions (Bharathidasan, Kumar, Bobji, Chakradhar, & Basu, 2014; Chen et al., 2012; Varanasi et al., 2010). Varanasi et al. (2010) reported that ice formation is unavoidable while the hydrophobicity is lost due to the constant surface energy. The argument is also sustained by Chen et al. (2012), who determined that the superhydrophobic surface can't cause a reduction in ice adhesion. Superhydrophobic coatings even displayed an irregular surface, which may be insufficient as a coating to prevent ice formations under different environmental conditions (Bharathidasan et al., 2014). Previously conducted studies have mainly been focusing on SWD, neglecting other icing conditions such as frost and mixed ice. At the same time, a thorough knowledge of microstructures is needed to achieve anti-icing properties. Even though superhydrophobic coatings are a controversial subject, Bharathidasan et al. (2014) found that silicon-based superhydrophobic coatings maintained a smooth surface, which is a significant factor for not altering the aerodynamics of a monoplane. In the same study, silicone-based hydrophobic coatings revealed an exceptional reduction in ice adhesion strength on aluminum alloys (23 – 43 kPa). In summary, superhydrophobic surfaces do not essentially entail icephobicity, especially for the aircraft during the flight icing scenario with high-speed influences of supercooled water droplets onto the wing areas.

There is another way to cause a reduction in the strength of ice adhesion by using SLIPS, because of adhesion strength of only a few kPa. The low strength of ice adhesion is quite suitable because it will rapidly remove the accrued ice over the surface. There is another concern to use SLIPS for anti-icing purposes is that the infused liquid could evaporate because of reduced pressure or high temperature. When the ice starts to flow through the lubricated surface,

so the liquid lubricant may be removed by the accrued ice, this will affect the durability. Moreover, the surface can be damaged by mechanical contact like penetrated liquid depletes and make the surface week (Liu, Ma, Wang, Kota, & Hu, 2018).

Other soft materials have been suggested for icing mitigation because of the dynamic deformation. As mentioned earlier, Beemer et al. (2016) showed that the soft material of PDMS gels has ultra-low strength of ice adhesion, good mechanical durability because of stiffness, and deformability. Hydrophobic gels occupy ultra-low ice adhesion due to the hydrophobic materials generally occupy low work of adhesion, and gels generally take a low shear modulus. Furthermore, hydrophobic gels have better mechanical durability as compared to the lubricated materials. Hydrophobic PDMS materials/gels offer excellent mechanical durability and ultra-low ice adhesion and reliable mechanical durability. Besides, the PDMS materials/gels are transparent with a visual transfer of more than 90% in the visible range.

Based on the current evaluation of the methods done in previous studies of icephobic surfaces, one will assess the following approaches based on what has been discussed. The creation of the icephobic surface using polymers with low cross-link density seems to be the most promising approach. According to Beemer et al. (2016), PDMS is the most suitable polymer due to the followings:

a) *"It is a hydrophobic material that results in low work of adhesion."*
b) *"It can be cross-linked to generate gels with low shear modulus."*
c) *"The shear modulus of gel can be blended by modifying the cross-link density."*
d) *"It is available without additives (e.g., silicon dioxide particles) in different molecular masses in the market. "*
e) *"It is economical, non-corrosive, and environmentally friendly."*

3.3.8 Findings

Of the methods studied, two are the most promising:

1. Preparation of PDMS gel via hydrosilylation as described by Beemer et al. (2016).

2. Preparation of slide-ring PDMS through the cross-linking reaction of the methylhydrosiloxane-dimethylsiloxane copolymer (HPDMS) with vinyl functionalized polyrotaxane (slidable cross-linker, SA3403P) as described by Zhuo et al. (2019).

The first method is more straightforward and accessible, as well as more studied. The second method is a more technically complex solution, but it probably has more serious prospects.

The aviation industry has several requirements and regulations for safety, especially during icing conditions, such as the FAR-25 appendix. Chemicals are also limited according to regulations, such as the REACH regulations (EC, Commission Regulation, 2006). Whether or not the international standards are met, a successful icephobic coating should prevent or delay ice formations on airfoils and laminar components of the airframe. Additional outcomes are to reduce fuel consumption and maintenance, and at the same time, increase the performance (Huang et al., 2019). Accordingly, further research paths include laboratory testing of materials prepared using methods for compliance with these requirements.

3.3.9 Results

1. Methods for creating anti-icing coatings suitable for use in aircraft have been studied. To date, it has been unveiled that neither of industrial products nor amongst scientific solutions, there are no coatings capable of independently functioning as a passive anti-icing system. Modern aviation uses active systems.
2. Superhydrophobic coatings revealed disadvantages that limit their use in extreme icing conditions. Among the developed approaches, the most promising is the use of polymers with a low cross-linking density.
3. For further research, two different methods for developing icephobic substances are proposed.

3.4 The Preparation of a Highly Hydrophobic coating based on Zinc Stearate and a Platinum-Curable Polydimethylsiloxane (PDMS).

The following method is based on the first finding from the previous landscape assessment. The reason for choosing the first method is that the second method is too complicated and requires more research based on extensiveness.

3.4.1 Objective

The scope of this preliminary trial is the development, on a laboratory scale, of a highly effective hydrophobic and icephobic coating. Since the final material will be applied in the field of aviation and aerospace, a necessary feature for the proposed coating is the high adhesion to metals, specifically to aluminum.

Based on the literature sources previously cited, one of the proposed approaches is based on the use of a hydrophobic Zinc salt dispersed into a polymer matrix that can efficiently adhere to aluminum. This study was developed by taking a leaf from a previously cited paper by Yang et al. (2015). In this study, the authors successfully dispersed Zinc oxide (ZnO) into curable polydimethylsiloxane (PDMS), obtaining a highly effective ice-phobic coating. Despite the high efficiency of the obtained coating, the cited method needs the use of 1-dodecanethiol (DC). DC is a corrosive and toxic chemical with a bad smell even at low concentrations.

To avoid the use of 1-dodecanethiol, one decided to use another hydro-phobic zinc salt, which is easily dispersed into a polymer matrix without further modifications. Zinc Stearate (ZnSt) is an organic salt that is well dispersible in a wide range of polymers and widely used as a polymer additive (Anneken et al., 2006). ZnSt has familiar hydrophobic properties (Richarda, Anandana, & Arunaa, 2016) and has already been used for the realization of long-lasting hydrophobic materials (Lanzón, Martínez, Mestre, & Madrid., 2017; Wu, Wu, Yang, & Ye, 2020). Moreover, ZnO combined with stearic acid has been proficiently used with a PDMS matrix by Yu, Xiao, Pan (2019). In this case, ZnO was treated with stearic acid. The treated ZnO were highly organophilic and was then dispersed in silicone, allowing it to obtain a long-lasting and superhydrophobic coating.

The following report shows a simple way to develop a highly hydrophobic and ice-phobic coating based on ZnSt and a Pt-curable PDMS. The chosen curable silicone rubber was Easy Composite AS 40 (silicone rubber + curing agent); it was chosen based on its high affinity toward metals and its extremely low post-curing shrinkage.

3.4.2 Materials and Methods

Materials

AS40 PDMS (Part A) and Pt curing agent (Part B) were purchased from Easy Composites Ltd; both polymer and curing agent composition are proprietary and not specified. Zinc stearate (USP- Ph. Eur., Zinc stearate approx. 98,5%; free fatty acid 1%, water approx. 0,5%) was purchased from Pharmalabor. Aluminum plates (thickness 3mm) were purchased from Bi-metal. All reagents and materials were used without any further purification.

Methods

Aluminum plates coated with ZnSt-curable PDMS with different compositions were prepared according to the following procedure: ZnSt powder was weighed into a beaker and mechanically mixed with PDMS (Part A). After 10 minutes of stirring, Part B (curing agent) was added to the mixture. The mixture was briefly stirred, then poured on a sanded aluminum plate and spread using a plastic blade. Different amounts of ZnSt and curing agents were used in the preparation of the coating. All the quantities are reported in table 9.

Table 9: Various compositions in the mixture.

PDMS (g)	Curing Agent (g)	ZnSt (g)	ZnSt %
10	1	1,1	10%
5	1	0,6	10%
5	1	1,2	20%
5	2	2,4	40%

The coated aluminum plates were left to cure at room temperature for 24 hours at 60°C for 2 hours.

3.4.3 Results and discussion

Morphological properties

In nearly all cases, the ZnSt resulted in a well-mixable PDMS, leading to a homogeneous dispersion; the only exception was the last case (40%), where the ZnSt showed the tendency to form lumps into the PDMS (probably because of the high concentration). However, all the mixture resulted as highly homogeneous after the addition of the curing agent.

The blade-spreading allowed one to obtain highly uniform layers of the ZnSt-PDMS mixture on the aluminum plates. The first test was executed using the silicone to curing agent ratio recommended by the supplier (10:1). Nevertheless, the resulting mixture had not optimal viscosity and gave fewer uniform layers. Moreover, after curing (both the one cured at room temperature and that cured at 60°C), the final coating resulted slightly sticky. Because of the latter, it was decided to use higher amounts of curing agent to increase the coating's viscosity while decreasing the "sticky effect." The samples were prepared with increased curing agents (5:1 and 5:2), resulting in highly viscous liquids and were not sticky after curing.

All samples obtained at higher concentrations of curing agents displayed similar behavior. After curing, uniform layers with a matt white color were obtained; the final thickness resulted from 700 to 800 µm (measured by caliber) for each composition.
In all cases, no distinct differences in the final morphology of the layers were noticed between the sample cured at room temperature for 24 hours, and those cured at 60°C for two hours.

Wettability properties

A first test was carried on by merely dropping some water droplets on the surface of uncoated aluminum and on the ZnSt-PDMS coated aluminum. The results are shown in figure 64-66:

Figure 66:Uncoated aluminum.

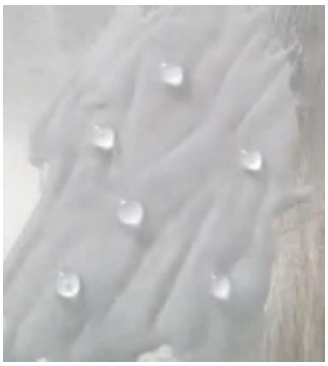

Figure 66: 10% of ZnSt, 10:1 PDMS to curing agent.

Figure 66: 40% of ZnSt, 5:2 PDMS to curing agent.

As shown in figure 64, the water droplets on the uncoated aluminum result flatter than those on the coated aluminum (figure 65, figure 66).

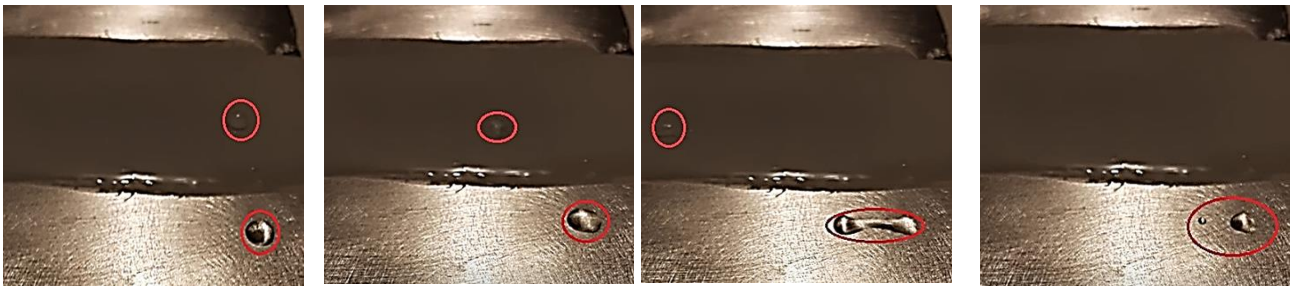

0 seconds **1 second** **3 seconds** **4 seconds**

Figure 67: Adhesion test under compressed air.

The low interaction between coated aluminum and water results is also evident in figure 44, where one droplet of water was applied on the uncoated aluminum surface. In comparison, one droplet was added on the ZnSt-PDMS treated aluminum (40% of ZnSt, 5:2 PDMS/curing agent ratio). The two droplets were subjected to compressed air (2 atm). It is possible to notice that, under a flux of compressed air, the water droplet on the untreated aluminum flows more slowly due to the higher wettability of the surface (figure 67). Moreover, it is possible to see that a small part of the droplet on the untreated aluminum does not move at all, remaining adhered to the aluminum surface. In contrast, no water residues can be found on the coated aluminum.

Note: A video of the process is provided in Appendix A.

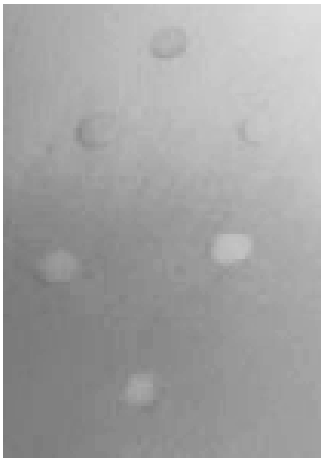

Figure 68: Uncoated aluminum.

Figure 69: 10% of ZnSt, 10:1 PDMS to curing agent ratio.

Figure 70: 40% of ZnSt, 5:2 PDMS to curing agent ratio.

The results are similar for the droplets after freezing at -20°C for 3 hours, (figure 68-70). The frozen droplets show a reduced contact angle on the ZnSt-PDMS treated aluminum. The ZnSt-PDMS coating showed a lower grade of interaction with the frozen droplets, which are easily removable from the coated aluminum (figure 69-70); in contrast, the frozen droplet remains solidly anchored to the untreated aluminum, (figure 68).

Water contact angle (WCA)

The contact angle is a measure of the wettability of a surface, and it is the angle measured through the liquid, where a liquid-vapor interface meets a solid surface. By convention, hydrophobic surfaces have a contact angle θ >90°, while hydrophilic surfaces have a contact angle θ < 90°.

The images collected for the contact angle dimensions are obtained by a MACRO lens mounted on a 2220 x 1080-pixel camera and processed with ImageJ software, 1.47 version.

The WCA measurements for the untreated aluminum are reported in figure 71.
The water droplet results flat, with measured contact angles of θ_{Left} = 79.39° and θ_{Right} = 80.31°. The defined values indicate a hydrophilic aluminum surface (0 – 90°).

The WCA on the PDMS-ZnSt coating is displayed in figure 72.

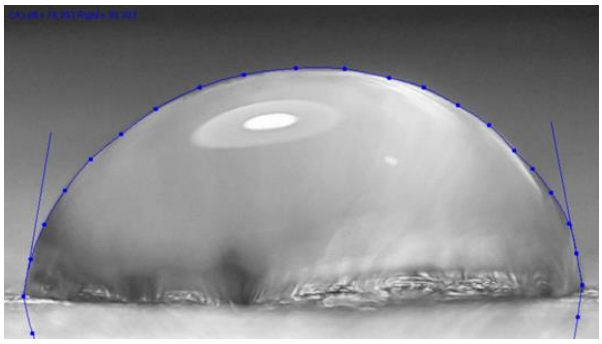

Figure 72: A water droplet measured on an un-coated aluminum surface.

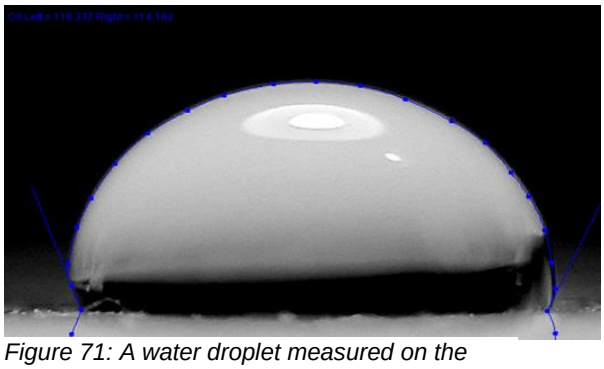

Figure 71: A water droplet measured on the ZnSt-PDMS coating.

The water droplet displays a slightly rounded shape than the uncoated surface (figure 72), and the measured contact angles are θ_L = 123.34° and θ_R = 124,18°. Since θ_{Total} = ~124°, (θ > 90) the PDMS-ZnSt confirms a hydrophobic surface, compared to the hydrophilic uncoated aluminum.

Ice adhesion

A preliminary test of the ice adhesion on the ZnSt-PDMS coating (40% of ZnSt, 5:2 PDMS to curing agent ratio) was performed using a procedure based on the work of Makkonen (2012): An ice cylinder with 1 cm radius and about 0,5 cm height was obtained on both uncoated and ZnSt-PDMS coated aluminum using a silicone mold (figure 73).

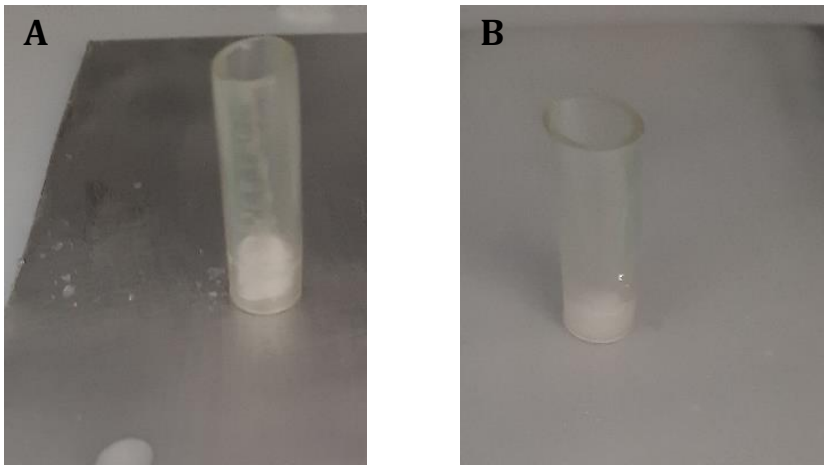

Figure 73: Ice sample deposition on aluminum (A) and on ZnSt-PDMS coating (B).

A shear force was then applied on both ice cylinders at -20°C for 2 hours, using a belt moving at a constant rate of 200 mm/min. The shear force was measured by a precision spring dynamometer (3B Scientific, 5 N of maximum load). Adhesion was then measured as the peak of the shear force divided by the interface area (314 mm^2).

The shear force for the ice sample deposited on the ZnSt-PDMS coating resulted in 2,65 N, which corresponds to an ice adhesion of 8,4 x 10^{-3} MPa. In contrast, the sample on the uncoated aluminum surface broke during the examination, and its base remained firmly adhered to the surface, as reported in figure 74 (circled in red).

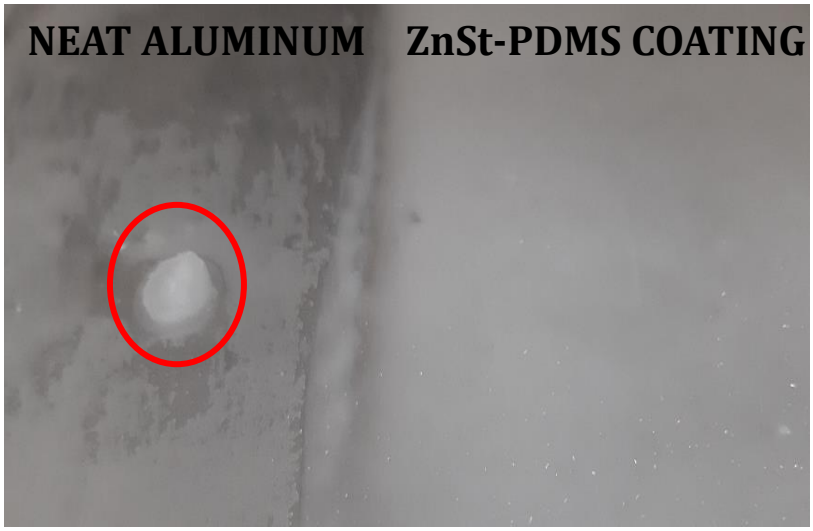

Figure 74: Ice adhesion between neat aluminum and ZnSt-PDMS coating.

This behavior further confirms the excellent efficiency of the designed coating in reducing the ice adhesion force on the aluminum.

3.4.4 Results

The present report shows an easy way to prepare a highly hydrophobic and icephobic material by dispersing Zinc Stearate (ZnSt) in curable polydimethylsiloxane (PDMS).

$$C_{36}H_{70}O_4Zn + (C_2H_6OSi)n$$

The high efficiency of the ZnSt-PDMS coating was confirmed by testing a higher Water Contact Angle (WCA) in interaction with the coating - both in liquid and solid state. Indicatively,

the ZnSt-PDMS coating offers lower resistance to water flow than the untreated aluminum, as well as reducing the interaction between the material and frozen water droplets by more than 50%. Ice adhesion measures confirmed the lower interaction between the ice and the ZnSt-PDMS coating, with a lower adhesion force determined through the ice adhesion test.

4 Conclusion

Based on previous assessments and results, the sub-conclusion will be given in accordance with research questions 1 and 2, addressed in subchapter 1.1.

4.1 RQ1

RQ1: How do different ice formations affect the aircraft's aerodynamic performance?

The partial conclusion from RQ1 is **that severe ice accretions lead to critical degradation of the aerodynamic effectiveness.** Structural ice formations reconstruct the airframe, which leads to **reduced lifting capacity and increased drag** – increasing stall speed. Since aircraft varies in altitude, different icing conditions will occur rapidly in different altitudes, under various weather conditions. It was also found that mixed ice, rime ice, and frost are detrimental under freezing conditions but not as severe as glaze icing.

Through cross-tabulation, an attempt was made to classify the risks related to different flight phases. According to flight-phase, risk assessment revealed that the **most adverse and fatal events occurred in <u>cruising altitude</u> at 0-2 AoA**.

- By evaluating the components by individual risk significance in icing conditions (Tab le 4), one can neglect parts based on sustainability. The alleged theory suggests that the **<u>wing</u> part is most susceptible to aerodynamic degradability.**
- A CFD analysis compared the wing of the Airbus-A320 in 0° AoA, with and without glaze ice. It was found that glaze ice accumulates at a very high rate. **After 100 seconds of simulation, the total mass of accreted ice was around 2.3kg.** Under glazed ice, airflow's primary obstruction correlates with the structural reformation in the airfoil, as the change in velocity streamlines and pressure is evident.
    - The aerodynamic impairment resulted in an approximately **17% increment in airfoil drag, while the wing lift was almost unaffected with a decrement of 0,15%.** The relationship between the velocity and pressure in glazed conditions indicates that a constant **AoA of 0° (cruising conditions) will have a prominent increment in the drag coefficient (C_D)**. In contrast, the lift coefficient (C_L) is close to stagnant in both conditions at 0° AoA.

The **main threat for severe icing conditions is caused by super cooled water droplets under freezing rain.** While small super cooled droplets may freeze instantly and may stay unnoticeable as both frost and rime ice, super cooled large droplets can remain avoidant and less influenced to the airflow surrounding the aircraft. The latter causes it to stick more easily to the surface of the plane and creating a structure of glaze ice. Glaze ice is the structure most difficult to spot and usually has the highest risk of severely disrupting the airflow and impairing the planes aerodynamics.

- **Glaze ice is the most harmful ice structure for aerodynamic functions.** It creates more extensive reconstructions on the airframe, leading to a **drag penalty about six times more extensive than mixed ice while reducing lifting capacity.** It was also found that glaze ice develops beyond the wings IPS (Ice Protection System).
- Rime ice is a function of time and **does not possess a severe risk until prolonged exposure.** Even though it accretes with a similar amount as glaze ice, it only leads to about 1/3 drag compared to glaze ice.
- Mixed ice is a combination of rime ice and glaze ice and incorporates supercooled droplets with various MVD (Median Volume Diameter). Compared to glaze ice, **it can achieve a drag penalty of about 1/2 compared to glaze ice conditions**, and it mainly affects the initial climb phase.
- **Frost** is both challenging to notice and possesses greater danger in larger quantities, especially during climbing, but is **considered least hazardous compared to glaze, rime, and mixed conditions.**
- **IPS systems are the most effective active ice removal systems in-flight**, to date. However, they exhibit weaknesses in terms of reliability because of low thermal flux, limited wattage to generate a significant melting process, while at the same time reliant on pilots' risk perception.

4.2 RQ2

RQ2: How can one create a passive anti-icing system for aircraft, and improve risk mitigation through hydrophobic nanocomposite?

According to RQ2, the following work has shown that a coating of Zinc Stearate (ZnSt) in curable polydimethylsiloxane (PDMS) can provide safer aviation. **The high efficiency of the ZnSt-PDMS coating was confirmed by a higher Water Contact Angle (WCA) of ~124 °** (compared to water on the uncoated aluminum surface (~80°)) in interaction with the coating - both in liquid and solid state. The ZnSt-PDMS coating offers lower resistance to water flow than untreated aluminum and **reduces the interaction between the material and frozen water droplets by more than 50%.** Ice adhesion measures confirmed the lower interaction between the ice and the ZnSt-PDMS coating, with a lower adhesion force determined through the ice adhesion test.

The "Landscape assessment" revealed that to date there are no coatings in industrial production capable of independently functioning as a passive anti-icing system. Modern aviation uses active systems.

Hydrophobic coatings revealed disadvantages that limit their use in extreme icing conditions. Among the developed approaches**, the most promising was the use of polymers with a low cross-linking density.**

- However, findings revealed **two promising methods** for **creating anti-icing coatings suitable for aircraft**, where number 1 was prepared:
    1. **Preparation of PDMS gel via hydrosilylation as described by Beemer et al. (2016).**
    2. Preparation of slide-ring PDMS through the cross-linking reaction of the methylhydrosiloxane-dimethylsiloxane copolymer (HPDMS) with vinyl functionalized polyrotaxane (slidable cross-linker, SA3403P) as described by Zhuo et al. (2019).
- Icing conditions are reported by the intensity of the atmospheric surroundings and based on the rate of ice accretion. Even though there are procedures to handle icing threats,

severe conditions may not be voidable even with the current anti- and de-icing equipment available.

- Current de-icing methods in the aviation industry have high reliability until the take-off phase but is still expensive and not considered environmentally friendly. De-icing maintenance also creates repercussions in delays. In an already complex industry where the highest risk of unwanted events is related to traffic on ground – such procedures should be modernized.

4.3 Further research

Even though the demonstrated Zn-St-PDMS coating has proven effective in preventing water and ice adhesion on aluminum, further analysis and testing is needed before giving a main conclusion in respect to safety and reliability. Since the chemical are only tested under static conditions and with a “weather-still” environment, further research should produce more accurate results in terms of usability. The most important criteria are as follows.

4.3.1 Mechanical tests

The first property of the material which should be tested is the adhesion force to the metal. This test would give a measure of the durability of the interaction between the coating and the aluminum. A standard method for measuring the adhesion force of organic compounds, ASTM D2197 (Standard Test Method for Adhesion of Organic Coatings by Scrape Adhesion), is recommended.

Due to aerodynamics and an unsteady airflow, the coating would likewise be subjected to vibrations, mainly if applied to components such as the wings upper and lower surface, ailerons, and the vertical and horizontal stabilizer.

The material would be exposed to long cycles of oscillation, which would cause mechanical stress on the substance. In the long term, it may cause cracks into the coating, leading to its partial or total detachment. Testing the resistance to vibrations could be performed by subjecting a sample to vibrations at different times and frequency, registering the eventual formation of cracks, holes, or the partial or total detachment of the coating from the aluminum.

4.3.2 Thermal test

The Zn-St-PDMS would be exposed to high thermal excursion during its consistent utilization. Although silicone rubbers work well even at -80°C, the difference in the thermal expansion coefficient of the two materials could cause mechanical stress that could cause the coating to deteriorate. The resistance to thermal excursion could be tested by subjecting the coated aluminum to several thermal cycles, from -80°C to +60°C, registering the partial or total detachment of the coating from the aluminum.

Differential Scanning Calorimetry analysis (DSC), in a temperature range between 0 and -100°C, is also suggested to determine the material properties (e.g., thermal stability, and temperature transitions) at low temperatures.

During its frequent use, the coating would be subjected to a high dosage of UV radiation, which can cause the polymer/material to change. The resistance of the surface to UV-alteration can be tested irradiating a sample with a UV-lamp at different times, then analyzing it by FT-IR spectroscopy to determine the eventual formation of degradation products.

Based on test results, it could be necessary to modify the coating formulation, adding mechanical reinforcing fillers, photo-stabilizers, or adhesion reinforcers.

5 Bibliography

Aerotoolbox. (2017). Retrieved: 10.07.20. Available from: https://aerotoolbox.com/angle-of-attack/.

Ahrens, C. Donald. (2007). Meteorology today: an introduction to weather, climate, and the environment. Belmont, CA: Thomson/Brooks/Cole.

Airbus Industry. (2000). Getting to grips with cold weather operations. France, Blagnac: Customer Services Directive.

Airbus. (n.d). Retrieved: 10.07.20. Available from: https://www.airbus.com/aircraft/passenger-aircraft/a320-family/a320neo.html#details.

Alizadeh, A., Bahadur, V., Kulkarni, A., Yamada, M., & Ruud, J. (2013). Hydrophobic surfaces for control and enhancement of water phase transitions. MRS Bulletin, 38(5), 407-411. doi:10.1557/mrs.2013.1049/5-2004_N90AG.pdf.

American Meteorological Society. (2012). *Precipitation.* Available from: http://glossary.ametsoc.org/wiki/Precipitation.

Amescorp. (n.d). Retrieved: 29.06.20. Available from: https://amescorp.com/what-we-do/aerospace-and-aircraft-components.

Anneken, D. J., Both, S., Christoph, R., Fieg, G., Steinberner, U. & Westfechtel, A. (2006) Fatty Acids. In Wiley-VCH Verlag (Eds): *Ullmann's Encyclopedia of Industrial Chemistry* (pp. 74-116)

AOPA Air Safety Foundation. (2008). *Safety Advisor; Aircraft Icing.* Available from: https://www.aopa.org/-/media/Files/AOPA/Home/Pilot-Resources/ASI/Safety-Advisors/sa11.pdf. Retrieved 18.06.20.

AOPA. (2010). WX WATCH: FREEZING RAIN FACTS: Becoming aware of the worst icing. Available from: https://www.aopa.org/news-and-media/all-news/2010/november/01/wx-watch-freezing-rain-facts. Retrieved: 09.06.20.

AOPA. (2016). WEATHER: JACK FROST: first one to arrive when winter weather is forecast. Available from: https://www.aopa.org/news-and-media/all-news/2016/december/flight-training-magazine/weather-jack-frost. Retrieved 10.06.2020.

AOPA. (2018). *How it works: Pitot-static system.* Retrieved: 24.10.19. Available from: https://www.aopa.org/news-and-media/all-news/2018/november/flight-training-magazine/how-it-works-pitot-static-system.

Association of European Airlines. (2008). *Recommendations for De-Icing / Anti-Icing of Aircraft on the Ground: 23.edition.* Available from: https://www.icao.int/safety/airnavigation/OPS/Documents/aea_deicing_v23.pdf.

Basu, B. B. J. & Paranthaman, A. K. (2009) 'A simple method for the preparation of superhydrophobic PVDF–HMFS hybrid composite coatings', Applied Surface Science, vol. 255, no. 8, pp. 4479–4483, doi: 10.1016/j.apsusc.2008.11.065.

Baumert, A., Bansmer, S., Trontin, P., & Villedieu, P. (2018). Experimental and numerical investigations on aircraft icing at mixed phase conditions. International Journal of Heat and Mass Transfer, 123, 957-978. doi: 10.1016/j.ijheatmasstransfer.2018.02.008.

Beemer, D. L., Wang, W. & Kota, A. K. (2016). 'Durable gels with ultra-low adhesion to ice', J. Mater. Chem. A, vol. 4, no. 47, pp. 18253–18258, doi: 10.1039/C6TA07262C.

Beeram, P. S. R. (2017). Characterization of ice adhesion strength over different surfaces pertinent to aircraft anti-/de-icing (p. 11413627) [Master of Science, Iowa State University, Digital Repository]. https://doi.org/10.31274/etd-180810-5702.

Bernstein, B. C. (2000). Regional and local influences on freezing drizzle, freezing rain, and ice pellet events. Weather and Forecasting, 15(5), 485-508. doi: 10.1175/1520-0434(2000)015<0485:Raliof>2.0.Co;2.

Bharathidasan, T., Kumar, S. V., Bobji, M. S., Chakradhar, R. P. S., & Basu, B. J. (2014). Effect of wettability and surface roughness on ice-adhesion strength of hydrophilic, hydrophobic and superhydrophobic surfaces. Applied Surface Science, 314, 241-250. doi: 10.1016/j.apsusc.2014.06.101.

Biolin Scentific. (2018). *What is contact angle hysteresis?* Retrieved: 30.06.20. Available from: https://www.biolinscientific.com/blog/what-is-contact-angle-hysteresis.

Boeing. (2000). Aero no.12: Angle of Attack. Retrieved 07.07.20. Available from: https://www.boeing.com/commercial/aeromagazine/aero_12/attack_story.html

Boeing. (2008). *Engine power loss in ice crystal conditions.* Retrieved: 24.10.19. Available from: https://www.boeing.com/commercial/aeromagazine/articles/qtr_4_07/article_03_2.html.

Bohn, H. F. & Federle, W. (2004). 'Insect aquaplaning: Nepenthes pitcher plants capture prey with the peristome, a fully wettable water-lubricated anisotropic surface', Proc. Natl. Acad. Sci. USA, vol. 101, no. 39, pp. 14138–14143, doi: 10.1073/pnas.0405885101.

Bureau of Meteorology. *(2013). Hazardous weather phenomena: Airframe Icing.* Retrieved: 29.10.19. Available from: [http://rrwx.com/wp-content/uploads/2013/04/hwp-icing.pdf].

Cao, Y., Zhang, Q., & Sheridan, J. (2008). Numerical simulation of rime ice accretions on an aerofoil using an Eulerian method. Aeronautical Journal, 112, 243-249. doi:10.1017/S0001924000002189

Cao, M., Guo, D., Yu, C., Li, K., Liu, M. & Jiang, L. (2016). 'Water-Repellent Properties of Superhydrophobic and Lubricant-Infused "Slippery" Surfaces: A Brief Study on the Functions and Applications', ACS Appl. Mater. Interfaces, vol. 8, no. 6, pp. 3615–3623, doi: 10.1021/acsami.5b07881.

Cao, Y., Tan, W. & Zhenlong. W. (2018). Aircraft icing: An ongoing threat to aviation safety. Aerospace Science and Technology. 75. 10.1016/j.ast.2017.12.028.

Centre For Atmospheric Icing (n.d). *Ice and Mixed Phase Clouds.* Retrieved: 11.12.19. Available from: http://www.cas.manchester.ac.uk/resactivities/cloudphysics/background/ice/.

Chen, B., Evans, J. R., Greenwell, H. C., Boulet, P., Coveney, P. V., Bowden, A. A., & Whiting, A. (2008). A critical appraisal of polymer-clay nanocomposites. Chem Soc Rev, 37(3), 568-594. doi:10.1039/b702653f.

Chen, J., Liu, J., He, M., Li, K., Cui, D., Zhang, Q., Zeng, X., Zhang, Y., Wang, J. & Song, Y. (2012). 'Superhydrophobic surfaces cannot reduce ice adhesion', Appl. Phys. Lett., vol. 101, no. 11, p. 111603, doi: 10.1063/1.4752436.

Civil Aviation Authority. (2000). *Aircraft Icing Handbook.* New Zealand: Civil Aviation Authority.

Commons. (2007). *Aircraft Parts.* Retrieved: 26.06.20. Available from: https://commons.wikimedia.org/wiki/File:Aircraft_Parts_eng.jpg.

Cortinas Jr, J. V., Bernstein, B. C., Robbins, C. C., & Strapp, J. W. (2004). An analysis of freezing rain, freezing drizzle, and ice pellets across the United States and Canada: 1976-90. Weather and Forecasting, 19(2), 377-390. doi:10.1175/1520-0434(2004)019<0377:AAOFRF>2.0.CO.

COSCAP. (1984). ICAO ANNEX: References for Ramp Inspection Guidance. Retrieved: 14.10.19. Available from: [https://webcache.googleusercontent.com/search?q=cache:DecObkA6Cx0J:https://www.icao.int/safety/fsix/Library/Reference_ANNEXES_for_ICAO_Ramp_Inspections_Guidance_2009_07_02.pdf+&cd=1&hl=no&ct=clnk&gl=no].

DNVGL (2019). DNVGL-RP-A203, Technology Qualification. DNVGL, Oslo. Høvik.

Eastlake, C. N. (2002) An Aerodynamicist's View of Lift, Bernoulli, and Newton: The Physics Teacher vol. 40. Embry-Riddle Aeronautical university.

EC, Commission Regulation (EU). (2016). No 1321/2014. On the continuing airworthiness of aircraft and aeronautical products, parts and appliances, and on the approval of organizations and personnel involved in these tasks. Available from: https://eur-lex.europa.eu/legal-content/EN/TXT/?uri=CELEX%3A32003R2042.

EC, Commission Regulation. (2006). No 1907/2006. *Concerning the Registration, Evaluation, Authorisation and Restriction of Chemicals (REACH).* Available from: https://eur-lex.europa.eu/legal-content/EN/TXT/?uri=CELEX%3A02006R1907-20140410.

Electropaedia. (n.d). Available from: https://www.mpoweruk.com/flight_theory.htm.

Farhadi, S., Farzaneh, M. & Kulinich. S. A. (2011). 'Anti-icing performance of superhydrophobic surfaces', Applied Surface Science, vol. 257, no. 14, pp. 6264–6269, doi: 10.1016/j.apsusc.2011.02.057.

FAA. (2008). *Instrument Flying Handbook.* Washington DC: US Government Printing Office.

FAA. (2014). *ALC-33: Inflight icing.* Retrieved 26.10.19. Available from: https://www.faasafety.gov/gslac/ALC/course_content.aspx?cID=33&sID=155&preview=true.

FAA. (2015). *Advisory Circular: 91-74B.* retrieved: 10.07.20. Available from: https://www.faa.gov/documentLibrary/media/Advisory_Circular/AC_91-74B.pdf.

FAA. (2016). *Pilot´s Handbook of Aeronautical Knowledge.* USA: Department of Transportation.

Federal Aviation Administration & National Weather Service (1975). *Aviation Weather: AC 00-6A.* Washington DC: US Government Printing Office.

Federal Aviation Administration & National Weather Service (2016). *Aviation Weather: AC 00-6B.* Washington DC: US Government Printing Office.

Fikke, M. S., Heimo, A., Säntti, K. (2007). COST 727 – Report from Phase 1. Yokohama: The European Cooperation of Scientific and Technical Research.

Florio F. (2016). *Airworthiness. An Introduction to Aircraft Certification*, 3rd edition, Butterworth-Heinemann.

Frega, F. (2018). *A320 Fuel System.* Available from: https://www.scribd.com/document/369597642/A320-Fuel-System.

Gao, S., Liu, G., Peng, J., Zhu, K., Zhao, Y., Li, X. & Yuan, X. (2019). 'Icephobic Durability of Branched PDMS Slippage Coatings Co- Cross-Linked by Functionalized POSS', ACS Appl Mater Interfaces, vol. 11, no. 4, pp. 4654–4666, doi: 10.1021/acsami.8b19666.

Ghalmi, Z., Menini, R., & Farzaneh, M. (2009). Theoretical Studies and Quantification of Ice Adhesion Mechanisms. 7.

Golovin. K., Kobaku. S. P. R., Lee, D. H., DiLoreto, E. T., Mabry, J. M. & Tuteja, A. (2016). 'Designing durable icephobic surfaces', Sci Adv, vol. 2, no. 3, p. e1501496, doi: 10.1126/sciadv.1501496.

Han, Yiqiang. (2011). Theoretical and Experimental Study of Scaling Methods for Rotor Blade Ice Accretion Testing. Doi: 10.13140/RG.2.1.2585.0485.

Heinrich, A., Ross, R., Zumwalt, G., Provorse, J., Padmanabhan, V., Thompsom, J. & Riley, J. (1993). Aircraft Icing Handbook, (Volumes 1–3), FAA Technical Report DOT/FAA/CT–88/8–1. Available from: http://www.tc.faa.gov/its/worldpac/techrpt/ct888-1.pdf.

Himma, F. N., Prasetya, N., Anisah, S., & Wenten, G. (2019). Superhydrophobic membrane: progress in preparation and its separation properties. Reviews in Chemical Engineering, 35(2), 211-238. doi: 10.1515/revce-2017-0030.

Hong, S., Wang, R., Huang, X. & Liu, H. (2019) 'Facile one-step fabrication of PHC/PDMS anti-icing coatings with mechanical properties and good durability', Progress in Organic Coatings, vol. 135, pp. 263–269, doi: 10.1016/j.porgcoat.2019.06.016.

Hosseini, S., Ibrahim, F., Rothan, H. A., Yusof, R., Marel, C. v. d., Djordjevic, I., & Koole, L. H. (2015). Aging effect and antibody immobilization on COOH exposed surfaces designed for dengue virus detection. Biochemical Engineering Journal, 99, 183-192. doi: 10.1016/j.bej.2015.04.001

Huang, X., Tepylo, N., Pommier-Budinger, V., Budinger, M., Bonaccurso, E., Villedieu, P., & Bennani, L. (2019). A survey of icephobic coatings and their potential use in a hybrid coating/active ice protection system for aerospace applications. Progress in Aerospace Sciences, 105, 74-97. doi: 10.1016/j.paerosci.2019.01.002.

Häusler, T., Witek, L., Felgitsch, L., Hitzenberger, R., Grothe, H. (2017). *Heterogeneous freezing of super cooled water droplets in micrometer range-freezing on a chip.* Atmospheric Chemistry and Physics Discussions. 1-19. 10.5194/acp-2017-31. Available from: https://www.researchgate.net/publication/312477668_Heterogeneous_freezing_of_super_cooled_water_droplets_in_micrometre_range-freezing_on_a_chip.

ICAO (International Civil Aviation Organization). (2000). Manual of aircraft ground de-icing/anti-icing operations: Second edition. Available from: https://code7700.com/pdfs/icao/icao_doc_9640_manual_of_aircraft_ground_de-Icing_anti-Icing_operations.pdf

ICAO (International Civil Aviation Organization). (2014). Doc 9760 Airworthiness Manual, 3rd Edition, ICAO. Available from: https://www.icao.int/MID/Documents/2014/Airworthiness%20Manual%20Seminar/PPT.pdf.

Ideas Engineering. Wing Analysis. Available from: https://ideasengineering.blogspot.com/2016/12/motogp-wings-analysis.html.

InnovateCee. (2017*). Surface that keeps water and ice away.* Retrieved: 09.10.19. Available from: [http://www.innovatecee.com/technology/surface-that-keeps-water/]

Instras Scientific. (2013) Retrieved: 30.06.20. Available from: https://instras.com/index.php/dip-coater-dck-100/.

Johnson, R. W. (1998). The handbook of fluid dynamics. Boca Raton, Fla: CRC Press.

Jung, S., Tiwari K. M. & Poulikakos, D. (2012). *Frost halos from super cooled water droplets.* New Jersey: Princeton University.

Kajikawa, M., Kikuchi, K., Asuma, Y., Inoue, Y., & Sato, N. (2000). Supercooled drizzle formed by condensation-coalescence in the mid-winter season of the Canadian Arctic. Atmospheric Research, 52(4), 293-301. doi:Doi 10.1016/S0169-8095(99)00035-6.

Kim, P., Wong, T.-S., Alvarenga, J., Kreder, M. J., Adorno-Martinez, W. E. & Aizenberg, J. (2012). 'Liquid-infused nanostructured surfaces with extreme anti-ice and anti-frost performance', ACS Nano, vol. 6, no. 8, pp. 6569–6577, doi: 10.1021/nn302310q.

Klein-Paste, A. & Potova, J. (2014). *Thermal Aspects of Melting Ice with Deicer Chemicals.* Available from: https://journals.sagepub.com/doi/10.3141/2440-09.

Kulinich, S. A. & Farzaneh, M. (2009). 'Ice adhesion on superhydrophobic surfaces', Applied Surface Science, vol. 255, no. 18, pp. 8153–8157, doi: 10.1016/j.apsusc.2009.05.033.

Lanzón, M., Martínez, E., Mestre, M. & Madrid, J. A. (2017). 'Use of zinc stearate to produce highly-hydrophobic adobe materials with extended durability to water and acid-rain', Construction and Building Materials, vol. 139, p. 114-122, doi: 10.1016/j.conbuildmat.2017.02.055

Law, K.-Y. (2014). Definitions for Hydrophilicity, Hydrophobicity, and Superhydrophobicity: Getting the Basics Right. The Journal of Physical Chemistry Letters, 5(4), 686-688. doi:10.1021/jz402762h.

Lester, F. Peter. (1995). *Aviation Weather.* Englewood: Jeppesen Sanderson Training Products.

Li. J., Zhao, Y., Hu, J., Shu, L. & Shi, X. (2012) 'Anti-icing Performance of a Superhydrophobic PDMS/Modified Nano-silica Hybrid Coating for Insulators', Journal of Adhesion Science and Technology, vol. 26, no. 4–5, pp. 665–679 ,doi: 10.1163/016942411X574826.

Li, X., Zhao, Y., Li, H. & Yuan, X. (2014). 'Preparation and icephobic properties of polymethyltrifluoropropylsiloxane–polyacrylate block copolymers', Applied Surface Science, vol. 316, pp. 222–231, doi: 10.1016/j.apsusc.2014.07.097.

Liu, M., Hou, Y., Li, J., Tie, L. & Guo, Z. (2018). 'Transparent slippery liquid-infused nanoparticulate coatings', Chemical Engineering Journal, vol. 337, pp. 462–470 , doi: 10.1016/j.cej.2017.12.118.

Liu, Y., Ma, L., Wang, W., Kota, A. K., & Hu, H. (2018). An experimental study on soft PDMS materials for aircraft icing mitigation. Applied Surface Science, 447, 599-609. doi: 10.1016/j.apsusc.2018.04.032.

Lovdata. (2018). Lov om luftfart – Vedlikehold av fly. Available from: https://lovdata.no/dokument/NL/lov/1993-06-11-101?q=luftfart

Lynch, F. T., & Khodadoust, A. (2001). Effects of ice accretions on aircraft aerodynamics. Progress in Aerospace Sciences, 37(8), 669-767. doi:https://doi.org/10.1016/S0376-0421(01)00018-5.

MachineDesign. (2016). *What's the Difference Between Turbine Engines?* Available from: https://www.machinedesign.com/motorsdrives/what-s-difference-between-turbine-engines

Mahapatra, P., Doviak, R.J., Mazur, V., Zrnić D.S. (1999). Aviation Weather Surveillance Systems. USA: The Institution of Electrical Engineers.

Makkonen, L. (2012). Ice Adhesion —Theory, Measurements and Countermeasures', Journal of Adhesion Science and Technology, vol 26, 413-455, doi: 10.1163/016942411X574583.

Massachusetts Institute of Technology. (2015). *Explained: chemical vapor deposition.* Retrieved: 02.07.20. Available from: https://news.mit.edu/2015/explained-chemical-vapor-deposition-0619.

Mobarakeh, L. F., Jafari, R. & Farzaneh, M. (2013). 'The ice repellency of plasma polymerized hexamethyldisiloxane coating', Applied Surface Science, vol. 284, pp. 459–463, doi: 10.1016/j.apsusc.2013.07.119.

Nanoproject. (2013) Retrieved: 10.07.20. Available from: https://nanoproject2b.wordpress.com/2013/06/06/hydrophobic-textile/.

NASA. (1984). *Performance Degradation of a Typical Twin-Engine Commuter Type Aircraft in Measured Natural Icing Conditions.* Available from: https://ntrs.nasa.gov/archive/nasa/casi.ntrs.nasa.gov/19840005105.pdf.

NASA. (2008). Subsonic Aircraft Safety Icing Study: NASA/TM—2008–215107. Available from: https://ntrs.nasa.gov/search.jsp?R=20080008836.

NASA. (2008b). Current Methods for Modeling and Simulating Icing Effects on Aircraft Performance, Stability and Control. NASA/TM-2008215453. Retrieved: 11.07.20.

NASA. (2011). *What is Aerodynamics?* Retrieved: 22.06.20. Available from: https://www.nasa.gov/audience/forstudents/k-4/stories/nasa-knows/what-is-aerodynamics-k4.html

NASA. (2012). *Pitot-Static Tube.* Retrieved: 24.10.19. Available from: https://www.grc.nasa.gov/WWW/K-12/airplane/pitot.html.

NASA (2015). What is Lift? Retrieved: 07.07.20. Available from: https://www.grc.nasa.gov/WWW/K-12/airplane/lift1.html.

NASA. (2016). *A Pilot's guide to inflight icing: Weather – Frontal Effects.* Retrieved: 24.06.20. Available from: https://aircrafticing.grc.nasa.gov/1_1_5_4.html.

NASA. (2018). Inclination Effects on Lift. Retrieved: 10.07.20. Available from: https://www.grc.nasa.gov/WWW/K-12/airplane/incline.html.

National Weather Service. (n.d). *Icing.* Retrieved: 13.05.20. Available from https://www.weather.gov/source/zhu/ZHU_Training_Page/icing_stuff/icing/icing.html.

Nguyen, T.-B., Park, S., Jung, Y. & Lim, H. (2019). 'Effects of hydrophobicity and lubricant characteristics on anti-icing performance of slippery lubricant-infused porous surfaces', Journal of Industrial and Engineering Chemistry, vol. 69, pp. 99–105, doi: 10.1016/j.jiec.2018.09.003.

NTSB. (1994*). Aircraft Accident Report-Runway Overrun Following Rejected Takeoff, Continental Airlines Flight 795 McDonnell Douglas MD-82, N18835 LaGuardia Airport Flushing, New York March 2, 1994 (NTSB-AAR-95-01; DCA94MA038; NTIS-PB95- 910401), February 14, 1995.* USA: Washington, D.C. Retrieved: 14.01.2019. Available from: https://www.fss.aero/accident-reports/dvdfiles/US/1994-03-02-US.pdf.

NTSB. (2004). A Statistical Review of Aviation Airframe Icing Accidents in the U.S. Washington, DC. Available from:https://www.researchgate.net/publication/287186718_A_statistical_review_of_aviation_airframe_icing_accidents_in_the_US.

NTSB. (2008). *Activate Leading Edge Deice Boots as Soon as Airplane Enters Icing Conditions.* Retrieved: 10.06.20. Available from: https://www.skybrary.aero/bookshelf/books/547.pdf.

O'Brien, P. J., Ross, F. R., Education, U. S. N., Command, T., Education, N., & Activity, T. P. M. S. (1990). Aerographer's Mate Second Class: The Activity.

Oxford Aviation Academy. (2010). *Meteorology: second edition.* UK: Oxford Aviation Academy.

Pellissier, M. P. C., Habashi, W. G., & Pueyo, A. (2011). Optimization via FENSAP-ICE of Aircraft Hot-Air Anti-Icing Systems. Journal of Aircraft, 48(1), 265-276. doi:10.2514/1.C031095.

Peng, C., Xing, S., Yuan, Z., Xiao, J., Wang, C. & Zeng, J. (2012). 'Preparation and antiicing of superhydrophobic PVDF coating on a wind turbine blade', Applied Surface Science, vol. 259, pp. 764–768, doi: 10.1016/j.apsusc.2012.07.118.

Perrow, C. (1999). Normal Accidents. Living With High-Risk Technologies. USA: Basic Books.

Petrenko, V. F., & Ryzhkin, I. A. (1997). Surface States of Charge Carriers and Electrical Properties of the Surface Layer of Ice. The Journal of Physical Chemistry B, 101(32), 6285–6289. https://doi.org/10.1021/jp963216p.

Petty, K.R., Floyd, C.D.J. (2004). A Statistical Review Of Aviation Airframe Icing Accidents In The U.S. Available from: https://www.researchgate.net/publication/287186718_A_statistical_review_of_aviation_airframe_icing_accidents_in_the_US.

Pourbagian, M., Talgorn, B., Habashi, W. G., Kokkolaras, M., & Le Digabel, S. (2015). Constrained problem formulations for power optimization of aircraft electro-thermal anti-icing systems. Optimization and Engineering, 16(4), 663-693. doi:10.1007/s11081-015-9282-1

Pruppacher, H. R., & Klett, J. D. (1997). Microphysics of clouds and precipitation (2nd rev. and enl. ed.). Dordrecht ; Boston: Kluwer Academic Publishers.

Rathakrishnan, E. (2013). Theoretical Aerodynamics (1. Aufl. ed.). SG: Wiley.

Rauber, R. M., Olthoff, L. S., Ramamurthy, M. K., & Kunkel, K. E. (2000). The relative importance of warm rain and melting processes in freezing precipitation events. Journal of Applied Meteorology, 39(7), 1185-1195. doi:Doi 10.1175/1520-0450(2000)039<1185:Triowr>2.0.Co;2.

Reason, J. (1997). Managing the Risks of Organizational Accidents. Ashgate: Ashgate Publishing Company.

Richarda, E., Anandana, C. & Arunaa, S. T. (2016). 'Fabrication of Superhydrophobic Zinc Stearate Hierarchical Surfaces from Different Precursors', Materials and Manufacturing Processes, vol 31, no 9, p 1171-1176, doi: 10.1080/10426914.2015.1019123.

Richoffmanclass. (n.d.). *Chapter 5: Forms of Condensation and Precipitation.* Retrieved: 24.10.19. Available from: http://www.richhoffmanclass.com/chapter5.html.

Robards, K., Haddad, P.R & Jackson, P.E. (2004). *Sample Handling in Chromatography*. Principles and Practice of moderns Chromatographic Methods, Science direct, pp. 407-455, doi: 10.1016/B978-0-08-057178-2.50011-X.

Rutherford, R.B & Dudman, L. R. (2001). Aircraft de-icing system. Retrieved: 04.06.2020. Available from: https://patentimages.storage.googleapis.com/a4/ce/8a/6b14510fe46fbb/US6330986.pdf.

Ryerson, C. C. (2011). Ice protection of offshore platforms. Cold Regions Science and Technology, 65(1), 97-110.

Scavuzzo. R. J., & Chu, M.L. (1987). 'Structural properties of impact ices accreted on aircraft structures". US: Ohio. The University of Akron.

Sforza, P. (2014). Chapter 5 - Wing Design. In P. Sforza (Ed.), Commercial Airplane Design Principles (pp. 119-212). Boston: Butterworth-Heinemann.

Shaylesh, R. (2020). *AIRBUS A320neo*. Retrieved and adapted from: https://grabcad.com/library/airbus-a320neo-1).

Skybrary (2018). *A332, en-route, Atlantic Ocean, 2009.* Retrieved: 22.10.19. Available from: [https://www.skybrary.aero/index.php/A332,_en-route,_Atlantic_Ocean,_2009]

Skybrary. (2019a). *AT43, en-route, Folgefonna Norway, 2005.* Retrieved: 22.10.19. Available from: [https://www.skybrary.aero/index.php/AT43,_en-route,_Folgefonna_Norway,_2005].

Skybrary. (2019b). *Hoar Frost.* Retrieved 10.06.20. Available from: https://www.skybrary.aero/index.php/Hoar_Frost.

Skybrary. (2019c). *Ice Formation on Aircraft.* Retrieved: 23.06.20. Available from: https://www.skybrary.aero/index.php/Ice_Formation_on_Aircraft.

Sojoudi, H., Wang, M., Boscher, N. D., McKinley, G. H., & Gleason, K. K. (2016). Durable and scalable icephobic surfaces: similarities and distinctions from superhydrophobic surfaces. Soft Matter, 12(7), 1938-1963. doi:10.1039/C5SM02295A

Sparaco, P. White Chaos (2011) – *Extreme cold climate in Europe disrupts air travel.* Retrieved: 14.10.19. Available from: [http://archive.aviationweek.com/].

Stoye, D., & Freitag, W. (1998). Paints, coatings, and solvents (2nd ed.). Weinheim, Germany: Wiley-VCH.

Susoff, M., Siegmann, K., Pfaffenroth, C. & Hirayama, M. 'Evaluation of icephobic coatings—Screening of different coatings and influence of roughness'. (2013). Applied Surface Science, vol. 282, pp. 870–879, doi: 10.1016/j.apsusc.2013.06.073.

Thompson, G., Bruintjes, RT., Brown, B.G. & Hage, F. (1997): Intercomparison of in-flight icing algorithms. Part I: WISP94 Real-time Icing Prediction and Evaluation Program. Weather and Forecasting 12: 878–889.

Varanasi, K. K. & Deng, T. (2010). 'Controlling nucleation and growth of water using hybrid hydrophobic-hydrophilic surfaces', in 2010 12th IEEE Intersociety Conference on Thermal and Thermomechanical Phenomena in Electronic Systems, pp. 1–5, doi: 10.1109/ITHERM.2010.5501324.

Varanasi, K. K., Deng, T., Smith, J. D., Hsu, M., & Bhate, N. (2010). Frost formation and ice adhesion on superhydrophobic surfaces. Applied Physics Letters, 97(23), 234102. doi:10.1063/1.3524513

Vertuccio, L., De Santis, F., Pantani, R., Lafdi, K., & Guadagno, L. (2019). Effective de-icing skin using graphene-based flexible heater. Composites Part B: Engineering, 162, 600-610. doi:https://doi.org/10.1016/j.compositesb.2019.01.045.

Vindportalen. (n.d). *Weather condition and different types of icing.* Retrieved: 01.11.2019. Available from: https://www.vindportalen.no/Vindportalen-informasjonssiden-om-vindkraft/Vindkraft/Cold-climate-English/Weather-condition-and-different-types-of-icing.

Vukits, T. (2002). Overview and risk assessment of icing for transport category aircraft and components.

Waagbø, G. A. (2013). *Numeriske modeller for prediksjon av underkjølt skyvann.* Available from: https://www.duo.uio.no/handle/10852/35638.

Wang, H., He, G. & Tian, Q. (2012). 'Effects of nano-fluorocarbon coating on icing', Applied Surface Science, vol. 258, no. 18, pp. 7219–7224, doi: 10.1016/j.apsusc.2012.04.043.

Wang, S., Li, Y., Fei, X., Sun, M., Zhang, C., Li, Y., Yang, Q. & Hong, X. (2011). 'Preparation of a durable superhydrophobic membrane by electrospinning poly (vinylidene fluoride) (PVDF) mixed with epoxy–siloxane modified SiO2 nanoparticles: A possible route to superhydrophobic surfaces with low water sliding angle and high water contact angle', Journal of Colloid and Interface Science, vol. 359, no. 2, pp. 380–388, doi: 10.1016/j.jcis.2011.04.004.

Wang, N., Xiong, D., Lu, Y., Pan, S., Wang, K., Deng, Y. & Shi, Y. (2016). 'Design and Fabrication of the Lyophobic Slippery Surface and Its Application in Anti-Icing'. (2016). J. Phys. Chem. C, vol. 120, no. 20, pp. 11054– 11059, doi: 10.1021/acs.jpcc.6b04778.

Wang, N., Xiong, D., Pan, S., Wang, K., Shi, Y. & Deng, Y. (2017). 'Robust superhydrophobic coating and the anti-icing properties of its lubricants-infusedcomposite surface under condensing condition', New J. Chem., vol. 41, no. 4, pp. 1846–1853, doi: 10.1039/C6NJ02824A.

Wang, Y., Yao, X., Chen, J., He, Z., Liu, J., Li, Q., Wang, J. & Jiang, L. (2015). 'Organogel as durable anti-icing coatings', Sci. China Mater., vol. 58, no. 7, pp. 559–565, doi: 10.1007/s40843-015-0069-7.

Watson, C. R., Dolan, R. C., Putnam, J. W., Bonarrigo, B. B., Kurz, P. L. & Weisse. M. A. (2015). 'Erosion resistant anti-icing coatings', EP1849843B1.

Whiteman, C. D. (2000). Mountain Meteorology. US: Oxford University Press.

Wong, T.-S., Kang, S. H., Tang, S. K. Y., Smythe, E. J., Hatton, B. D., Grinthal, A. & Aizenberg, J. (2011). 'Bioinspired self-repairing slippery surfaces with pressurestable omniphobicity', Nature, vol. 477, no. 7365, pp. 443–447, doi: 10.1038/nature10447.

Yang, C., Wang, F., Li, W., Ou, J., Li, C. & Amirfazli, A. (2015). 'Anti-icing properties of super-hydrophobic ZnO/PDMS composite coating', Appl. Phys. A, vol. 122, no.1, p. 1, doi: 10.1007/s00339-015-9525-1.

Yang, S., Xia, Q., Zhu, L., Xue, J., Wang, Q., & Chen, Q.-m. (2011). Research on the icephobic properties of fluoropolymer-based materials. Applied Surface Science, 257(11), 4956-4962. doi:https://doi.org/10.1016/j.apsusc.2011.01.003.

Yeong, Y. H, Sokhey, J. & Loth, E. (2017). 'Ice Adhesion on Superhydrophobic Coatings in an Icing Wind Tunnel', pp. 1–23, doi: 10.1007/12_2017_32.

Young, T. (1805). An Essay on the Cohesion of Fluids. Philosophical Transactions of the Royal Society of London, 95, 65-87. Retrieved: 15.06.20. Available from www.jstor.org/stable/107159.

Yr. (2009). *Værkart og fronter*. Retrieved: 24.06.20. Available from: https://www.yr.no/artikkel/vaerkart-og-fronter-1.6750800.

Yu, N., Xiao, X., & Pan, G. (2019). 'A stearic acidified-ZnO/methyl polysiloxane/PDMS superhydrophobic coating with good mechanical durability and physical repairability', Journal of Dispersion Science and Technology, vol 40, no 11, p 1548-1558, doi: 10.1080/01932691.2018.1484294

Zha, D., Mei, S., Wang, Z., Li, H., Shi, Z. & Jin, Z. (2011). 'Superhydrophobic polyvinylidene fluoride/graphene porous materials', Carbon, vol. 49, no. 15, pp. 5166–5172, doi: 10.1016/j.carbon.2011.07.032.

Zigmond, J. S., Pollack, K. A., Smedley, S., Raymond, J. E., Link, L. A., Sanders, A. P., Hickner, M. A. & Wooley, K. L. (2016). 'Investigation of intricate, amphiphilic crosslinked hyper-

branched fluoropolymers as anti-icing coatings for extreme environments', Journal of Polymer Science Part A: Polymer Chemistry, vol. 54, no. 2, pp. 238–244, doi: 10.1002/pola.27800.

Zhu, L., Xue, J., Wang, Y., Chen, Q., Ding, J. & Wang, Q. (2013). 'Ice-phobic coatings based on silicon-oil-infused polydimethylsiloxane', ACS Appl Mater Interfaces, vol. 5, no. 10, pp. 4053–4062, doi: 10.1021/am400704z.

Zhang, J., Gu, C. & Tu, J. (2017). 'Robust Slippery Coating with Superior Corrosion Resistance and Anti-Icing Performance for AZ31B Mg Alloy Protection', ACS Appl Mater Interfaces, vol. 9, no. 12, pp. 11247–11257, doi: 10.1021/acsami.7b00972.

Zhang, G., Zhang, Q., Cheng, T., Zhan, X. & Chen, F. (2018). 'Polyols-Infused Slippery Surfaces Based on Magnetic Fe3O4-Functionalized Polymer Hybrids for Enhanced Multifunctional Anti-Icing and Deicing Properties', Langmuir, vol. 34, no. 13, pp. 4052–4058, doi: 10.1021/acs.langmuir.8b00286.

Zhang, X., Wu, X., & Min, J. (2017). Aircraft icing model considering both rime ice property variability and runback water effect. *International Journal of Heat and Mass Transfer, 104*, 510-516.

Zhang, X. (2019). The Proceedings of the 2018 Asia-Pacific International Symposium on Aerospace Technology (APISAT 2018) (1st ed. 2019. ed., Vol. 459, Lecture Notes in Electrical Engineering). Singapore: Springer Singapore : Imprint: Springer.

Zhuo, Y., Li, T., Wang, F., Håkonsen, V., Xiao, S., He, J. & Zhang, Z. (2019). 'An ultra-durable icephobic coating by a molecular pulley', Soft Matter, vol. 15, no. 17, pp. 3607–3611, doi: 10.1039/c9sm00162j.

Zhuo, Y., Xiao, S., Håkonsen, V., Li, T., Wang, F., He, J., & Zhang, Z. (2020). Ultrafast self-healing and highly transparent coating with mechanically durable icephobicity. *Applied Materials Today, 19*, 100542. doi:10.1016/j.apmt.2019.100542.

6 Appendices

6.1 Appendix A

Wettability properties:

https://youtu.be/HrjlbM8_9c8

6.2 Appendix B

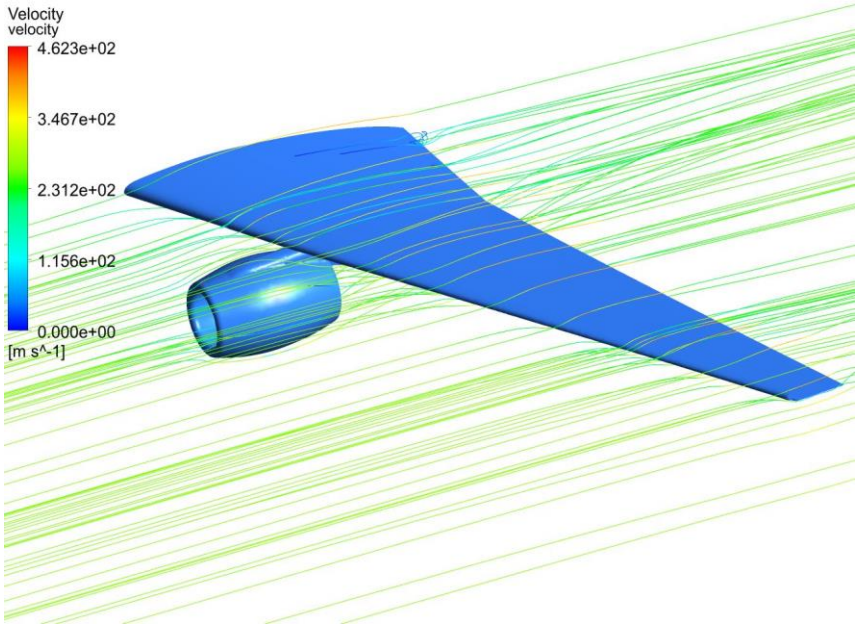

Figure 75: Velocity streamlines without glaze ice (side view).

Figure X illustrates the streamlines from a side angle without glaze ice. These streamlines show the path followed by different particles of air over the wing.

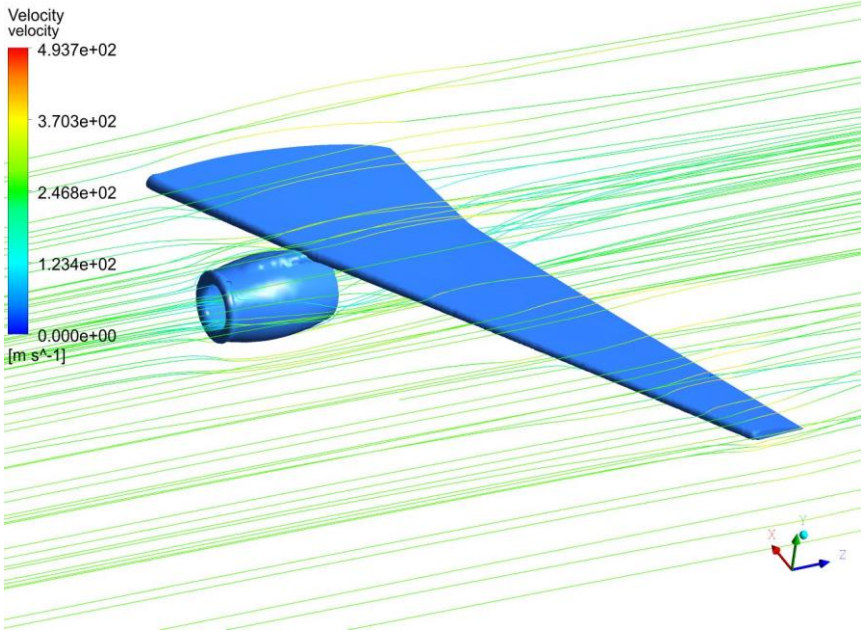

Figure 76: Velocity streamlines with glaze ice (side view).

Figure X illustrates the streamlines from a side angle with glaze ice accumulations, after 100 seconds. These streamlines show the path followed by different particles of air over the wing.

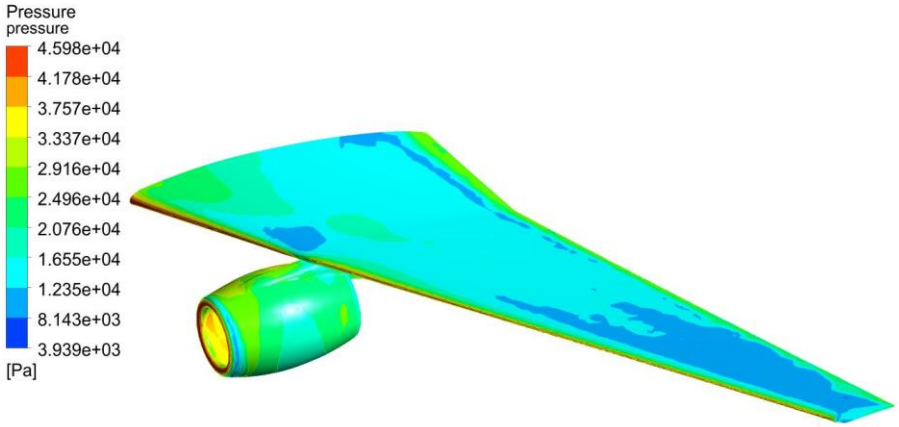

Figure 77: Pressure contour without glaze ice (side view).

Figure X shows the pressure contour from a side view without glaze ice.

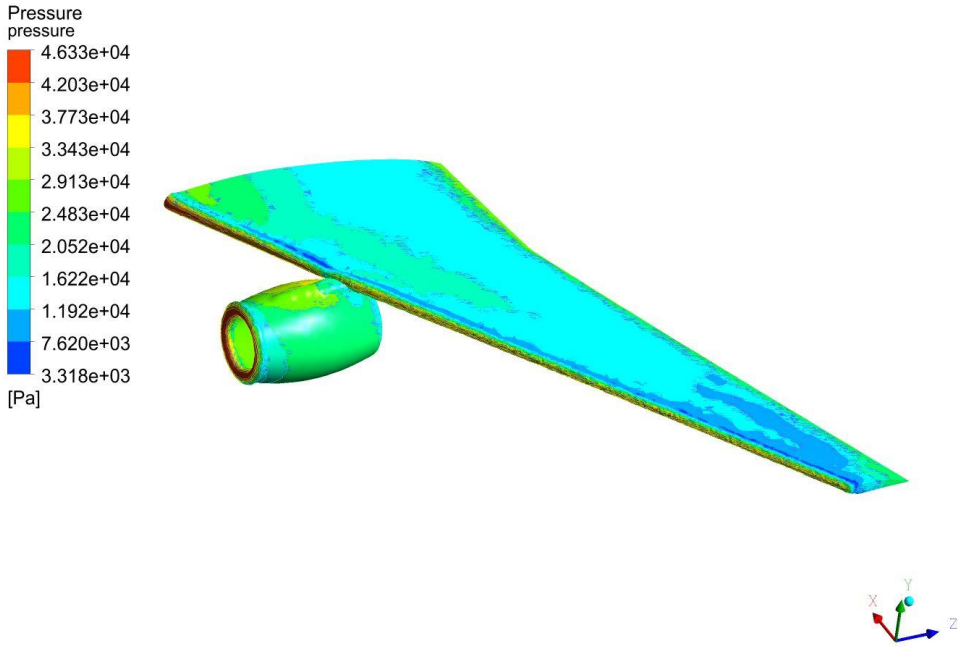

Figure 78: Pressure contour with glaze ice (side view).

Figure X shows the pressure contour from an isometric view with glaze ice accretions, after 100 seconds.

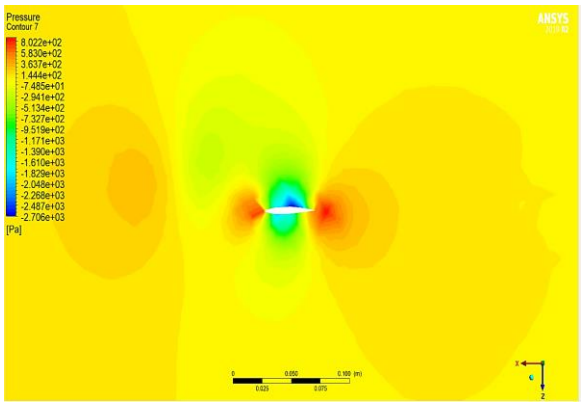

Figure 79: Pressure at cross-section 3.

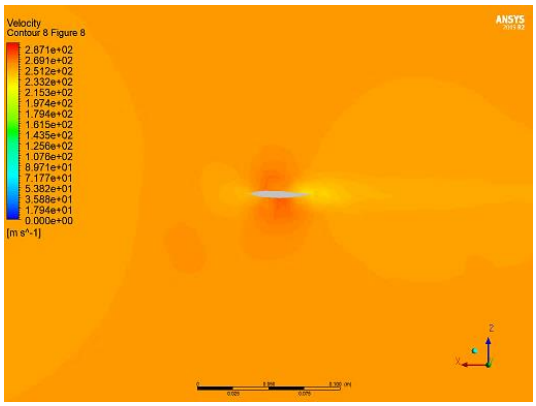

Figure 80: Velocity at cross-section 3.